Wallerian degeneration and Wallerian-related axon loss in disease

Inaugural-Dissertation

zur

Erlangung des Doktorgrades

der mathematisch-naturwissenschaftlichen Fakultät

der Universität zu Köln

vorgelegt von

Weiqian Mi

aus Köln

Köln 2003

ERKLÄRUNG

Ich versichere, daß ich die von mir vorgelegte Dissertation selbständig angefertigt, die benutzten Quellen und Hilfsmittel vollständig angegeben und die Stellen der Arbeit - einschließlich Tabellen, Karten und Abbildungen -, die anderen Werke im Wortlaut oder dem Sinn nach entnommen sind, in jedem Einzelfall als Entlehnung kenntlich gemacht habe; daß diese Dissertation noch keiner anderen Fakultät oder Universität zur Prüfung vorgelegen hat; daß sie - abgesehen von unten angegebenen Teilpublikationen - noch nicht veröffentlicht worden ist sowie, daß ich eine solche Veröffentlichung vor Abschluß des Promotionsverfahrens nicht vornehmen werde. Die Bestimmungen dieser Promotionsordnung sind mir bekannt. Die von mir vorgelegte Dissertation ist von Prof. Dr. S. I. Korsching betreut worden.
Köln, den 26. Juli, 2003

Weiqian Mi

ACKNOWLEGMENT

List of publications related to the Ph.D. thesis

Manuscripts in peer reviewed journals

I.   **Mi W**., Beirowski B., Gillingwater T.H., Coleman M.P. *et al*. Wallerian degeneration shares a regulatory step with axonal spheroid pathology caused by defective ubiquitin metabolism. Submitted.

II. **Mi W**., Glass J.D., Coleman M.P. Stable inheritance of an 85-kb triplication in C57BL/*Wld*^{S} mice. *Mutat. Res.* May 15; 526(1-2): 33-7 (2003).

III. Samsam M., **Mi W**., Wessig C., Zielasek J., Toyka K.V., Coleman M.P. and Martini R. The *Wld*^{S} mutation delays robust axonal loss of motor and sensory axons in a genetic model for myelin-related axonopathy. *J. Neurosci.* Apr 1; 23(7): 2833-9 (2003).

IV. **Mi W**., Conforti L., Coleman M.P. A genotyping method to detect a unique neuroprotective factor for axon (*Wld*^{S}). *J. Neurosci. Meth.* Jan 30; 113(2): 215-8 (2002).

V.   Mack T.G.A., Reiner M., Beirowski B., **Mi W**., Coleman M.P. *et al*. Wallerian degeneration of injured axons and synapses is delayed by a *Ube4b/Nmnat* chimeric gene. *Nat. Neurosci.* Dec; 4(12): 1199-1206 (2001).

VI. Conforti L., Tarlton A., Mack T.G.A., **Mi W**., Buckmaster E.A., Wagner D., Perry V.H., and Coleman M.P. A chimeric protein and overexpression of Rbp7 in the slow wallerian degeneration (*Wld*^{S}) mouse. *Proc. Natl. Acad. Sci.* Oct 10; 97 (21): 11377-11382 (2000).

Chapter Contents

List of Figures

List of Tables

CHAPTER 1

INTRODUCTION

1.1 Wallerian degeneration and slow Wallerian degeneration Mouse, C57BL/Wld^S

Wallerian degeneration is the degeneration of the distal stump of an injured axon (Waller, 1850). It normally occurs over a time course of around 24-48 hr of a lesion, such as mechanical (transection, crush, blunt trauma), chemical toxic (acrylamide), or metabolic (ischemia) injuries. It includes disintegration of the axonal cytoskeleton and fragmentation of the axon, followed by breakdown of myelin sheath, macrophage infiltration and Schwann cell proliferation (Figure 1.1). It is not known how Wallerian degeneration is initiated, but the mechanism clearly involves an active and regulated program of self-destruction and is distinct from neuronal cell body apoptotic degeneration: in Wld^S, neurites of sympathetic ganglia undergo slow Wallerian degeneration after deprivation of their physiological trophic factor (nerve growth factor), however the neuronal soma degenerates normally as wild type (Deckwerth & Johnson, 1994); overexpression of Bcl-2, a anti-apoptosis protein, prevents motoneuron cell body loss but not axonal degeneration in a mouse model of motor neuron disease (progressive motor neuronopathy, *pmn/pmn*)(Sagot *et al*, 1995); Wallerian degeneration and NGF-withdrawal-induced axonal degeneration do not activate classical caspase cascade happening in cell body's apoptosis, and caspase inhibitors do not block axonal degeneration (Finn *et al*, 2000).

The slow Wallerian degeneration mouse, C57BL/Wld^s, carries a dominant mutation that delays Wallerian degeneration in the distal stump of an injured axon. It is a spontaneous mutant that was revealed by experiments to investigate the role of macrophages in peripheral-nerve repair (Lunn *et al*, 1989). Transected axons from the PNS (such as sciatic nerve and tibial nerve) or CNS (such as optic nerve) of the Wld^s retain the ability to transmit a compound action potential for up to 3 weeks (Lunn *et al* 1989; Ludwin and Bisby, 1992; Watson *et al*, 1993), and continue the anterograde and retrograde transport of proteins for a similar length of time (Smith & Bisby, 1993; Glass & Griffin, 1994). In fact, all PNS and CNS neuronal subtypes studied show delayed Wallerian degeneration, including motor and sensory neurons, sympathetic neurons, and retinal gangalion cells (Lunn *et al*, 1989; Perry *et al*, 1991; Deckwerth & Johnson, 1994). The neuroprotective phenotype is dominant and intrinsic to the axon (Perry *et al*, 1990; Glass *et al*, 1993; Deckwerth & Johnson, 1994; Buckmaster *et al*, 1995). The existence of a putative

regulatory molecule in axons suggests that Wallerian degeneration is not a passive process, as previously thought, but an active one that removes damaged axons (Buckmaster *et al*, 1995). Surprisingly, such mutant is developmentally normal, with unaltered axon numbers or synapse elimination (Perry *et al* 1990; Parson *et al*, 1997). Thus Wld^S offers an attractive route to therapy that may have few side effects.

Axonal degeneration, including Wallerian degeneration, is considered to occur through the activation of a local self-destruct program, which is distinct from apoptosis (programmed cell death) (Raff and Finn, 2002). So far, apoptosis is considered as responsible for neuronal cell death in the developing nervous system and probably in certain pathological states such as ischemia and neurodegenerative diseases. It relies on a cascade of enzymes. Most of these are caspases, enzymes that are expressed as inactive precursors (procaspases) and are activated by being cleaved at specific peptide bonds. Likewise, activated caspases in turn activate procaspases at the next point in the enzyme chain by cleaving them at specific bonds. Caspases early in the cascade are activated after a death-inducing signal propagates to the mitochondria, which release several proteins including cytochrome *c*. Cytochrome *c*, the adaptor protein Apaf-1, the enzyme precursor procaspase-9 and dATP form the 'apoptosome' death complex. Procaspase-9 is cleaved to form the active enzyme, caspase-9, which activates caspases 3, 6 and 7 in the same way. These enzymes cleave several intracellular substrates, such as *ICAD* (resulting eventually in DNA fragmentation) and other cell-death regulators, ensuring the death of the cell. Several different proteins acting as 'roadblocks' prevent unwanted cell death by controlling the cytochrome *c* release or the ability of caspases to bind to linker molecules. For example, Bcl-2 proteins regulate the release of proteins from mitochondria; inhibitor-of-apoptosis proteins (IAPs) bind procaspases (to prevent them being activated) and active caspases (to inhibit their activity).

Wallerian degeneration was, until recently, considered as a passive mechanism, with axons degenerating through loss of the inhibitory influence of neuronal trophic substance on the Schwann cell due to the nerve interruption, loss of protein synthesis in the cell body or activation of Ca^{2+}-dependent protease (Lubinska, 1977; Schlaepfer and Hasler, 1979). The picture has changed dramatically with the discovery of the Wld^S mutant and further the identification of the responsible 85 kb triplication region and chimeric gene

(*Ube4b*/*Nmnat*) within the region (Lunn *et al*, 1989; Coleman *et al*, 1998; Conforti *et al*, 2000; Mack *et al*, 2001). Although the molecular mechanism of Wallerian degeneration is still not clear, *Wld*^{S} offers an attractive route into this problem because identifying the gene should lead to regulators of Wallerian degenration. In addition to that, the *Wld*^{s} mutant also gives a great potential to investigate its role in protecting or alleviating neurological diseases, such as myelin-related neuropathy, multiple sclerosis and amyotrophic lateral sclerosis (Coleman and Perry, 2002)**.**

1.2 Molecular genetics of *Wld*^{S}

The *Wld*^{S} mutation has been mapped to distal mouse chromosome 4 (Lyon *et al*, 1993), and a tandem triplication of an 85-kb genomic region has been identified within a genetic candidate interval (Coleman *et al*, 1998). Exons of three genes were identified within the 85-kb tandem triplication unit (Conforti *et al*, 2000) (Figure 1.2). Ubiquitination factor E4B (*Ube4b*) and nicotinamide mononucleotide adenylytransferase (*Nmnat*), span the distal and proximal boundaries of the repeat unit, respectively. They have the same chromosomal orientation and form a chimeric gene when brought together at the boundaries between adjacent repeat units in *Wld*^{S}. The chimeric mRNA is abundantly expressed in the nervous system and consists of the N-terminal 210 coding nucleotides of *Ube4b*, the entire 855 coding nucleotides of *Nmnat*, and 54 nucleotides formed at the junction (Figure 1.2 and Figure 1.3b). The third gene altered by the triplication, *Rbp7*, is a novel member of the cellular retinoid-binding protein family. Although the function of *Rbp7* is unknown, cellular retinoid-binding proteins, most of which are belonging to the fatty acid-binding protein/cellular retinol-binding protein family, have been well characterized in controlling the concentration of free retinoids and in directing protein-bound retinoids to key enzymes responsible for their metabolism. For example, the cellular retinol-binding protein, CRBP, has been implicated in retinol uptake, retinol esterification, mobilization of retinyl esters, and the initial oxidation of retinol to retinaldehyde. It is also conceivable that an alternation in retinoid metabolism could influence axonal survival given that retinoic acid can induce neuronal differentiation, increase nNOS (neuronal nitric oxide synthase) levels *in vitro*, and participate in the cholinergic potentiation of synaptic activity (Sidell *et al*, 1983; Ando *et al*, 1996; Personett *et al*, 2000). However, while *Rbp7* is highly expressed in white adipose tissue

and mammary gland, it is undetectable on northern blots of Wld^S brain. This suggests that it is unlikely to play a role in delaying Wallerian degeneration of axons, but does not rule it out.

1.3 Triplication and its genomic stability

Germ-line triplication is a rare event. However, Reddy and Logan (2000) found a triplication with an inverted middle repeat in 13q22q33 in a new born boy with multiple complications including meconium aspiration syndrome (Reddy and Logan, 2000) and also found triplications in 15q11q13 and 2q112q21. Thus they suggest that intrachromosomal triplication may be more prevalent than previously assumed and can sometimes be mistaken for duplications. Some rare triplications have also found within the α globin gene cluster (Villegas *et al*, 1995). An 85-kb tandem triplication has been identified in the Wld^S mouse (Coleman *et al*, 1998). There are very few reports of tandem triplications in a vertebrate. Perhaps the best-studied tandem triplication is that of the *Drosophila double Bar* mutant, which was shown to arise following a recombination event of the original *Bar* duplication, using polytene banding patterns long before the advent of molecular genetics (Sturtevant *et al*, 1925; Muller *et al*, 1936; Bridges *et al*, 1936). Such triplication is mediated by homologous, but unequal, crossing-over between tandem head-to-tail repeated DNA sequences (Jeffreys *et al*, 1988; Tartof, 1988).

Very little is known about genomic instability of triplications, although it is clear that duplications of similar repeat unit length can be unstable in mammals, for examples the 70-kb pink-eyed unstable (p^{un}) duplication that frequently reverts to wild type (Gondo *et al*, 1993). Initial experiments in Wld^s mice showed that some duplication alleles also existed in two out of seven mice analyzed (Coleman *et al*, 1998). So, like *double Bar*, the tandem triplication in the Wld^S mouse is very likely to have developed from duplication, which, like the mouse pink-eyed unstable (p^{un}) mutation, was unstable. However, unlike pink-eyed, Wld^S contains no genes that are harmful at the increased dosage.

A study of the genomic instability of the triplication in Wld^S is important to understand the gene dosage that is present in Wld^S mice and to facilitate the study of the potential role of *Wld* in neuroprotection, such as crossing Wld^S with mouse model of neurodegenerative diseases.

1.4 The chimeric gene is the Wld^S gene

During the course of the experiments described, it has been confirmed that the *Ube4b*/*Nmnat* chimeric gene confers the slow Wallerian degeneration phenotype using transgenic mice expressing the *Ube4b*/*Nmnat* cDNA from an β-actin promoter. The *Wld*^S phenotype was reproduced fully in one line (line 4836) and partially in three other lines (lines 4830, 4858 and 4839) with a phenotype strength determined by transgene expression level, thus proving that the chimeric gene is the *Wld* gene (Mack *et al*, 2001). The protective gene thus confers a dose-dependent block of Wallerian degeneration. Expression of *Wld* needs to reach a threshold level to exert a significant protective effect: transected distal axons (69%-73%) survived for two weeks in transgenic line 4836 homozygotes which has the highest expression level, however the protection was considerably weaker with only 7% surviving in line 4836 hemizygotes. In addition, motor nerve conduction, synaptic transmission, vesicle recycling and motor nerve terminal morphology were also preserved in a dose-dependent manner.

Ube4b/*Nmnat* chimeric gene encodes a 43-kDa in-frame fusion protein consisting of the N-terminal 70 amino acid of Ube4b, the C-terminal 285 amino acids of Nmnat, and 18 amino acids formed at the junction (Figure 1.3).

The protective mechanism is unknown. Using an antibody described in section 6.2.1, the Wld^S protein was detected predominantly in the nucleus of *Wld*^S and transgenic neurons, indicating an indirect protective mechanism. Although we could not rule out that a possible extremely low and undetectable level of Wld^S protein might exist in axons, it is unlikely that the predominantly nuclear localization of Wld^S does not play a role in protecting axons. The yeast homologue (Ufd2) of Ube4b is required to multi-ubiquitinate some substrate proteins (Koegl *et al*, 1999) and a direct link between ubiquitination and axon degeneration comes from the *Uch-l1* mutation in gracile axonal dystrophy (Saigoh *et al*, 1999 and see section 1.6). However, the Wld^S protein contains only 70 of 1,173 amino acids from Ube4b, and these are absent from the yeast homologue Ufd2. So far ubiquitin-protein ligases (E3s) had been classified into several established families including HECT, RING-finger families and U-box proteins (Hershko and Ciechanover, 1998; Joazeiro and Weissman, 2000; Hatakeyama and Nakayama, 2003). HECT domain E3 family was first characterized by its representative member, the E6 associated protein (E6-AP). The U-box is a domain of approximately 70 amino acids that is present from

yeast to humans. The prototype U-box is present in the C-terminal region of yeast Ufd2, an ubiquitin chain assembly factor (E4), however absent in the Ube4b-derived N-terminal 70 amino acids of chimeric protein in Wld^S. They are therefore unlikely to confer multi-ubiquitination activity, but may have a related role, such as substrate binding or regulation of E3 activity. The protective mechanism may be linked to the nuclear location of the Wld^S protein. Possibilities include sequestering of ubiquitination factors by protein-protein interactions and ubiquitination within the nucleus altering transcription factor stability or RNA processing, leading to an axon effect mediated by unknown proteins. Nmnat is a nuclear protein and has two isoforms of mammalian enzymes catalyzing the reaction $NMN + ATP \rightarrow NAD^+ + Ppi$ (Magni *et al*, 1999; Raffaelli *et al*, 2002), a reaction generally assumed not to be at equilibrium because of the constitutive action of pyrophosphatases. We confirmed that Wld^S protein has Nmnat enzyme activity and found a fourfold increase of Nmnat activity in Wld^S brain homogenates compared to C57BL/6J, but the total content of NAD^+ was not significantly altered (see section 6.2.1). Thus, the increase in Nmnat activity in Wld^S should increase NAD^+ synthesis, and the maintenance of normal steady-state levels suggests that the putative additional NAD^+ is metabolized. The product of a compensatory reaction could itself be involved in axon protection. For example, poly-ADP ribosylation uses NAD^+, influencing protein activity and cellular NAD^+ and ATP content, especially in response to stress (Smith, 2001; Ha and Snyder, 1999). Mild activation of PARP-1 without NAD^+ depletion can be neuroprotective (Nagayama *et al*, 2000). Another metabolite, NADH, is a coenzyme for nitric oxide synthase, an enzyme linked to axon damage, and synthesis of the signaling molecule cyclic ADP ribose from NAD^+ regulates calcium release from intracellular stores, potentially influencing calcium activated proteases in Wallerian degeneration (Smith *et al*, 2001; Di Lisa & Ziegler, 2001).

1.5 Slow Wallerian degeneration Mouse, C57BL/Wld^S and human disease

The morphological features of Wallerian degeneration – the granular disintegration and beading of an axon distal to a site of injury – can be triggered by neurotoxins, and by defects in myelin, axonal transport or oxygen delivery (Waller, 1850; Cliffer *et al*, 1998**;** Frei *et al*, 1999; Probst *et al*, 2000; Oosthuyse *et al*, 2001; Garbern *et al*, 2002). Wallerian degeneration *per se* is a model for the mechanism of axon death in many

diseases of the central and peripheral nervous system such as multiple sclerosis, amyotrophic lateral sclerosis and peripheral neuropathy (Waller, 1850; Dal & Gurney, 1995; Fujimura, 1991). In addition, other diseases, such as dying-back type neuropathies, are traditionally considered distinct from Wallerian degeneration, although there is no evidence that their mechanisms are unrelated (Saigoh *et al*, 1999; Frei *et al*, 1999; Cifuentes-Diaz *et al*, 2002). Recent data shows that Wallerian degeneration and dying-back axon degeneration might share some mechanism in common (Wang *et al*, 2002); and this could be extended to other neurodegenerative disorders, see section 3.2.2. Since axon loss is a major cause of symptoms, even in disorders where the primary defect lies elsewhere, identification of the *Wld*[S] gene facilitates studies to determine whether it protects axons in clinically relevant situations. The *Wld*[S] mutation is already known to protect neuronal processes on primary sensory neuronal culture *in vitro* from the toxic effects of vincristine, suggesting a possible role in combating neurodegeneration induced by chemotherapy (Wang *et al*, 2001). Studies in which I collaborated indicate that distal axon loss in myelin protein zero deficient mutants (*P0*) is partially rescued by *Wld*[S] (Samsam *et al*, 2003 and see section 3.2.2), and that *Wld*[S] protects axon loss in *Pmn*, a mouse model of motor neuron disease (Ferri *et al*, 2003 and see section 3.2.2). In addition to that, *Wld*[S] should shed light on the roles of axon loss in multiple sclerosis (MS), amyotrophic lateral sclerosis (ALS), axonal transport defects (such as Charcot-Marie-Tooth disease type 2A, peripheral neuropathy) (Zhao *et al*, 2001; Cliffer *et al*, 1998), and acute disorders (such as brain trauma and stroke) (Sherriff *et al*, 1994; Graham *et al* 2000; Stys, 1998)**.** *Wld*[S]-derived knowledge might even lead towards a therapy for axons in such clinical situations. Since axon injury has recently emerged as a substantial, and perhaps the key component of MS pathology, manipulating the survival of axons, such as *Wld*[S] does, could lead more axons to survive a period of demyelination and then recover, thus arresting the decline from a relapsing-remitting disease to a progressive one (Narayanan *et al*, 1997; Sherriff *et al*, 1994). As in MS, there is considerable axonal loss in human ALS and in animal models of ALS and spinal muscular atrophy (Oosthuyse *et al*, 2001; Cifuentes-Diaz *et al*, 2002; Dal & Gurney, 1994). It has been reported, that prevention of axonal loss in *pmn* does improve the phenotype (Sagot *et al*, 2000; Ferri *et al*, 2003). Delaying Wallerian degeneration might

well preserve axons, although could not unblock axonal transport, while another treatment removes the blockage. In brain trauma, axon transection is not necessarily instantaneous upon injury and can occur hours later, giving a window of opportunity in which to save axons (Jafari *et al*, 1997). In stroke, there is large component of damage in white matter, thus minimizing the loss of the axons could offer new therapeutic opportunities (Dewar *et al*, 1999).

Those observations above have many important implications: 1) a pathway related to Wallerian degeneration occurs in disease-related processes. Thus, understanding the Wallerian degeneration mechanism is relevant to non-injury disorders such as dying-back neuropathies; 2) Wld^S is a valuable and unique experimental tool with which to probe the contribution of axonal degeneration to numerous neurodegenerative models; 3) such studies could lead to the development of novel therapeutic strategies.

1.6 The *gad* mouse (gracile axonal dystrophy)

The gracile axonal dystrophy mouse is an autosomal recessive mutant that shows sensory ataxia at an early stage (first detectable at 30 days after birth), followed by motor ataxia (detectable about 60 days after birth) (Yamazaki *et al*, 1988). Pathologically, the mutant is characterized by 'dying-back' type axonal degeneration in both the central and peripheral distal ends of primary sensory neurons and the lower motor neurons and formation of spheroid body in the central distal ends of gracile tract (Mukoyama *et al*, 1989; Kikuchi *et al*, 1990; Oda *et al*, 1992; Miura *et al*, 1993). Recent pathological observations have associated neurodegenerative diseases with progressive accumulation of ubiquitinated protein conjugates (Arnold *et al*, 1998; Alves-Rodrigues *et al*, 1998). In *gad* mice, accumulation of amyloid β-protein and ubiquitin-positive deposits occur retrogradely along the sensory and motor nervous system (Ichihara *et al*, 1995; Wu *et al*, 1996). The *gad* mutation is caused by an in-frame deletion including exons 7 and 8 of *Uchl1*, encoding the ubiquitin carboxy-terminal hydrolase (UCH) isozyme (Uch-l1) selectively expressed in the nervous system and testis (Day & Thompson, 1987; Wilkinson *et al*, 1989; Day *et al*, 1990; Kajimoto *et al*, 1992; Saigoh *et al*, 1999)(Figure 1.4). The *gad* allele encodes a truncated *Uch-l1* lacking a segment of 42 amino acids containing a catalytic residue (Larsen *et al*, 1996). *Uch-l1* is known to be involved in the process of de-ubiquitination and UCHs are thought to hydrolyse bonds between small

adducts and ubiquitin to generate free monomeric ubiquitin (Dang *et al*, 1998; Larsen *et al*, 1998). Recent data also suggests this neuronal-abundant protein (Uchl1) mediates the ubiquitin stability and function in neurons (Osaka *et al*, in press). Thus, UCHs are essential in continuing the function of the ubiquitin system, and the defect in Uch-l1 in *gad* mutation appears to affect protein turnover (Saigoh *et al*, 1999). The *gad* mouse is the first mammalian model of neurodegeneration with a defect in the ubiquitin system. In addition to that, dying-back degenerative process is thought to underlie several neurodegenerative diseases in human such as motor neuron disease and peripheral neuropathy (Schmalbruch *et al*, 1991, Samsam *et al*, 2003), and *gad* mutant is characterized by dying-back type degeneration in both sensory and motor nerve fibers, thus it could be also expected to provide important information on the pathogenesis of some neurodegenerative diseases.

1.7 Ubiquitin metabolism in neurodegeneration

The integrity of cellular processes depends upon the proper balance of different proteins. In cells, there are two major destruction pathways to regulate such activities involving either a collection of proteolytic enzymes within the lysosome or the multicatalytic proteolytic core of the proteasome. The majority of proteins that are destined for proteasome degradation are marked by the covalent attachment of multiple ubiquitin molecules, which provide a recognition signal for the 26S proteasome. Such ubiquitin-proteasome pathway involves two discrete and successive steps: a specific recognition process, employing the ubiquitin conjugation cascade, and secondly, an indiscriminate destruction process, mediated by the proteolytic proteasome core. The ubiquitin conjugation cascade uses E1 (ubiquitin-activating enzyme), E2 (ubiquitin-conjugating enzyme), E3 (ubiquitin ligase) and E4 (ubiquitin elongation factor) to shuttle ubiquitin and eventually link ubiquitin to the protein substrates, which then targeted by proteasome for degradation (Myung *et al*, 2001; Koegl *et al*, 1999).

Such ubiquitin-proteasome pathway is considered to play a central role in the processing of damaged and toxic protein, and thus impairing such a pathway could lead to the abnormal accumulation and processing of mutant or damaged intra- and extracellular proteins and finally cause neuronal dysfunction and cell death. In a variety of neurodegenerative diseases, such ubiquitin-positive protein aggregates or inclusion

bodies could be found, for example in the prion protein (PrP) plaques in prion disease, amyloid plaques and neurofibrillary tangles in Alzheimer's disease (AD), Lewy bodies in Parkinson's disease (PD) and nuclear inclusion in the poly-glutamine repeat diseases such as Huntington's disease (HD), spinocerebellar ataxias (SCA) (Hardy and Gwinn-Hardy, 1998; Alves-Rodringues *et al*, 1998; Kenward *et al*, 1994). The mutation of two genes (*Uch-l1* and *Parkin*) within the ubiquitin-proteasome pathway in hereditary PD and recent proof of a mutation in *Usp14* encoding a ubiquitin-specific protease in *ataxia* mice, clearly indicate that ubiquitin-proteasome pathway plays a crucial role in the pathogenesis of neurodegenerative diseases (Kitada *et al*, 1998; Leroy *et al*, 1998; Wilson *et al*, 2002). A missense mutation (Ile93Met) in ubiquitin carboxy-terminal hydrolase L1 (*UCH-L1*) gene was identified in a small German pedigree composed of two affected family members (Leroy *et al*, 1998). Since such mutation causes a partial loss of the catalytic activity of this protease, which involves in the release of ubiquitin from the degraded end products containing small molecules (amines and thiols) and has a potential role in mediating ubiquitin stability in axons (Osaka *et al*, in press), the mutation could impair the overall efficiency of the ubiquitin system leading to aggregation of proteins. The deletion of exon7 and exon8 of *Uchl1* was found to be the causative gene in the first mice model (*gad*) of neurodegeneration with defect in ubiquitin system as well, and such ablation of Uch-l1 expression causes the primary defect in the gracile tract of *gad* mutant, which will be discussed in detail in chapter 5. As described before, E3 ubiquitin-ligase is involved in recognizing the substrates and mediating the attachment of polyubiquitin chains to the substrates, thus it is an important factor in the regulation and selectivity of substrates targeted for degradation. Missense mutations in *Parkin* were identified in familial Parkinson disease and further parkin was found to be a ubiquitin-protein ligase E3 (Kitada *et al*, 1998; Shimura *et al*, 2000). Familial-associated mutations in parkin cause impaired binding to E2 and defective E3 ligase activity, which might cause the autosomal recessive PD (Shimura *et al*, 2000; Imai *et al*, 2000; Zhang *et al*, 2000). Several potential substrates for parkin have recently been identified: CDCrel-1 (potential role in regulating synaptic vesicle release in nervous system) (Beites *et al*, 1999), α-synuclein interacting protein synphilin-1 (Chung *et al*, 2001), Pael-R (parkin-associated endothelin-receptor-like receptor) (Imai *et al*, 2000) and α-Sp22 (a glycosylated form of α-

synuclein)(Shimura *et al*, 2001). Interestingly, ubiquitinated synphilin-1 is enriched in Lewy bodies, the hallmark of PD, and thus suggests that familial-associated mutations in parkin involve in the pathogenesis of PD. Recently, a mutation in *Usp14*, encoding an ubiquitin-specific protease was identified as the causative gene for ataxia mice (Wilson *et al*, 2002). The function of Usp14 might be associated with cleaving the mono-ubiquitin side chain from substrate, and the removal of such mono-ubiquitin would regulate processes such as protein localization and protein activity (Katzmann *et al*, 2001; Hicke, 2001; Shih *et al*, 2000). Although neither ubiquitin-positive protein aggregates nor neuronal cell loss is detectable in the central nervous system (CNS) of *ataxia* mice, there are defects in synaptic transmission in both the central and peripheral nervous systems, and thus suggest that ubiquitin proteases are important in regulating synaptic activity in mammals.

It is clear that the defects in the components of ubiquitin-proteasome pathway play a major role in neurodegenerative diseases, thus a full understanding of such intricate system could contribute to understand the pathogenesis of these disorders.

1.8 XFP (especially YFP-H) mice in studying Wallerian degeneration

A series of methods have been developed before to image individual neurons: from Golgi stain to electron microscopy to anterograde and retrograde labeling methods to immunohistochemical labeling protocols to confocal microscopy. The introduction of the jellyfish green fluorescent protein (GFP) as a vital stain has rendered several useful features: GFP is a protein, so the cells could be rendered fluorescent stably and heritably by introduction of a cDNA; the GFP chromophore is derived entirely from the polypeptide chain without a need of exogenous cofactors or substrates, thus it can be used to view living cells with minimal perturbation; GFP can be fused to other proteins without loss of fluorescence, thus it can be directed to specific subcellular compartments; GFP can be mutated to generate variants (named as XFP) with altered spectral properties and improved translational efficiency, thermostability, and quantum yield. As a result of these favorable properties, GFP and its variants have been used to follow molecules and cells in a lot species (Chalfie *et al*, 1994; Chalfie and Kain, 1998; Tsien, 1998; Conn, 1999) and recently, transgenic mice in which red, green, yellow, or cyan fluorescent proteins (together termed XFPs, termed RFP, GFP, YFP and CFP respectively) were

selectively expressed in neurons were also generated to image individual neurons (Feng *et al*, 2000)(Figure 1.5). All four XFPs labeled neurons in their entirety, including axons, nerve terminals, dendrites, and dendritic spines (XFPs label axons over centimeter-long distances and dendrites over millimeter-long distances). Expression of XFP for up to 9 months has no discernible effect on synaptic structure and that multiple imaging of XFP-labeled neurons in vivo is not detectably toxic. Although there is a remarkable variability in patterns of XFP expression among mice generated from the same construct (under the neuron-specific *thy1*-derived regulatory element), expression is unique and heritable among offspring of each transgenic founder, indicating the difference due to integration site and/or copy number.

Since YFP-fluorescence is intense in both live and paraformaldehyde-fixed tissues, shows good quality of staining axons and nerve terminal and is commercial available, it was chosen as a useful tool to study Wallerian degeneration in following attempts: 1) to study how Wallerian degeneration initiates and progresses in the axotomised axons. Although Wallerian degeneration was described as a process starting from proximal to distal at the transection site with fragmentation of axons, the evidence is indirect; introducing YFP into Wld^S mice should give us a clear picture of it; 2) to study synaptic changes in Wld^S mice. Since XFP could label neurons in their entirety including synapses, CFP-expressing mice were crossed with Wld^S mice to study the undergoing mechanism of synapse withdrawal and degeneration (Gillingwater *et al*, 2002); 3) to study synaptic and axonal change in mice model of neurological disorders with Wld^S. Crossing YFP-H mice with gad/Wld^S mice could give us the information of the difference in the nerve terminal of *gad* with Wld^S or without Wld^S and thus give us a better picture to understand the potential rescue-function of Wld^S in neurodegenerative disorders (see 5.2.1 and 5.2.6); 4) to facilitate the mechanism study of Wallerian degneration. Crossing YFP with transgenic mice with the expression of N-terminal of 70 amino acid of the chimeric gene with NLS or NES could make it easy to visualize the preservation of the axon (see section 6.2.2 in detail).

Figure 1.1 A schematic diagram shows undergoing Wallerian degeneration: disintegration of axonal cytoskeleton and fragmentation of the axon, followed by breakdown of the myelin sheath, macrophage infiltration and Schwann cell proliferation.

Figure 1.1 Schematic diagram of Wallerian degeneration.

Axon fragmentation, myelin degradation

Macrophage infiltration

Schwann cell proliferation

Axon Regeneration
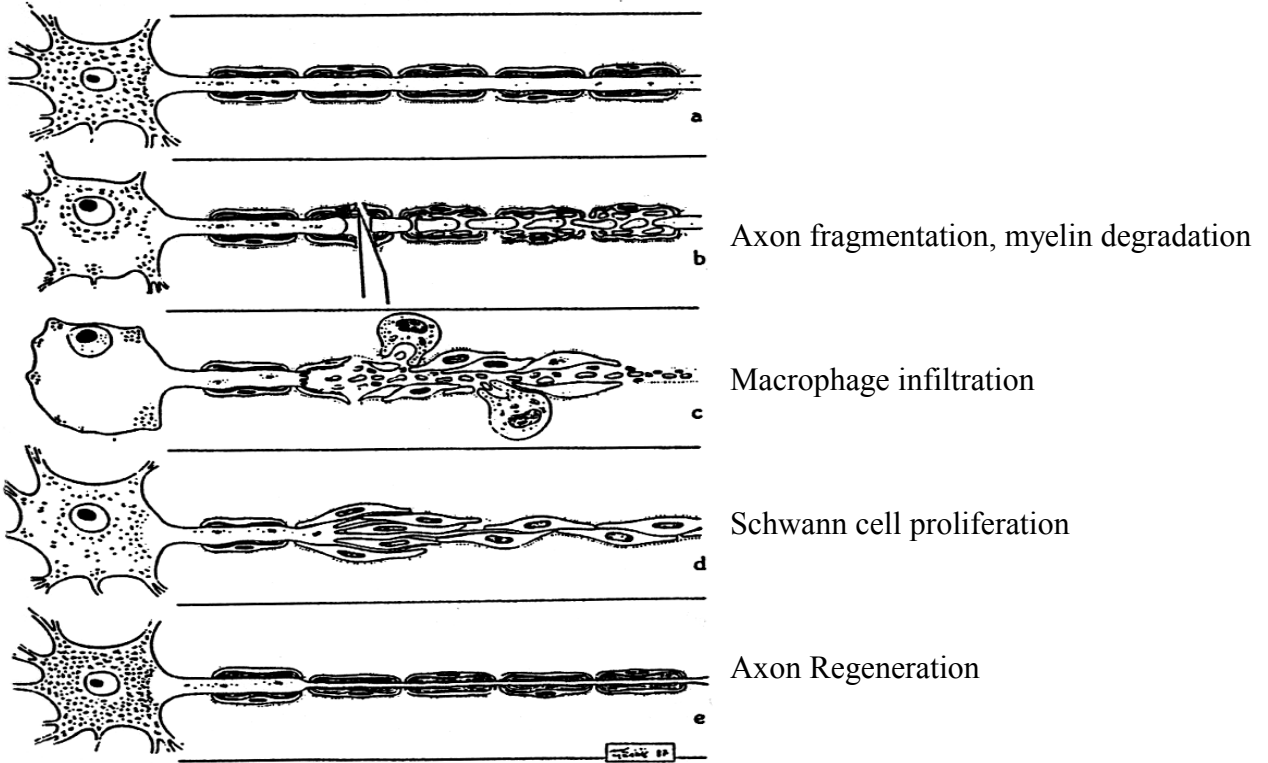
Figure 1.2 Location of exons within the 85-kb Wld^S triplication repeat unit. In Wld^S, three adjacent repeat units are shown to indicate (i) how N-terminal of $Ube4b$ and $Nmnat$ are brought together to form a chimeric gene (ii) that normal copies of $Ube4b$ and $Nmnat$ exist still at either end of the repeat array (the complete genes are not shown), and (iii) how $Rbp7$ is present at three time the normal copy number.

Figure 1.2 Location of exons within the 85-kb *Wld*^S triplication repeat unit.

C57BL/6J
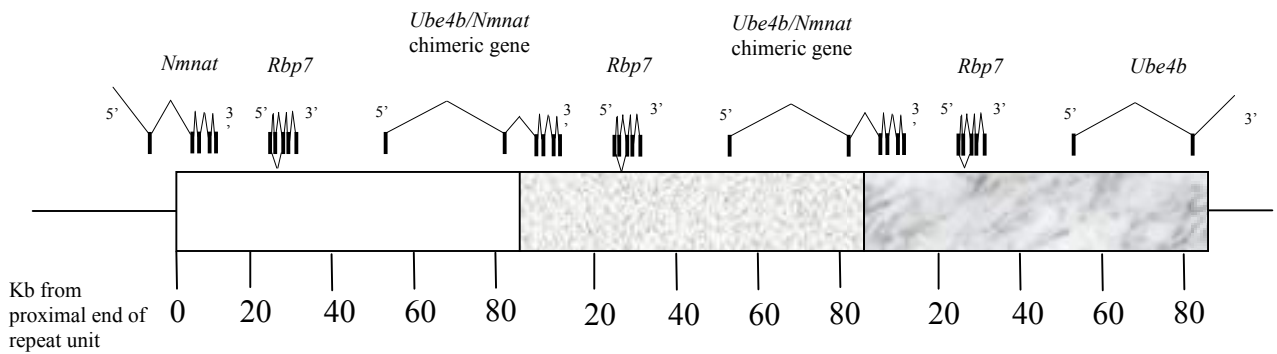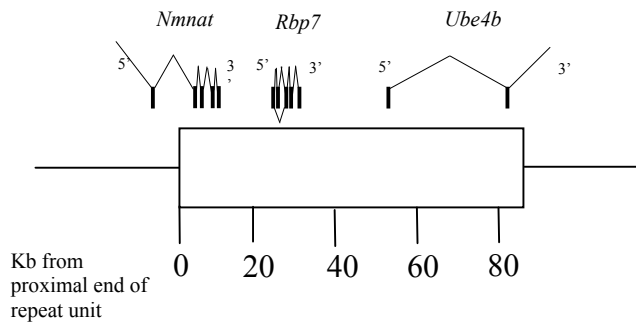
C57BL/*Wld*^S

Figure 1.3a *Wld^S* express novel and wild type proteins: (i) a 43-kDa *Wld^S*-specific chimeric protein; (ii) Ube4b and Nmnat which express both in wild type C57BL/6J and C57BL/*Wld^S*.

Figure 1.3b Sequence of the chimeric cDNA and the predicted coding sequence. The vertical arrow indicates the junction between Ube4b and Nmnat (starting from 71aa and ending at 88aa), and the amino acid shown in bold are those used to make peptides for generation of polyclonal antisera 183 (Ile-325 to Lys-339) and 185 (Thr-64 to His-79) (see section 3.2.1 and section 6.2.1).

Figure 1.3a *Wld*[S] express novel and wild type proteins.

C57BL/6J: Ube4b   1174

Nmnat   285

C57BL/*Wld*[S]:   Ube4b

Nmnat

70   18   285

Chimeric Protein

∗
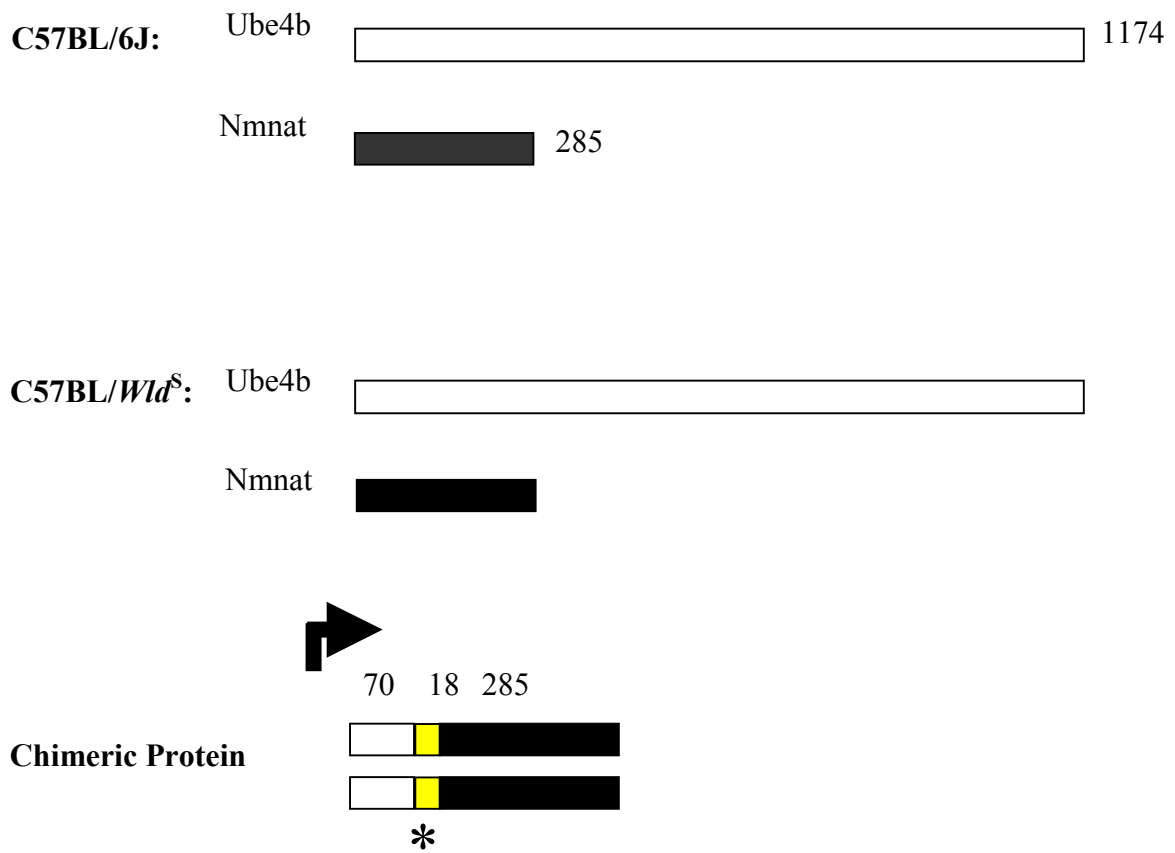
Figure 1.3b Sequence of the chimeric cDNA and the predicted coding sequence.

```
     ATGGAGGAGCTGAGCGCTGACGAGATTCGACGGAGGCGCCTGGCACGACTTGCTGGTGGA
1    MetGluGluLeuSerAlaAspGluIleArgArgArgArgLeuAlaArgLeuAlaGlyGly

     CAGACCTCCCAGCCGACCACCCCGCTTACATCTCCCCAGAGGGAGAACCCTCCGGGACCT
21   GlnThrSerGlnProThrThrProLeuThrSerProGlnArgGluAsnProProGlyPro

     CCAATAGCTGCATCAGCCCCAGGCCCCTCCCAGAGTCTTGGTCTCAATGTCCACAACATG
41   ProIleAlaAlaSerAlaProGlyProSerGlnSerLeuGlyLeuAsnValHisAsnMet
                              ▼
     ACCCCAGCTACCTCCCCCATAGGTGCAGCAGACAACATCGCTGTCAGAGGGTTGCATGTA
61   ThrProAla**ThrSerProIleGlyAlaAlaAspAsnIleAlaValArgGlyLeuHis**Val
                      ▼
     GGTCAACACCACCAACTTCTCCCCATGGACTCATCCAAGAAGACAGAGGTGGTTCTCCTG
81   GlyGlnHisHisGlnLeuLeuProMetAspSerSerLysLysThrGluValValLeuLeu

     GCCTGTGGCTCTTTTAACCCCATCACCAACATGCACCTCAGGCTGTTCGAGCTGGCCAAG
101  AlaCysGlySerPheAsnProIleThrAsnMetHisLeuArgLeuPheGluLeuAlaLys

     GACTATATGCATGCTACAGGAAAATACAGTGTTATCAAAGGCATTATCTCACCGGTCGGT
121  AspTyrMetHisAlaThrGlyLysTyrSerValIleLysGlyIleIleSerProValGly

     GATGCGTACAAGAAGAAAGGGCTCATCCCAGCCCACCACCGAATCATCATGGCAGAACTT
141  AspAlaTyrLysLysLysGlyLeuIleProAlaHisHisArgIleIleMetAlaGluLeu
```

20

```
     GCCACCAAGAACTCACACTGGGTGGAAGTGGATACGTGGGAAAGTCTTCAGAAGGAGTGG
161  AlaThrLysAsnSerHisTrpValGluValAspThrTrpGluSerLeuGlnLysGluTrp


     GTGGAGACTGTGAAGGTGCTCAGATACCATCAGGAGAAGCTGGCAACTGGCAGCTGCAGT
181  ValGluThrValLysValLeuArgTyrHisGlnGluLysLeuAlaThrGlySerCysSer

     TACCCACAAAGCTCACCTGCACTGGAAAAGCCTGGGCGGAAGAGGAAGTGGGCTGATCAA
201  TyrProGlnSerSerProAlaLeuGluLysProGlyArgLysArgLysTrpAlaAspGln


     AAGCAAGATTCTAGCCCACAGAAGCCCCAAGAGCCCAAACCAACAGGTGTGCCCAAGGTG
221  LysGlnAspSerSerProGlnLysProGlnGluProLysProThrGlyValProLysVal


     AAATTGCTGTGTGGGGCAGATTTACTGGAGTCCTTCAGCGTGCCCAACTTGTGGAAGATG
241  LysLeuLeuCysGlyAlaAspLeuLeuGluSerPheSerValProAsnLeuTrpLysMet


     GAGGACATCACGCAAATCGTGGCCAACTTTGGGCTCATCTGTATCACTCGGGCTGGCAGT
261  GluAspIleThrGlnIleValAlaAsnPheGlyLeuIleCysIleThrArgAlaGlySer


     GACGCTCAGAAATTCATCTACGAGTCCGATGTGCTGTGGAGACATCAGAGCAACATCCAC
281  AspAlaGlnLysPheIleTyrGluSerAspValLeuTrpArgHisGlnSerAsnIleHis


     CTGGTGAACGAGTGGATCACCAATGACATCTCGTCCACCAAGATCCGGAGGGCGCTCAGG
301  LeuValAsnGluTrpIleThrAsnAspIleSerSerThrLysIleArgArgAlaLeuArg
```

```
321  AGGGGCCAGAGCATCCGCTACTTGGTACCGGACCTGGTCCAAGAGTACATTGAGAAGCAT
     ArgGlyGlnSerIleArgTyrLeuValProAspLeuValGlnGluTyrIleGluLysHis


     GAGCTGTACAACACGGAGAGCGAAGGCAGGAATGCTGGGGTCACCCTGGCTCCTCTGCAG
341  GluLeuTyrAsnThrGluSerGluGlyArgAsnAlaGlyValThrLeuAlaProLeuGln


     AGGAACGCCGCAGAGGCCAAGCACAACCATTCCACTCTGTGA
361  ArgAsnAlaAlaGluAlaLysHisAsnHisSerThrLeu*** 373
```

Figure 1.4 Scheme of the deleted region of *Uch-l1* in *gad* mice. *gad* mutation is caused by an in-frame deletion including exon7 and exon 8 of *Uchl1*, encoding the ubiquitin carboxy-terminal hydrolase l1.

Figure 1.4 Scheme of the deleted region of *Uchl1* in *gad* mice.
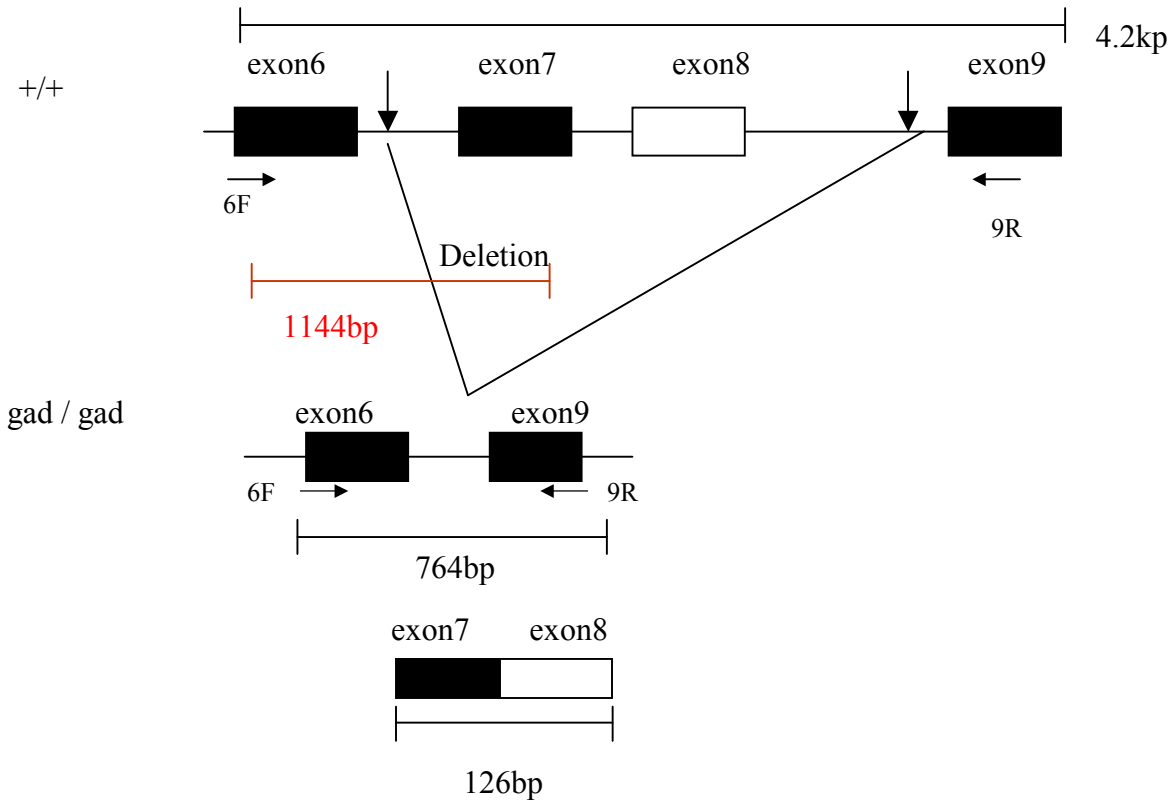
Figure 1.5 Four spectrally distinct XFPs serve as vital stains in transgenic mice. Neuromuscular junctions from *thy1-YFP* line H (a), *thy1-GFP* line H (b), *thy1-CFP* line D (c), and *thy1-RFP* line 8 (d) transgenic mice.

Figure 1.5 Four spectrally distinct XFPs serve as vital stains in transgenic mice.
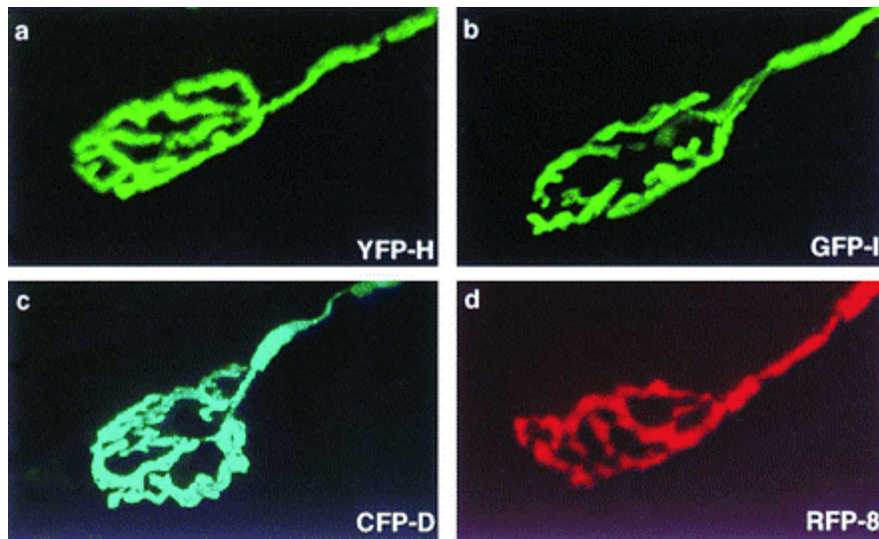
CHAPTER 2

MATERIAL AND METHODS

2.1 Molecular and cellular biology

2.1.1 Extraction of Genomic DNA and preparation of DNA agarose plugs for PFG.

Solution DNA was extracted from mouse spleen or tail tip by using the Nucleon II kit (Amersham Pharmacia) (referred to Appendix 1) according to the manufacturer's instructions. One-third of spleen was homogenized in 2.5 ml Reagent A (10 mM Tris-HCl, 320 mM sucrose, 5 mM $MgCl_2$, 1% (v/v) Triton X-100, pH 8.0) and spun down at 3,000xg. Cell pellet was lysed in 0.5 ml Reagent B containing SDS (supplied by Nucleon II kit) with RNase A treatment (final concentration 400 ng/ml) at 37°C for 30 minutes, deproteinized by adding 150 μl sodium perchlorate and extracted by adding 0.5 ml chloroform and 150 μl Nucleon resin (supplied by Nucleon II kit). Upper DNA phase was transferred to a clean tube and precipitated with 2 volumes of cold absolute ethanol. DNA pellet was washed once with 70% ethanol and suspended in 100-μl sterile water (a rough concentration of 0.25 μg/μl). For hard tissue preparation, half centimeter tail tip was lysed in 0.35 ml Reagent B containing SDS (supplied by Nucleon II kit) with proteinase K to a final concentration of 50 ng/ml, overnight, and deproteinized by adding 100 μl sodium perchlorate. DNAs were extracted by adding 0.6 ml chloroform and 150 μl Nucleon resin, Upper DNA phase was transferred to a clean tube and precipitated with 2 volumes of cold absolute ethanol. DNA pellet was washed once with 70% ethanol and suspended in 40-μl sterile water (a rough concentration of 0.25 μg/μl).

High Molecular weight DNA for pulsed-field gel electrophoresis (PFG) also was extracted from spleen as follows. Half a spleen was dissociated in 1ml of PBS by multiple passages through increasingly narrower needles (from 1.1 mm down to 0.6 mm) and strained through a Becton Dickinson cell strainer (70 μm). The cells were mixed with an equal volume of 1% low-melting point agarose (Flowgen Lichfield, U. K.) in distilled water and poured into a Bio-Rad plug mould on ice (Bio-Rad, Richmond, CA). The embedded cells then were lysed by three overnight incubations in 0.5 M EDTA, 1% sodium-*N*-laurylsarcosine, and 25 μg/ml of proteinase K at 48°C, washed three times in Tris·HCl (10 mM, pH 7.5) and stored long term in Tris·HCl (10 mM, pH 7.5) plus PMSF (0.04 mg/ml).

2.1.2 Genotyping methods to track *Wld*^S triplication.

PCR. Wld^s and 6J genomic DNA was extracted by using the Nucleon II kit (Amersham Pharmacia) (section 2.1.1 and Appendix 1) and used as template. WldF and WldR were used as primers: (WldF) 5'-CGTTGGCTCTAAGGACAGCAC-3'; (WldR) 5'-CTGCAGCCCCCACCC CTT-3'.

Amplification conditions are: 1 cycle of denaturation at 94°C for 2 minutes; 35 cycles of (denaturation at 94°C for 45 seconds; annealing at 60°C for 45 seconds; extension at 72°C for 45 seconds); and a final cycle of extension at 72°C for 10 minutes. Reaction agents referred to Appendix 5.

Southern blotting (refers to Appendix 6). To track the Wld^S triplication, genomic DNA extracts were digested by *EcoR*V at 37°C overnight, and run on 1 % TAE gel overnight. The gel was denatured in 0.4 M NaOH with two changes at 30-minute intervals. DNA on the gel was Southern-blotted overnight onto Hybond N+ (Amersham) in 0.4 M NaOH. Probe GS11 (sequence see below) was radiolabelled by using the Amersham Megaprime kit and [α-^{32}P] dCTP (DuPont/NEN). Posthybridization washes were normally done at a stringency of 0.5 x standard saline citrate (SSC), 0.1% SDS. Radioactive filters were exposed to X-ray film (X-Ograph, Malmesbury, UK) for 24 hours at -80°C or longer when necessary.

Probe GS11 corresponds to nt.5370-6084 in Genbank entry AF260927 was amplified from Wld^S genomic DNA using primers WldF2 (5'-ACATCATACATACTAGGTAAGC-3') and WldR2 (5'-AACTGGATTCTGAACTGATGT-3').

Pulsed-Field Gel Electrophoresis (refers to Appendix 7). Before digestion, agarose plugs (preparation described in 2.1.1) were equilibrated with three changes of 30ml of Tris·HCl (10 mM, pH 7.5), 1mM EDTA, and then with 1ml of the restriction buffer 3 (Invitrogen, USA). Thirty units of *Not*I in a volume of 100 μl was used to digest ½ fragments of plugs for 5 hours at 37ºC. Pulsed-field gel electrophoresis was performed in 0.5 X TBE (90 mM Tris/64.6 mM boric acid/2.5 mM EDTA, pH 8.3) by using a Bio-Rad Chef-DR electrophoresis cell and running conditions of 6V/cm, 10ºC, switch times ramped from 20 to 60 sec, and a run length of 22 hours. After electrophoresis the gel was depurinated for 2 x 10 minutes in HCl (0.3% v/v), Southern-blotted and the DNA was hybridized with

the probe 2 (sequence see below), located centrally within the repeat unit (Figure 3.1) (hybridization procedure is the same as above in southern blotting).

Probe2 was generated by primers WldF3 (5'-TGTAGGTCAACACCACCAAC-3') and WldR3 (5'-TTCCCACGTATCCACTTCCA-3') from Wld^S genomic DNA.

2.1.3 Genotyping of transgenic mice and *gad* (gracile axonal dystrophy) mice.

Transgenic mice N70-NLS and N70-NES: DNA was prepared from a 5-mm tail biopsy using the Nucleon II kit (Amersham Pharmacia, Freiburg, Germany) (Appendix 1). The ~5 kb transgene coding region plus promoter region (constructs shown in Figure 6.1b and Figure 6.1c) was detected using Southern blotting of a *Hind*III single digest on Hybond N+ (Amersham Pharmacia) and hybridization with a corresponding ^{32}P-labeled probe Hg (Probe Hg corresponds to nt.5370-6084 in Genbank entry AF260927, covers the full length sequence of Wld^S gene *Ube4b/Nmnat*).

gad genotyping: For *gad* genotyping tail, genomic DNA was extracted at 3 weeks using the Nucleon II kit (Amersham Pharmacia)(section 2.1.1 and Appendix 1), digested with *Pvu*II, and Southern blotted (See section 2.1.2 and Appendix 6). It was then hybridized with a ^{32}P labeled 764bp probe generated by PCR from *gad* homozygous genomic DNA using primers *gad*F (5'ATCCAGGCGGCCCATGACTC3') and *gad*R (5'AGCTGCTTTGCAGAGAGCCA3'). Positively hybridizing fragments indicative of the *gad* (0.75 kb) and wild-type (1.6 kb) alleles were then identified by autoradiography.

2.1.4 Generation of transgenic mice.

Generation of transgenic mice expressing N70-NLS-Flag-tag.

PCR: DNA encoding N70 (N-terminal 210 nucleotides of *Ube4b/Nmnat*) was amplified by PCR (refers to Appendix 5) from pHβAPr-1-Wld^S (Novagen, Germany), which was used as transgenic construct for expressing *Ube4b/Nmnat* (Wld^S gene)(Mack *et al*, 2001), using Platinum Pfx polymerase (Life Technologies, Karlsruhe, Germany). The primers were designed to contain a *BamH*I and a *Hind*III restriction site at the 5' and 3' ends flanking the N70 sequence. An arbitrary 4 or 5 base was added to 5' end of each primer to facilitate cloning. The amplification conditions are: 1 cycle of denaturation at 94˚C for 2 minutes; 35 cycles of (denaturation at 94˚C for 45 seconds; annealing at 56˚C for 45 seconds; extension at 72˚C for 45 seconds)(Appendix 5). Primers used are FT1A (5'ATC CC**A AGC TT**A ACC TTT CAC CAT TAA GAG GAA AGC G<u>AT G</u>3') and N70-TGR

(5'ACG **CGG ATC C**CT GCT GCA CCT <u>ATG</u> GGG GA3')(letters in bold are the restriction site of *BamH*I and *Hind*III and the start codon is underlined).

Cloning: The amplified N70 flanked with recognition sequence of *Hind*III and *BamH*I was purified by phenol extraction (Appendix 8). N70 products were digested by *BamH*I/*Hind*III and ligated into downstream of the β-actin promoter in *BamH*I/*Hind*III double-digested pHβAPr-1 vector (Figure 6.1b). Ligation product was transformed into bacterial strain XL-10 Gold (Stratagene, Amsterdam, Netherlands). Transformants on LB agar plate with ampicillin (100 µl/ml) were screened using PCR (Appendix 10). The amplified products were analyzed by electrophoresis on a 1% agarose gel. Colonies that gave a PCR product around 210 bp were then chosen for plasmid isolation using Plasmid Mini Kit (Qiagen, Germany)(Appendix 2). Commercially synthesized and phosphorylated primers (the nuclear localization signal (NLS) of the SV40 large T antigen) (Invitrogen, Germany) flanked with restriction site of *BamH*I were digested by *BamH*I and ligated with *BamH*I-digested Flag-tag sequence at the C-terminal (sequence see Figure 2.1)(ligation refers to Appendix 9). Such ligation products were further ligated downstream of a *BamH*I single digested β-actin/pHβAPr-1-N70 backbone (construct see Figure 6.1b). Ligation products were transformed into bacterial strain XL-10 Gold (Stratagene, Amsterdam, Netherlands) and transformants on LB agar plate with ampicillin (100 µl/ml) were screened using PCR (Appendix 10). The amplified products were analyzed by electrophoresis on a 1% agarose gel. Colonies that gave a PCR product around 300 bp were then chosen for plasmid isolation using Plasmid Mini Kit (Qiagen, Germany)(Appendix 2). The orientation and sequence of insert (N70 / 3 x NLS / Flag-tag) were confirmed by DNA-sequencing service in ZMMK (center of molecular medicine in Köln) (ABI Prism 377 DNA-sequencer, Applied Biosystems).

Transfection and pronuclear injection: The construct was transfected to COS-7 cells to confirm the nuclear protein location (see 2.1.9). A 5-kb fragment containing promoter, N70-NLS-Flagtag, and polyadenylation signal was released using *Nde*I and *EcoR*I and gel-purified using QIAquick extraction (Qiagen, Hilden, Germany) (Appendix 3). Pronuclear injection into CBA x C57 F1 single-cell embryos (G. Kollias, Vari, Greece) resulted in one founder from 23 pups that were screened by Southern blotting (refers to genotyping transgenic mice in 2.1.3).

Generation of transgenic mice expressing N70-NES-Flag-tag.

PCR: DNA encoding N70 (N-terminal 210 nucleotides of *Ube4b/Nmnat*) was amplified by PCR (refers to Appendix 5) from pHβAPr-1-*Wld*[S] (Novagen, Germany), which was used as transgenic construct for expressing *Ube4b/Nmnat* (*Wld*[S] gene)(see above), using Platinum Pfx polymerase (Life Technologies, Karlsruhe, Germany). The primers were designed to contain a *BamH*I and a *Hind*III restriction site at the 5' and 3' ends flanking the N70 sequence. An arbitrary 4 or 5 base was added to 5' end of each primer to facilitate cloning. The amplification conditions are: 1 cycle of denaturation at 94°C for 2 minutes; 35 cycles of (denaturation at 94°C for 45 seconds; annealing at 56°C for 45 seconds; extension at 72°C for 45 seconds)(Appendix 5). Primers used are FT1A (5'ATC CC**A AGC TT**A ACC TTT CAC CAT TAA GAG GAA AGC G<u>AT G</u>3') and N70-TGR (5'ACG C**GG ATC C**CT GCT GCA CCT ATG GGG GA3')(letters in bold are the restriction site of *BamH*I and *Hind*III and the start codon is underlined).

Cloning: The amplified N70 flanked with recognition sequence of *Hind*III and *BamH*I was purified by phenol extraction (Appendix 8). N70 products were digested by *BamH*I/*Hind*III and ligated into downstream of the β-actin promoter in *BamH*I/*Hind*III double-digested pHβAPr-1 vector (Figure 6.1c). Ligation products were then transformed into bacterial strain XL-10 Gold (Stratagene, Amsterdam, Netherlands). Transformants on LB agar plate with ampicillin (100 μl/ml) were screened using PCR (Appendix 10). The amplified products were analyzed by electrophoresis on a 1% agarose gel. Colonies that gave a PCR product around 210 bp were then chosen for plasmid isolation using Plasmid Mini Kit (Qiagen, Germany)(Appendix 2). Commercial synthesized and phosphorylated primers (the nuclear export signal (NES) of HIV-Rev (Invitrogen, Germany)(Fukuda *et al*, 1997; Wen *et al*, 1995) flanked with restriction site of *BamH*I were digested by *BamH*I and ligated with *BamH*I-digested Flag-tag sequence at the C-terminal (sequence see Figure 2.1) (ligation refers to Appendix 9). Ligation products were then cloned downstream of a *BamH*I single digested β-actin/pHβAPr-1-N70 backbone (construct see Figure 6.1c). Ligation products were transformed into bacterial strain XL-10 Gold (Stratagene, Amsterdam, Netherlands) and transformants on LB agar plate with ampicillin (100 μl/ml) were screened using PCR (Appendix 10). The amplified products were analyzed by electrophoresis on a 1% agarose gel. Colonies that gave a

PCR product around 300 bp were then chosen for plasmid isolation using Plasmid Mini Kit (Qiagen, Germany)(Appendix 2). The orientation and sequence of insert (N70 / NES / Flag-tag) were confirmed by DNA-sequencing service in ZMMK (center of molecular medicine in Köln) (ABI Prism 377 DNA-sequencer, Applied Biosystems).

Transfection and pronuclear injection: The construct was transfected to COS-7 cells to confirm the cytoplasmic localization (see 2.1.9). A 5-kb fragment containing promoter, N70-NES-Flagtag, and polyadenylation signal was released using *Nde*I and *EcoR*I and gel-purified using QIAquick extraction (Qiagen, Hilden, Germany)(Appendix 3). Pronuclear injection into CBA x C57 F1 single-cell embryos (G. Kollias, Vari, Greece) resulted in 8 founder from 68 pups which were screened by Southern blotting and PCR (refers to genotyping transgenic mice in 2.1.3).

2.1.5 Cloning and expression of recombinant proteins.

N-terminal 210 nucleotides (N70) of chimeric gene (*Wld*[S]) was PCR-amplified from transgene construct using Pfx polymerase (Life Technologies) (Primers see below) (PCR refers to Appendix 5). The primers were designed to contain a *Nhe*I and a *Xho*I restriction site at the 5' and 3' ends flanking the N70 sequence. An arbitrary 4 or 5 base was added to 5' end of each primer to facilitate cloning. PCR products were purified by phenol extraction (Appendix 8). N70 double-digested by *Nhe*I/*Xho*I was ligated into *Nhe*I/*Xho*I double-digested pET-28b (+) vector (Novagen, Schwalbach, Germany) (Figure 2.2 and ligation reaction see Appendix 8) and transformed into high transformation efficiency strain, XL-10 Gold (Stratagene, Amsterdam, Netherlands). Plasmids isolated using the Plasmid Mini Kit (Qiagen, Germany)(Appendix 2) and the orientation and sequence of the insert were confirmed by DNA-sequencing service in ZMMK (**C**enter of **M**olecular **M**edicine in **K**öln) (ABI Prism 377 DNA-sequencer, Applied Biosystems). The plasmids containing N70 insert were retransformed into bacterial strain BL21 (DE3) (Novagen, Germany) because BL21 (DE3) is ideal for high-level protein expression using T7 RNA polymerase promoter, easy induction by Isopropyl-1-thio-β-D-galactopyranoside (IPTG), and with tighter control of protein expression for expression of toxic proteins. Protein expression was induced with 1mM IPTG for 3h at OD_{600}=0.8 (Optimization of conditions for N70 expression see Appendix 11).

Full length chimeric gene (*Wld*^{S}) was PCR-amplified from transgene construct using Pfx polymerase (Life Technologies) (Primers see below) (PCR refers to Appendix 5). The primers were designed to contain a *Nhe*I and a *Xho*I restriction site at the 5' and 3' ends flanking the N70 sequence. Arbitrary 3 or 5 bases were added to 5' end of each primer to facilitate cloning. Full length chimeric gene double-digested by *Nhe*I/*Xho*I were ligated into *Nhe*I/*Xho*I double-digested pET-28b (+) vector (Novagen, Schwalbach, Germany)(Figure 2.2 and ligation reaction see Appendix 8) and transformed into XL-10 Gold (Stratagene, Amsterdam, Netherlands). Plasmids isolated using the Plasmid Mini Kit (Qiagen, Germany)(Appendix 2) and the orientation and sequence of insert were confirmed by DNA-sequencing service in ZMMK (center of molecular medicine in Köln) (ABI Prism 377 DNA-sequencer, Applied Biosystems). The plasmids containing chimeric gene insert were retransformed into BL21 (DE3) (Novagen, Germany). Protein expression was induced with 1mM IPTG for 3h at OD_{600}=0.8 (Optimization of conditions for N70 expression see Appendix 11).

The procedure of purifying recombinant chimeric protein refers to that for recombinant N70 protein in 2.1.6.

Primers for N70 were 5'-GACTA**GCTAGC**<u>ATG</u>GAGGAGCTGAGCGCTGAC-3' (*Nhe*I restriction sites were indicated in bold, the start codons were underlined) and 5'-ATCCG**CTCGAG**CTAGTCTGCTGCACCTATGGGGGA-3' (*Xho*I restriction sites were indicated in bold).

Primers for full-length chimeric gene were 5'-GACTA**GCTAGC**<u>ATG</u>GAGGAGCTGAGCGCTGAC-3' (NheI restriction sites were indicated in bold, the start codons were underlined) and 5'-CGC**CTCGAG**TCACAGAGTGGAATGGTTGTGC-3' (*Xho*I restriction sites were indicated in bold).

2.1.6 Purification of recombinant protein (N70 and Wld^S)

The N70 (or Wld^S protein) bacterial pellet was resuspended in native binding buffer (20 mM sodium phosphate, 500 mM sodium chloride pH7.8, 100µg/ml egg white lysozyme), sonicated on ice (6 x 15s with 15-s intervals) and centrifuged at 4°C (3,000 g, 15 min). N70 was purified using a ProBond^{TM} Resin column (Invitrogen, Groningen,

Netherlands)(refersto Appendix 4) and concentrated using a YM-3 Centricon centrifugal filter (Millipore, Bedford, Massachusetts).

2.1.7 Generation of polyclonal antisera

Antisera (60ml) were raised commercially (Eurogentec, Belgium) by intradermal immunization of rabbits with 20-100 µg of recombinant N70 / per injection per animal at days 14, 28 and 56, and a final bleed at 80 days. Antigens (recombinant N70) were emulsified with complete Freund's adjuvant for the first injection, and with incomplete Freund's adjuvant for the booster injections. Small volume of bleeds (2-3 ml) were taken at days 0, 38 and 66 and shipped on dry ice to us for antibody production test. The possibility of polyclonal antibody against recombinant N70 was tested by Western blot (refers to 2.1.8).

For affinity purification 500 µg N70 protein bound to ProBond resin (2 ml wet volume) was blocked with 5% (w/v) dried skimmed milk powder plus 1% (w/v) BSA in native binding buffer. Resin was incubated with crude antiserum (2 ml in 8 ml binding buffer), and washed with 10 bed volumes binding buffer. Specific antibodies, binding only Wld^S protein and Ube4b, were eluted with 100 mM ethanolamine (pH 11.5), neutralized with 1.5 M Tris and dialyzed against PBS. (Dr. Till Mack in the lab did this affinity purification).

2.1.8 Western blotting (Appendix 12)

Preparation of samples for western blotting

The expression level of proteins of interest was analysed in mouse brains, which were ground to a fine powder under liquid nitrogen and a few millgrammes placed on ice in 20 vol of BUST buffer (60mM Tris-Hcl (pH 6.8), 8.0M Urea, 2% (w/v) SDS, and 2% (v/v) 2-mercaptoethanol) for 4 hours on ice and then manually homogenized. The degree of preservation of heavy neurofilament protein was determined in the distal segment of lesioned sciatic nerves homogenized in 20 volumes of the same buffer. Segments of lumbar spinal cord (cut into fine pieces) and combined dorsal root ganglia (L4-L5) for checking the *Wld*^{S} protein expression level were placed on ice in 20 vol of BUST buffer for 4 hours with occasional manual homogenization.

Proteins separated by SDS-Polyacrylamide gels (refers to Appendix 13) and transferred to nitrocellulose filter (refers to Appendix 12)

The samples were mixed with half volume of 3-x SDS-PAGE buffer. Proteins were separated using standard SDS-PAGE (8-15% (w/v) acrylamide) depending on the molecular weight of proteins: 40~100 kDa, 8% (w/v) acrylamide; 20~70 kDa, 10 or 12% (w/v) acrylamide; 10~40 kDa, 15% (w/v) acrylamide. Proteins on SDS-PAGE were transferred onto nitrocellulose filters using a semi-dry blotter (BioRad, Germany)(Appendix 12). Membrane was incubated in Ponceau S staining solution (0.5% (w/v) Ponceau S (Sigma, Germany); 1% (v/v) glacial acetic acid) with gentle agitation for 2 minutes, and then destained in distilled water until bands are visible to check that proteins of different sizes have been transferred uniformly to the membrane.

Immunoblotting

Membranes were incubated for 1h in blocking buffer (5% skimmed milk) at room temperature, and then incubated with primary antibodies (dilution of primary antibody according to requirement) in the same blocking buffer overnight with gentle shaking at 4 °C. After washed twice for 10 minutes each in PBS-Tween (0.05% Tween®20) buffer at room temperature, membrane was incubated with secondary antibody coupled to horseradish peroxidase (goat-anti-mouse 1:2000, goat-anti-rabbit 1:2000; Dianova, Hamburg, Germany) for 1 h at room temperature. Signals were detected by enhanced chemiluminescence (ECL-detection; Amersham Pharmacia).

Blots could be stripped by stripping buffer (2% SDS, 100 mM β-mercaptoethanol, 50 mM Tris, pH 6.8), which can subsequently be reprobed with a different antibody.

2.1.9 Cells transfection and fixation for immunofluorescence examination.

Maintenance of stable cell line: COS-7 cells were maintained in DulBecco's MEM (D-MEM) with Glutamax-1 (Invitrogen, GIBCO) containing 10% fetal calf serum (FCS) at 37°C in 5% CO_2 in a humidified incubator, and passaged once or twice per week at 1:10 dilution. Cells (~ $2x10^5$) were then seeded to a 6 x well plate in D-MEM medium with FCS and incubated at 37°C in a CO_2 incubator the day before transfection.

Transfection: Transient transfections were carried out with Lipofectamine PLUS™ (Invitrogen Life Technologies). Two solutions were prepared before transfection: 1) diluted 4 µl of LipofectAMINE reagent into 100 µl specialized medium (reduced serum

medium) OPTI-MEM^{TM} (Invitrogen, GIBCO) for facilitating lipid-mediated transfection, and incubated for 5 minutes at room temperature; 2) diluted ~1 μg DNA into 100 μl OPTI-MEM^{TM} (Invitrogen, GIBCO), 4 μl PLUS reagent into DNA and mixed it. The solution 1) was added rapidly into the solution 2) and mixed. Such transfection complexes were incubated for 20 minutes at room temperature. The old medium was removed from the cells and replaced by 800 μl transfection medium (OPTI-MEM^{TM}). The transfection complexes (DNA-PLUS-LipofectAMINE) were added to cells and left to incubate at 37°C at 5% CO_2 for 3 hours. The medium with the complexes was removed and 2 ml fresh D-MEM with 10% FCS was added to the cells with an overnight incubation.

Fixation of transfected cells: The cells were fixed in 4% paraformaldehyde (PFA)/0.05% glutaraldehyde in PBS for 30 minutes, washed twice with PBS, and finally permeabilized in 0.1% Triton in PBS for 10 minutes. Low concentration of glutaraldehyde is to facilitate better cell fixation without destroying epitopes.

Immunostaining: fixed cells were blocked in 5% FCS in PBS for half an hour, and incubated at room temperature in anti-Flag M2 monoclonal antibody (1:100 in the same buffer) (Stratagene, USA) for 1 hour. Cells were then washed twice in PBS and incubated in Texas Red® X-goat anti-mouse IgG (H+L) (1:200) (Molecular Probes, Eugene, Oregon, USA) at room temperature for 45 minutes, washed twice with PBS, and incubated with mounting medium with DAPI (Vector Laboratories, USA) 5 minutes for nuclear staining. After washing twice with PBS, fixed cells were mounted with mounting medium (Vector Laboratories, USA) and covered with cover slip.

2.2 Animals breeding protocols and behavioral analysis

2.2.1 Animal breeding protocols

Crossing mouse model (P0$^{-/-}$ mouse) of myelin-related peripheral neuropathy with Wld^S. (done in the collaborator Martini's lab)

Homozygous C57BL/*Wld*^{S} mutants were obtained from Harlan-Winkelmann (Borchen, Germany) and cross-bred with heterozygous P0 mutants. According to Mendelian law, the individuals of the F1 generation were expected to consist exclusively of mice heterozygous for the *Wld*^{S} mutation. All of these individuals were genotyped for the P0

mutation by conventional PCR as described previously (Schmid *et al*, 2000), and individuals heterozygously deficient for P0 were intercrossed, leading to progenies with homozygous, heterozygous, and no P0 deficiency. Pulsed-field gel electrophoresis was used to genotype for Wld^S status (see detail in 2.1.2).

Crossing Uchl1$^{gad/gad}$ (gracile axonal dystrophy mice)(refers to as gad$^{-/-}$ below) with Wld^S. In the following text, $gad^{+/+}$, $gad^{+/-}$ and $gad^{-/-}$ refer to wild type, heterozygous and homozygous *gad* mice respectively.

Homozygous C57BL/$Wld^{S/S}$ (refers to as $Wld^{S/S}$ below) mutants were obtained from Harlan-Orlac (Netherland) and crossbred with heterozygous $Uch-l1^{gad/+}$ (refers to as $gad^{+/-}$ below) imported from Japan. According to Mendelian law, the individuals of the F1 generation were expected to consist exclusively of mice heterozygous for the Wld^S mutation. All of these individuals were genotyped for the *gad* status by Southern blotting (see section 2.1.2)(Appendix 6), and double heterozygotes ($gad^{+/-}$/$Wld^{S/+}$) were intercrossed, leading to progenies with $gad^{+/+}$, $gad^{+/-}$ and $gad^{-/-}$. Only $gad^{-/-}$ was chosen for behavioral and pathological analysis (*gad* genotyping see 2.1.3). Wld^S genotype was determined postmortem by pulsed-field gel electrophoresis of spleen DNA (Mi *et al*, 2002)(see detail in 2.1.2)(Appendix 7).

For assessment of Wallerian degeneration (section 5.2.1), heterozygous YFP-H mice were obtained from The Jackson Laboratories, Bar Harbor, Maine and mated with *gad*/Wld^S double heterozygotes to produce triple heterozygotes. These were then mated to *gad*/Wld^S double heterozygotes and YFP-H positive offspring genotyped for *gad* and Wld^S to identify *gad* homozygotes that were heterozygous for both Wld^S and YFP-H. The genotyping method for inheritance of the YFP-H transgene refers to below.

Crossing transgenic N70-NLS and N70-NES with YFP-H expressing mice.

Transgenic N70-NLS or transgenic N70–NES were crossbred with YFP-H expressing mice (Jackson Laboratories, Bar Harbour, ME, USA). To genotype for inheritance of the YFP-H transgene, the skin of a 1-2 mm ear punch at 21 days was pulled apart and fluorescent axons or neuronal cell bodies identified using a Zeiss Axiovert S100 inverted fluorescent microscope through the FITC filter. YFP-expression in axons was used as a tool to visualize the preservation of axons directly.

N70-NLS or N70-NES status was confirmed by Southern blotting (see section 2.1.3).

2.2.2 Rotarod analysis.

Tests were performed blind to the Wld^S genotype.

For the accelerating Rotarod (Model 7650, UGO BASILE), mice were trained twice for five minutes at constant speed (3.5 rpm) prior to five repeated testing at accelerating speed from 3.5 rpm to 35 rpm over five minutes. A minimum of 45 minutes recovery time was allowed between each trial. The median time in seconds to fall off from the Rotarod was taken as a measure of the maximum running speed achieved and the test repeated weekly from 9 to 18 weeks. Although mice may fall from the Rotarod for many reasons, it was clear from our observations that progressive hind limb paralysis was the primary cause for the *gad* mice to fall. This became evident also during normal walking for mice scoring below approximately 100 seconds. Wild-type mice typically remained on the Rotarod for the full 300 seconds and the Wld^S mutation did not alter this.

2.2.3 Clasping.

In the clasping test, the mouse was suspended by the tail more than 50 cm from any surface. Clasping time within a 1-minute test was scored as flexing or folding of the hind limbs tightly towards the trunk plus any spasmodic stretching. Mice were examined once per week through the period from 6 weeks to 16 weeks. No wild-type mice clasped, regardless of the presence of the Wld^S mutation.**2.2.4 Foot splay test.**

The foot splay test (Norreel *et al*, 2001) was used to estimate the reflex reaction speed of the hind limbs. Mice were gently taken by the neck and tail, the plantar surface of their hind feet painted using a non-toxic children's painting set, and the mouse released from a height of 15 cm to land on white paper. Wild-type mice bring their legs together during descent to land like a gymnast, whereas advanced *gad* mice fail to do this and land with their feet far apart. The distance between the two hind heels was averaged from 10 successive trials on each testing date (9 weeks and 13 weeks).

2.2.5 Peripheral nerves lesion (PNL).

Six- to eleven-week-old mice were anesthetized intraperitoneally with Ketanest (100mg/kg; Bayer, Leverkusen, Germany) and Rompun (5 mg/kg; Parke Davis/Pfizer, Karlsruhe, Germany). Right sciatic nerves (upper thigh) were transected and the wounds were closed with single sutures. Two to three days later (for transgenic N70-NLS and transgenic N70-NES), mice were killed, the swollen first 2 mm of the distal nerve was

discarded, the next 2 mm was used for Western blot, and further down tibial nerve (one branch of sciatic nerve at the lower thigh) was taken for fluorescence examination under light microscopy (the preparation of YFP nerves in section 2.2.6).

2.2.6 Processing YFP nerves.

Tibial and/or sciatic nerves were dissected from mouse ($gad^{+/+}/Wld^{S/S}$ or $gad^{+/+}/Wld^{+/+}$; gad wt/$Wld^{+/+}$; transgenic N70-NLS; transgenic N70-NES) with a minimum of attached adipose tissue and stretched approximately 10% by pinning them out on a Sylgard dish (Du Pont). Nerves were then fixed with 4 % paraformaldehyde (PFA) (BDH laboratory, England) in 0.1 M PBS in dark for 1 hour, further incubated in 1 % Triton X-100 (Sigma, Germany) in 0.1 M PBS for 10 minutes in dark. After 3 times wash with PBS for 5 minutes each, nerves were mounted in Vectashield (Vector Laboratories, USA) on a glass slide and stored dark at 4°C. View it on fluorescent microscope with standard FITC filter.

2.3 Histological analysis

2.3.1 Paraffin embedding of brain / spinal cord.

Mice aged 126-130 d were anaesthetized using Ketanest and Rompun (100 mg/kg and 5 mg/kg i.p. respectively) or a higher dose as required for deep terminal anaesthesia. After sternotomy, mice were killed by cardiac puncture and instantly intracardially perfused first with a solution containing 10 000 I.E. / l heparin (Liquemin N 25000, Hoffmann-La Roche) and 1% procainhydrochloride in 0.1M PBS (phosphate buffered saline) for 30 seconds and then with fixative (4% paraformaldehyde in 0.1M PBS) for 10 minutes. (Done by lab fellows Bogdan Beirowski and Dr. Robert Adalbert). Brain and spinal cord were carefully removed and fixed in 4% PFA/0.1M PBS overnight, with extensively buffer (0.1M PBS)-washing after fixation. Samples were then taken through a graded ethanol series for 3 days: 50% ethanol – 70% ethanol – 90% ethanol; followed by incubation in isopropyl alcohol overnight, chloroform overnight, and liquid paraffin overnight at 4ºC. The samples were then embedded in paraffin and harden in paraffin molds with ice. 6μm sections were taken on microtome (Type HM355, Microm GMBH) and mounted either on glass slides (Engelbrecht, Germany) for H&E staining or on same type of slides but coated with poly-L-Lysine for immunocytochemistry.

2.3.2 Haematoxylin / eosin staining (H&E).

6 μm sections were deparaffinized in Xylol (Carl-Roth, Germany) for 10 minutes, rehydrated in a descending ethanol series and rinsed in deionized H_2O for 1 minute. Sections were placed in Hematoxylin for 5 minutes, rinsed in tap water for 1 minute to allow stain to develop and then placed in eosin for 2 minutes, dehydrated and mounted in Entellan resin (Merck, Germany). The occurrence of clearly detectable eosinophilic spheroids, indicative of dystrophic axons (Yamazaki *et al*, 1998; Mukoyama *et al*, 1989; Kikuchi *et al*, 1990) was quantified in approximately 90 sections from gracile nucleus and approximately 30 sections from cervical gracile fascicle so that irregular results due to random deviations in spheroid numbers could be ruled out. H&E stained axonal spheroids were generally eosinophilic and appeared with a round or oval shape. They varied in diameter (5-50 μm) and sometimes reached a size larger than the nerve cells in gracile nucleus.

2.3.3 Luxol fast blue staining.

6 μm paraffin sections on poly-L-Lysine coated slides were deparaffinized in Xylol (Carl-Roth, Germany) for 15 minutes, and processed twice through 100% ethanol for 2 minutes each and a few seconds in 96% ethanol. Slides were transferred to Luxol fast blue solution (Luxol fast blue MBS chroma 0.1g (Merck, Germany); ethanol 96% 100ml; acetic acid 10% 0.5ml) and incubated at 60˚ C for 5 hours. Finally, sections were rinsed in 95% ethanol and distilled water for 1 minute each, dipped in a 0.05% Lithiumcarbonate (Merck, Germany) for 1 minute, and differentiated in 70% ethanol for another 1 minute. After rinsed in distilled water, sections were examined under light microscope for suitable differentiation between white and gray matter. Repeat the differentiation steps (1 minute in 0.05% Lithiumcarbonate and 1 minute in 70% ethanol) if necessary. Slides were then put into nuclear fast red staining solution (Aluminum sulfate 5% w/v; nuclear red 0.1% w/v; dH_2O 100 ml) for 10 minutes, followed by through distilled H_2O, 90% ethanol and 100% ethanol for 1 minute each. After putting in Xylol for 5 minutes, slides were covered by clover slips using Entellan (Merck, Germany) and left dry overnight in the hood.

Slides were examined under light microscopy (Nilcon Eclipse E200) for blue myelin staining and the density of blue staining was evaluated by Bioscan OPTIMAS 6.0 (Optimas Corp. Washington, USA) according to manufacturer's instructions. For

densitometric quantification, mean gray values were obtained for circumscribed areas of interest using a 3-chip monochrome CCD camera, and the background gray value (tissue-free area) was subtracted. Since demyelination occurs selectively in the gracile tract and not in the cuneate tract of *gad* mice by 126-130 d (Mukoyama, *et al*, 1989 and our own observations) we used cuneate fascicle as a reference area and expressed LFB staining in gracile tract as a percentage of that in cuneate tract. We applied this procedure to representative LFB stained sections of cranial gracile tract: two sections from level C2/C3 representing cervical gracile fascicle and two sections from level 535 representing gracile nucleus (Sidman *et al*, 1971)(Densitometric quantification was done by lab fellow Bogdan Beirowski).

2.3.4 Anti-GFAP (Glial fibrillary acidic protein) immunostaining.

Deparaffinizing: Slides were heated at 60˚C for 30 minutes, then processed through the following steps for 5 minutes each: Xylol – Xylol – 100% ethanol – 90% ethanol – 70% ethanol – 50% ethanol - dH$_2$O. Then slides were stored in 0.05 M TBS until usage.

Immunostaining: 6 μm paraffin sections on poly-L-Lysine coated slides were encircled with DAKO PAP-Pen and incubated in 0.05M TBS. After 10 minutes incubation with cell penetration solution (0.5 M NH$_4$Cl plus 0.25% Triton in 0.05M TBS), sections were washed twice with 0.05 M TBS. After 20 minutes incubation in 1.2 % H$_2$O$_2$ v/v in methanol and 2 times washed with 0.05 M TBS, sections were blocked by 5% w/v BSA in 0.05M TBS for 60 minutes. Then sections were incubated with anti-GFAP antibody (1:400 dilution) (Progen, Germany) at 4˚C overnight. After washing 4 times with 0.05M TBS, sections were incubated with goat anti-guinea pig globulin biotin conjugate (1:400 dilution) (Sigma, Germany) in 0.05M TBS for 1 hour. Sections were then washed again 4 times with 0.05M TBS, and incubated with avidin-coupled horseradish-peroxidase-complex (1:200 dilution) in 0.05M TBS for 1 hour. After 4 times wash with 0.05M TBS, sections were developed in filtered DAB (diaminobenzidine) solution (0.1 M PB pH7.4, 15ml; DAB 0.05g/ml, 150μl; NH$_4$Cl 0.04g/ml, 150μl; NiSO$_4$ x 6 H$_2$O 0.013g/ml, 300μl; 10% β-D-Glucose 0.1g/ml 300μl; Glucose-Oxidase 1.2 mg/ml, 50μl) for 25 minutes.

Dehydration and mounting: sections were dehydrated by through distilled H$_2$O and a grade series of ethanol for 5 minutes each: 50%, 70%, 90% and 100%. After putting into Xylol (Carl-Roth, Germany) for 5 minutes, slides were covered by clover slips using

Entellan (Merck, Germany) and left dry overnight in a fume hood. Quantification was similar to that described for LFB densitometry. GFAP immunostaining intensities in cranial gracile tract sections were expressed as percentage of GFAP staining intensity in wild-type sections at the same coronal level. We applied GFAP densitometry on representative cranial gracile tract sections from each examined mouse: two sections from level C2/C3 representing cervical gracile fascicle and two sections from level 535 representing gracile nucleus (Sidman et al., 1971)(Densitometric quantification was done by lab fellow Bogdan).

2.3.5 Statistical analysis of histopathological results.

All data (axonal spheroid numbers, TV-densitometry intensities) are presented as mean ± SD for the examined genotype groups. Data analysis was performed using PRISM (done by Dr. Michael Coleman) for Macintosh, SPSS for Windows (done by lab fellow Bogdan Beirowski) or Microsoft Excel including Student's t-test calculations for paired and unpaired data, where appropriate. Significance was considered at a p value < 0.05 and high significance at a p value < 0.01.

2.3.6 Analysis of neuromuscular pathology (done by collaborator Dr. Ribchester's lab in Edinburgh).

Mice were killed by cervical dislocation and lumbrical muscles immediately dissected under oxygenated Ringer solution. Fixation, immunocytochemistry and signal imaging were then carried out as previously described (Gillingwater *et al*, 2002). The denervation rate was determined by counting 100-200 endplates in each of 2-3 lumbrical muscles and the mean value taken for each mouse.

Figure 2.1 Sequence of NLS (nuclear localization signal), NES (nuclear export signal) and Flag-tag used in generation of transgenic mice in 2.1.7. The dash '-' indicates the corresponding sequence of NLS or NES. Flagtag is indicated by blue blocks. 4 (for NLS) or 3 (for NES) amino acids are used as 'Spacer' (which links 3 x NLS or NES and Flagtag) to facilitate the reorganization of Flag tag by anti-Flag antibody (Stratagene, USA).

3 x NLS – Flag tag:

        NLS1   NLS2   NLS3

5'GATCCAAAAAAGAAGAGAAAGGTAGATCCAAAAAAGAAGAGAAAGGTAGATCCAAAA

 AspProLysLysLysArgLysValAspProLysLysLysArgLysValAspProLys

AAGAAGAGAAAGGTAGATACGGCAGCA`GACTACAAGGACGATGACGACAAG`TGA3'
                    Spacer

LysLysArgLysVal   AspTyrLysAspAspAspAspLys*Stop
                             Flagtag

NES-Flag tag:

           NES   Spacer

5'CTGCAACTGCCGCCCCTGGAACGGCTGACGCTGCAAGGCGCA `GACTACAAGGACGAT`

 LeuGlnLeuProProLeuGluArgLeuThrLeu   AspTyrLysAspAsp

`GACGACAAG`TGA

AspAspLys*Stop

  Flagtag

Figure 2.2 pET-28 a-c (+) vectors map. The pET-28 b (+) vectors carry an N-terminal His·Tag®/thrombin/T7·Tag® configuration plus an optional C-terminal His·Tag sequence. The cloning/expression region of the coding strand transcribed by T7 RNA polymerase is shown as well. The *Nhe*I and *Xho*I restriction sites were chosen for cloning.

Figure 2.2

pET-28a-c(+) cloning/expression region

Figure 2.3 Abnormal limbs clasping in mice. Mouse clasps hind-limbs upon suspension by the tail (indicated by arrow). A) Normal control mouse spreads its hindlimbs when suspended by the tail. B) Mouse clasps its hind-limbs (Probst *et al*, 2000).
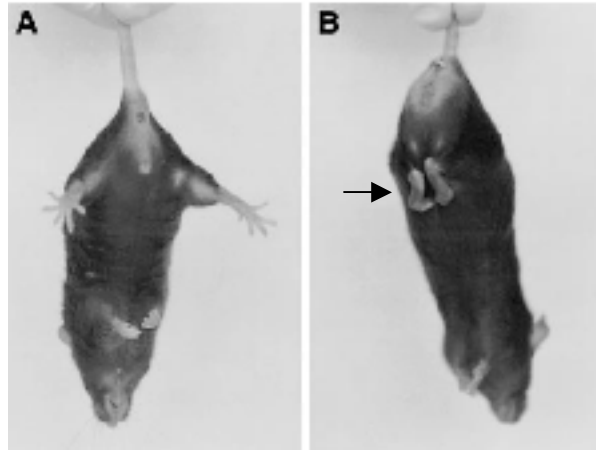
APPENDIX

1. **Principle of Nucleon II Kit (Amersham Pharmacia) for genomic DNA extraction**

Cells and nuclei from either soft tissue (spleen) or hard tissue (tail tip) were lysed by SDS, proteins precipitated with sodium perchlorate, removed with chloroform treatment and finally bound to the nucleon resin (supplied by the Nucleon II kit). DNA was then precipitated by absolute ethanol. DNAs were dissolved in distilled H_2O for future use.

2. **Principle of Plasmid Mini Kit (Qiagen, Germany) for plasmid purification**

The principle is based on a modified alkaline lysis procedure, followed by binding of plasmid DNA to Qiagen Anion-Exchange Resin under appropriate low-salt and pH conditions. RNA, proteins, dyes, and low-molecular-weight impurities are removed by a medium-salt wash. Plasmid DNA is eluted in a high-salt buffer and then concentrated and desalted by isopropanol precipitation.

3. **Principle of QIAquick extraction (Qiagen, Hilden, Germany)**

DNAs were recovered efficiently by binding to a uniquely-designed silica-gel in the presence of high salt while contaminants pass through the column; impurities are efficiently washed away by ethanol-containing buffer and the pure DNA is eluted with distilled H_2O.

4. **Principle of ProBond^{TM} Resin column (Invitrogen, Groningen, Netherlands)**

ProBond^{TM} resin is precharged with Ni^{2+} ions which has high affinity for recombinant fusion proteins that have been tagged with 6 x His-residues. Proteins with six histidine residues bound to the resin can be eluted with either low pH buffer or by competition with imidazole. The binding capacity of resin is 1-5 mg of protein per ml of resin.

5. **Reagents for PCR**

PCR is used to amplify a segment of DNA that lies between two regions of known sequence. Primers used in PCR were oligonucleotides that are complementary to sequences lying on opposite strands of the template DNA and flanking the segment of amplified DNA. PCR was typically performed in a total volume of 50 μl containing 1 x amplification buffer, 1.5 mM $MgCl_2$, 0.2 mM dNTPs, 1-μM primers, 50 ng

templates DNA and 2.5 units Taq DNA polymerase (Gibco-BRL, USA) or Platinum Pfx polymerase (Life Technologies, Karlsruhe, Germany) (with high reading-proof capacity). A programmable Thermal Cycler (Mastercycler gradient, Eppendorf, Germany) was used.

6. Principle for Southern blotting

Southern blotting is used to localize the particular sequences within genomic DNA (Southern, 1975). Genomic DNA is digested with one or more restriction enzymes, and the resulting fragments are separated according to size by electrophoresis through an agarose gel. The DNA is then denatured in situ by 0.4 M NaOH and transferred from the gel to a solid support such as positive charged nylon membrane. The DNA attached to the filter is hybridized to ^{32}P-radiolabeled DNA or RNA, unbound probe removed by washing and autoradiography is used to locate the positions of bands complementary to the probe.

7. Pulsed-Field Gel Electrophoresis

All linear double-stranded DNA molecules that are larger than a certain size migrate through agarose gels at the same rate. To solve such limit of resolution, pulsed fields of alternating direction is applied to a gel: large DNA molecules have to reorient themselves along the new axis of the electric field instead of migrating 'end-on' through the matrix in normal agarose gel apparatus. The larger the DNA molecule, the longer the time required for this realignment, thus it resolves the large DNA molecules to migrate according to their size.

8. DNA extraction using phenol / chloroform

The DNA of interest was cut out from low melting point agarose and melted in 200 μl TE buffer at 80°C for 10 minutes. Equal volume of phenol (200 μl + the volume of the melted agarose) was added to the melted agarose solution, and the mixture was spun at maximum speed (14, 000 rpm) in a benchtop Eppendorf centrifuge for 3-4 minutes. Then the supernatant aqueous layer was transferred to a clean tube and ½ volume of phenol and ½ volume of chloroform was added. The mixture was spun at maximum speed for 2-3 minutes and the supernatant aqueous layer was transferred to a clean tube. DNAs were precipitated by 10% sodium acetate pH 5.5, 1 μl glycogen, 2-3 volume absolute ethanol. The DNA pellet was dissolved in 10 μl distilled H_2O.

9. Ligation reaction

A typical ligation reaction contained 0.1 μg vector (pET-28b (+) or pHβAPr-1) linearized by corresponding restriction enzymes, 40 ng PCR insert digested by corresponding restriction enzymes, 2.5 units T4 DNA ligase (Promega, USA) and 1 x reaction buffer supplied by the manufacturer. Ligation was carried out in a final volume of 10 μl at 16˚C for 16 h.

10. PCR screening

Inserts in the selected colonies were detected via direct PCR screening. A pair of Actin primers (Actin forward primer: 5'ACT TCG GCT CAC AGC GCG3'; Actin reverse primer: 5'TCA CTG CAT TCT AGT TGT GG3') was used for screening plasmid pHβAPr with insert N70 / 3 x NLS / Flag-tag or N70/NES/Flag-tag. A pair of pET-28b (+) sequencing primers (primer for forward sequencing: 5'TAA TAC GAC TCA CTA TAG G3'; primer for reverse sequencing: 5'GCT AGT TAT TGC TCA GCG GT3') was used for screening plasmid pET-28b (+) with insert N70 or *Ube4b*/*Nmnat* (*Wld*^{S} gene). A pinhead quantity of each putative clone was inoculated into a reaction mixture comprising 0.5 μM of each primer, 0.25 mM dNTPs, 0.03 units / μl of *Taq* DNA polymerase (Gibco-BRL, USA) and 1 x PCR buffer. PCR was carried out as following condition: 1 cycle of denaturation at 94˚C for 2 minutes; 30 cycles of (denaturation at 94˚C for 45 seconds; annealing at 55˚C for 1 minute; extension at 72˚C for 1 minute); and a final cycle of extension at 72˚C for 10 minutes. Colonies that contained the inserts were identified and were prepared for sequencing.

11. Optimization of conditions for the expression of N70 or full length chimeric protein (Wld^S)

Optimization of conditions for the expression of N70 and full-length chimeric protein was performed using small-scale cultures. An overnight culture of the clone of interest was made in 1 ml LB containing kanamycin. The next day, a 1:50 dilution of the overnight culture was made in 10 ml of fresh media. Three flasks of the culture were prepared and incubated at 37˚C, with shaking, until OD_{600}=0.5, 0.8 and 1.0, respectively. The cultures were then induced with 1mM IPTG and examined for the production of the ~ 8 kDa N70 or ~ 43 kDa *Wld*^{S} recombinant protein after 0h, 1h, 2h, 3h, 4h of induction with 1mM IPTG. 2-ml aliquots of the cultures were pelleted and

lysed using 80 μl lysis buffer (8 M urea; 0.1 M NaH2PO4; 0.01 M Tris·Cl, pH 8.0). The pellet and supernatant fractions of the lysate were analyzed on 4% stacking / 15% resolving SDS-PAGE for N70 and 4% stacking / 10% resolving SDS-PAGE for full-length chimeric protein. According to recombinant protein expression level, protein expression condition with 1mM IPTG induction for 3h at OD_{600}=0.8 was chosen.

12. Western blotting

Western blotting (Towbin *et al*, 1979) is a technique for detecting specific proteins after electrophoretic separation by transferring from the gel to a more manageable solid phase support, as in Southern blotting DNA: electrophoretically separated protein components are transferred from a SDS-PAGE gel to a solid support (nitrocellulose filters) and probed with reagents (antibodies) that are specific for antigenic epitopes displayed by the target protein. The bound antibody is detected by one of several secondary immunological reagents (^{125}I-labeled protein A or anti-immunoglobulin, or anti-immunoglobulin or protein A coupled to horseradish peroxidase or alkaline phosphatase). As little as 1-5 ng of an average-sized protein can be detected by western blotting.

Semi-dry transfer: 12 pieces of filter paper and a piece of nitrocellulose membrane (7.5 cm x 6.5 cm) were soaked in semi-dry transfer buffer (25 mM Tris; 192 mM Gycin; 20% methanol). 6 sheets of filter paper were placed on the anode (positively charged), followed by the membranes, the gel and finally another 6 sheets of filter paper on the cathode (negatively charged). It is important to carefully avoid air bubbles during the procedure. Electrotransblotting was carried out at a constant voltage of 15 V for 45 minutes.

13. Buffers for SDS-polyacrylamide gel electrophoresis

3 x SDS-sample buffer: 150 mM Tris·HCl (pH 6.8); 300 mM DTT; 6% SDS; 0.25% Bromphenolblue; 30% Glycerol.

Separating gel:

1) 8%: Protogel (30% (w/v) Acrylamide: 0.8% (w/v) Bis-Acrylamide Stock Solution (37.5:1)(National diagnostics, USA), 2.67 ml; 1.5 M Tris·HCl, pH 8.8, 2.5 ml; 10% SDS, 0.1ml; deionized H2O, 4.62 ml.

2) 10%: Protogel (30% (w/v) Acrylamide: 0.8% (w/v) Bis-Acrylamide Stock Solution (37.5:1)(National diagnostics, USA), 3.33 ml; 1.5 M Tris·HCl, pH 8.8, 2.5 ml; 10% SDS, 0.1ml; deionized H2O, 3.96 ml.

3) 12%: Protogel (30% (w/v) Acrylamide: 0.8% (w/v) Bis-Acrylamide Stock Solution (37.5:1)(National diagnostics, USA), 4.00 ml; 1.5 M Tris·HCl, pH 8.8, 2.5 ml; 10% SDS, 0.1ml; deionized H2O, 3.29 ml.

4) 15%: Protogel (30% (w/v) Acrylamide: 0.8% (w/v) Bis-Acrylamide Stock Solution (37.5:1)(National diagnostics, USA), 5.00 ml; 1.5 M Tris·HCl, pH 8.8, 2.5 ml; 10% SDS, 0.1ml; deionized H2O, 2.29 ml.

100 µl Ammonium Persulfate (Sigma, Germany) and 10 µl TEMED (Sigma, Germany) were added to each solution above and mixed.

Stacking gel 4%: Protogel (30% (w/v) Acrylamide: 0.8% (w/v) Bis-Acrylamide Stock Solution (37.5:1)(National diagnostics, USA), 1.3 ml; ProtoGel stacking buffer (0.375 M Tris·HCl, pH6.8; 0.1% SDS), 2.5 ml; Deionized H2O, 6.1 ml; 100 µl Ammonium Persulfate (Sigma, USA) and 10 µl TEMED (Sigma, USA).

SDS-running buffer (10 x): 0.25 M Tris; 1.92 M Glycine; 1% SDS; pH 8.3.

Molecular standards is Precision Plus Protein standards (Bio-Rad, Germany): ten protein bands of 10 kD, 15 kD, 20 kD, **25 kD**, 37 kD, **50 kD**, **75 kD**, 100 kD, 150 kD and 250 kD are all recombinant proteins. Three reference bands are indicated in bold.

Coomassie Blue staining solution: methanol, 45% (v/v) (Carl-Roth, Germany); distilled H_2O, 45% (v/v) (Carl-Roth, Germany); glacial acetic acid, 10% (v/v) (Carl-Roth, Germany); Coomassie Blue, 0.25% (w/v) (Merck, Germany).

Destaining solution I: methanol, 50% (v/v); glacial acetic acid, 10% (v/v); distilled H_2O, 40% (v/v).

Destaining solution II: methanol, 5% (v/v); glacial acetic acid, 7% (v/v); distilled H_2O, 88% (v/v).

The sample (10 µl) was added to 5 µl of 3 x loading buffer and heated at 95°C for 5 minutes prior to application. Electrophoresis was carried out at a constant voltage of 100 V for about 2 hours. The gel was fixed and stained by placing the gel in Coomassie blue staining solution for 1 h with shaking, destained in a solution I for 1h, and then in a solution II until a clear background was obtained.

CHAPTER 3

GENOTYPING METHODS TO TRACK THE *Wld*^{S} TRIPLICATION

3.1 Introduction

The slow Wallerian degeneration mouse, C57BL/Wld^S, carries a dominant mutation that delays Wallerian degeneration in the distal stump of an injured axon. The protective gene (*Ube4b*/*Nmnat*) has been identified and also found to protect axons from the neurotoxin vincristine *in vitro* (Wang *et al*, 2001; Mack *et al*, 2001). Therefore, it is important to determine whether it has a widespread application to protect axons in neurological diseases, such as myelin related peripheral neuropathy, motoneuron disease etc. In principle, this can be done by crossing Wld^S to mouse model of neurological disorders, such as $P0^{-/-}$ mice (a mouse model of myelin-related peripheral neuropathy) and *pmn* (a mouse model of motoneuron disease), but first a method is needed to track the inheritance of the neuroprotective Wld^S allele. Due to the complex nature of the mutation, there is no simple method to distinguish Wld^S homozygotes, heterozygotes and wild-type mice. Therefore I carried on the study of finding a suitable genotyping method to track Wld^S triplication.

3.2 Result

3.2.1 Genotyping methods for the Wld^S triplication.

Three methods (PCR, Southern blotting and pulsed field gel eletrophoresis (PFGE) were discussed below.

1) PCR.

PCR primers Wld F and WldR are located at the proximal and distal ends of the 85 kb repeat unit, respectively (Figure 3.1 and Section 2.1.2), and thus amplify a 182 bp product from Wld^S genomic DNA which spans the boundary (Figure 3.2). No such product is produced from wild type mice, because the primers are separated by 85 kb and oriented in opposite directions.

2) Southern blotting

When a probe located close to the end of the repeat unit is used, additional restriction fragments are seen in Wld^S mice. Furthermore, the relative strength of the Wld^S-specific band and the constant band can be used to distinguish homozygotes from heterozygotes. Probe G11 which is located at the proximal boundary (Figure 3.1 and section 2.1.2), hybridized to a 6-kb fragment of identical size in C57BL/6J and in C57/Wld^S, but also to

a Wld^S-specific fragment (5 kb) of altered size and with an increased intensity (Figure 3.3). The Wld^s-specific band (5 kb) is always stronger than the constant band (6 kb) in homozygotes, however the two bands are almost the same intensity as each other in heterozygotes. This is because on the Wld^s chromosome there are two copies of the Wld^s-specific junction fragments and one normal fragment. Therefore Wld^s homozygotes have four copies of the Wld^s-specific fragments and two of the normal fragment. In heterozygotes, however, the fragments are present in equal copy numbers: two junction fragments on the Wld^s chromosome, plus one copy of the normal fragment on each chromosome 4. Since small fragments can blot more efficiently than bigger ones in Southern blotting, the constant band looks a slightly less intense in the heterozygotes when using an $EcoR$V where the constant band (6 kb) is slightly bigger than the Wld^s-specific band (5 kb).

3) Pulsed field gel electrophoresis (PFGE)

Using rare cutter restriction enzymes that do not cut within the repeat unit, it is possible to detect directly the 170 kb insertion corresponding to the 85 kb triplication in Wld^s. Any single-copy probe within the repeat unit can be used, including GS11 (see Figure 3.1). In the experiment shown in Figure 3.4, a different probe (probe 2, see section 2.1.2) was used. The probe detects a single NotI fragment of approximately 220 kb in C57BL/6J and a single fragment increasing in size to approximately 390 kb in C57BL/Wld^s (Figure 3.1 and Figure 3.4). In Wld^S heterozygotes, both fragments (220 kb and 390 kb) are detected.

3.2.2 The application of genotyping methods to track the Wld^S triplication

Since the axonal protective gene, the $Ube4b$/$Nmnat$ chimeric gene was identified within the tandem triplication in Wld^S, determination of Wld^S genotype could facilitate the investigation in the possible role of Wld^S preventing axon degeneration in diverse pathologies and its effect on the symptoms. This could be done by crossing Wld^S with neurodegenerative mutants in which axonal degeneration plays a primary or secondary role.

So far, these genotyping methods (Southern blotting and PFGE) have been applied to track Wld^S inheritance in following experiments: (1) is an extensive project reported in this thesis (chapter 5), (2) and (3) are collaborative projects for which I carried out the genotyping (2) or trained investigators from other laboratories (3), (4)-(7) are other

ongoing projects within our laboratory or collaborations and (8) has widespread applications in many laboratories and animal breeding companies.

1) Crossing recessive mutant gracile axonal dystrophy (*gad*) with Wld^S. To investigate whether Wld^S could prevent axon loss in the gracile tract of *gad* and then further alleviate the phenotype of *gad,* three groups of offspring are chosen by intercrossing double heterozygotes $gad^{+/-}/Wld^{+/S}$: *gad*/$Wld^{+/+}$, *gad*/$Wld^{+/S}$, and *gad*/$Wld^{S/S}$. *The Wld* genotype is confirmed by PFGE on postmortem tissue (spleen). The results in detail shown in chapter 5.

2) Crossing mouse model (*P0*$^{-/-}$ mouse) of myelin-related peripheral neuropathy with Wld^S.

   One of the major problems of myelin-related disorders, such as multiple sclerosis and demyelinating neuropathies, is the progressive loss of the axons that leads to irreversible symptoms and permanent disability (Trapp *et al*, 1998; Korneck *et al*, 2000; Martini, 2001). Mice deficient in the peripheral myelin component P0 mimic severe forms of inherited peripheral neuropathies in humans, with defective myelin formation and consequent axonal loss. It is presently not known how abnormal myelin or demyelination leads to axonal destruction.

   To investigate whether the robust myelin-related axonal loss in *P0*-deficient mutants follows a similar mechanism to that of Wallerian degeneration and whether Wld^S could rescue the myelin-related axonal loss in such mutant, our collaborators in Würzburg crossed *P0*-deificient mice with C57BL/Wld^S. Five groups of mice were chosen for analysis: *P0*$^{+/+}$/Wld^S-homozygotes (control), *P0*$^{+/+}$/WT (control), and *P0*$^{-/-}$/$Wld^{+/+}$, *P0*$^{-/-}$/$Wld^{S/S}$, *P0*$^{-/-}$/$Wld^{S/+}$. Genotyping Wld^S triplication in these mice were conducted in our lab using the shipped and frozen spleens, and in total I have genotyped 19 spleens from *P0*$^{-/-}$/$Wld^{+/+}$, 32 from P0$^{-/-}$/$Wld^{S/+}$ and 24 from P0$^{-/-}$/$Wld^{S/S}$. Our collaborators found that in the double mutants (*P0*$^{-/-}$/$Wld^{S/+}$ and *P0*$^{-/-}$/$Wld^{S/S}$), the robust myelin-related axonal loss in plantar nerves is reduced ~40% at 6 weeks age and ~30% at 3 months of age. Such rescue effect is also present in median nerve, showing ~25% reduction in axonal loss at 3 months age (Figure 3.5). Further, they found the rescued and morphologically normal axons are functionally intact and active in the 3-month-

old double mutants. The amplitude of compound muscle action potentials were reduced ~50% less in $P0^{-/-}/Wld^{S/S}$ than in $P0^{-/-}/Wld^{+/+}$ (Figure 3.6a). The result of retrograde transport of Fluorogold and counting of the corresponding spinal motoneurons further backs up the survival of preserved axons and indicates that some of the rescued axons are motor axons, which are mainly responsible for the disability in Charcot Marie Tooth Disease Type 1: the number of retrogradely labeled motoneurons (171±18) in $P0^{-/-}/Wld^S$-homo/hetero comparing to (136±21) in $P0^{-/-}$ mice and age-matched wild-type mice (177 ± 26), showing 100% preservation at 3 months age (Figure 3.6b). In addition to that, the result of the muscle strength by performing quantitative grip strength analysis shows significant more strength in $P0^{-/-}/Wld^{S/S}$ than $P0^{-/-}$ mice at 3 months age (Figure 3.7). Such rescue effect does not exist in 6-months-old double mutants compared to single mutant mice ($P0^{-/-}$). To investigate whether such loss of axonal protection in older double mutants is caused by any decrease in Wld^S expression, I examined the expression level of Wld^S protein in spinal cord or dorsal root ganglia between 6-week-old and 6-month-old double mutants ($P0^{-/-}/Wld^{S/S}$) by western blot using rabbit polyclonal anti-Wld 18 antibody (detail in Figure 1.3b). There is not a decrease of Wld^S protein level in older mutants (Figure 3.8).

The results indicate that myelin-related axonal loss is a process having some features in common with Wallerian degeneration, and introducing the Wld^S gene partially rescues axonal loss in mice model of peripheral neuropathy. This, and *pmn* (below) were the first examples of axon rescue in chronic disease by the Wld^S gene.

3) Crossing recessive mutant *pmn/pmn* (progressive motor neuronopathy) with Wld^S

Apoptosis is a hallmark of motoneuron diseases such as amyotrophic lateral sclerosis (ALS) and spinal muscular atrophy (SMA). In a widely used mouse model of motoneuron disease (*pmn*), transgenic expression of the anti-apoptotic bcl-2 gene or treatment with glial cell-derived neurotrophic factor prevents the apoptosis of the motoneuron soma; however they were unable to affect the life span of the animals (Sagot *et al*, 1995; Sagot *et al*, 1996). To determine whether Wld^S could rescue the *pmn* phenotype, Ann Kato's lab in Geneva crossed the

Wld^S with *pmn* mice and the PFG genotyping method helped them to confirm Wld^S genotype (hetero or homo) from wild type mice. In the crossing mice (*pmn/pmn* with Wld^S-homozygous or heterozygous)*, Wld^S attenuates symptoms, extends life span, prevents axon degeneration, rescues motoneuron number and size, and delays retrograde transport deficits in *pmn/pmn* mice (Ferri *et al*, 2003).

4) Crossing $Vegfa^{\delta/\delta}$ mice with Wld^S

Hypoxia stimulates angiogenesis through the binding of hypoxia-induced factors to the hypoxia-response element in the vascular endothelial growth factor (*Vegf*) promoter. VEGF is essential in the formation of new blood vessels (angiogenesis). Deletion of the hypoxia-response element in the *Vegf* promoter reduces hypoxic Vegf expression in the spinal cord and caused adult-onset progressive motor neuron degeneration, reminiscent of amyotrophic lateral sclerosis. To investigate whether axonal-protective protein Wld^S could play a protective role in mice homozygous for the deletion of the hypoxia-response element ($Vegfa^{\delta/\delta}$ mice), our group is crossing Wld^S with $Vegfa^{\delta/\delta}$ mice, and double mutants ($Vegfa^{\delta/\delta}/Wld^S$-heterozygous or homozygous, $Vegf^{\delta/\delta}/Wld^{+/+}$) will be selected for behavioral and pathological analysis. Southern blotting and PFGE will be applied to track the Wld^S inheritance in those mice. This project is carried out by Dr. Robert Adalbert, who I have trained in the PFG technique.

5) Crossing SOD1 with Wld^S

Amyotrophic lateral sclerosis (ALS) is a late-onset neurodegenerative disease involving upper and lower motoneurons. Approximately 15% of the total number of ALS cases are familial (FALS), and of these, ~20% are attributable to point mutations in cytosolic Cu/Zn superoxide dismutase (SOD1) (Deng *et al*, 1993; Pardo *et al*, 1995). Transgenic mice expressing high level of one of three FALS-associated SOD1 mutants (G93A) under the control of a human SOD1 minigene (hMg) were crossed with Wld^S to investigate whether Wld^S could rescue the axon loss in this mice model of late-onset ALS-like motoneuron disease. Such experiments are carried on in our collaborator's lab in US (Jonathan Glass). Again, our genotyping method (PFGE) will be applied to distinguish the Wld^S from $Wld^{+/+}$ and Wld^S-heterozygous from Wld^S-homozygous.

6) Crossing *Smn* mutants with *Wld*^{S}

Mutations of survival of the motor neuron gene (*SMN1*) are responsible for spinal muscular atrophy (*SMA*), a common genetic cause of death in childhood. Mice carrying a homozygous deletion of *Smn* exon 7 directed to neurons (*Smn* mutant mice) were generated in a collaborator's lab in France (Judith Melki). These mutant mice display a dramatic and progressive loss of motor axons involving both proximal and terminal regions, with aberrant cytoskeletal organization of synaptic terminal, thus *Smn* mutant mice represent a valuable model of SMA. To test whether *Wld*^{S} could rescue such axonal loss in *Smn* mutant mice, these mutants were crossed with *Wld*^{S} and Southern blotting was applied to genotype *Wld*^{S}. In this experiment it is only necessary to identify *Wld*^{S} heterozygotes so the *EcoR*V genotyping method is used.

7) Generation of CFP/*Wld*$^{S/S}$ double homozygotes.

To facilitate examining the nerve terminals (such as axons and synapses) and NMJs (neuronal muscular junctions) in *Wld*^{S} and thus give us the hints of the mechanism of Wallerian degeneration, Richard Ribchester's lab in Edinburgh generated CFP/*Wld*$^{S/S}$ double homozygotes mice. Again, genotyping method (PFGE) was applied to confirm *Wld*^{S} genotype in our lab, which was done by Arzu Celik, following training from myself.

8) Confirmation of mouse imports and breeding colony maintenance.

Whenever the *Wld*^{S} mice were shipped to the lab from different sources, either from collaborators' lab or from Harlan Orlac, UK, we need to use genotyping method to confirm the presence of *Wld*^{S} in the genome. For the living mice, we used Southern blotting with the genomic extraction from mice tail tips, and for the postmortem samples, we use PFGE with spleen as a starting material (methods see 2.1.1 and 2.1.2). To maintain the *Wld*^{S} breeding colony, the same strategy also can be applied to either living or postmortem samples.

3.3 Discussion

We describe methods to determine the genotype of Wld^s using PCR, Southern-blotting or pulsed field gel electrophoresis (PFGE). PFGE is the only qualitative method to distinguish homozygotes from heterozygotes.

In the PCR assay, there is a Wld^s-specific product but given the nature of the mutation, it is not possible to design a PCR that yields a wild-type specific product. Therefore it is difficult to distinguish homozygotes from heterozygotes, or wild-type from false negative. The Southern blotting assay resolves this false negative problem because the constant wild-type band acts as an internal control. It also resolves the homo/heterozygotes problem to some extent because this can be determined from the relative strength of Wld^s-specific band and the constant band. However, we do not recommend this quantitative approach for genotyping for experiments where it is important to distinguish homozygotes from heterozygotes, as the result could be affected by artifacts such as Southern blotting efficiency and partial digestion. The pulsed field gel electrophoresis method is based on altered fragment size rather than altered fragment intensity and is therefore more reliable. However since spleen is the usual starting material in order to yield enough high molecular weight DNA from a soft tissue, this determination will usually have to be made post-mortem. In cases where the mouse is perfused, it is clearly important to remove the spleen or a fragment of it before fixation.

Determination of genotype of Wld^s has become more important after the identification of the protective gene, the $Ube4b/Nmnat$ chimeric gene within tandem triplication in Wld^s (Mack et al, 2001; Conforti et al, 2000). The possibility of Wld^s preventing axon degeneration in diverse pathologies and its effect on the symptoms should now be actively investigated by crossing Wld^s with neurodegenerative mutants in which axon degeneration plays a primary or early secondary role. By reporting several genotyping protocols and discussing their relative merits we make it possible to follow inheritance of the Wld^s chromosome in such studies. Genotyping can now also be used to confirm the Wld^s strain when breeding or shipping mice.

Figure 3.1 Tandem triplication schematic diagram model. Probe GS11 was used in Southern blotting. Probe 2 was used in pulsed-field gel electrophoresis. The restriction cutting cites for *Not*I (N) and *EcoR*V (E) were indicated. WldF and WldR were primers used in PCR.

Figure 3.1

C57BL/6J

C57BL/*Wld*ˢ
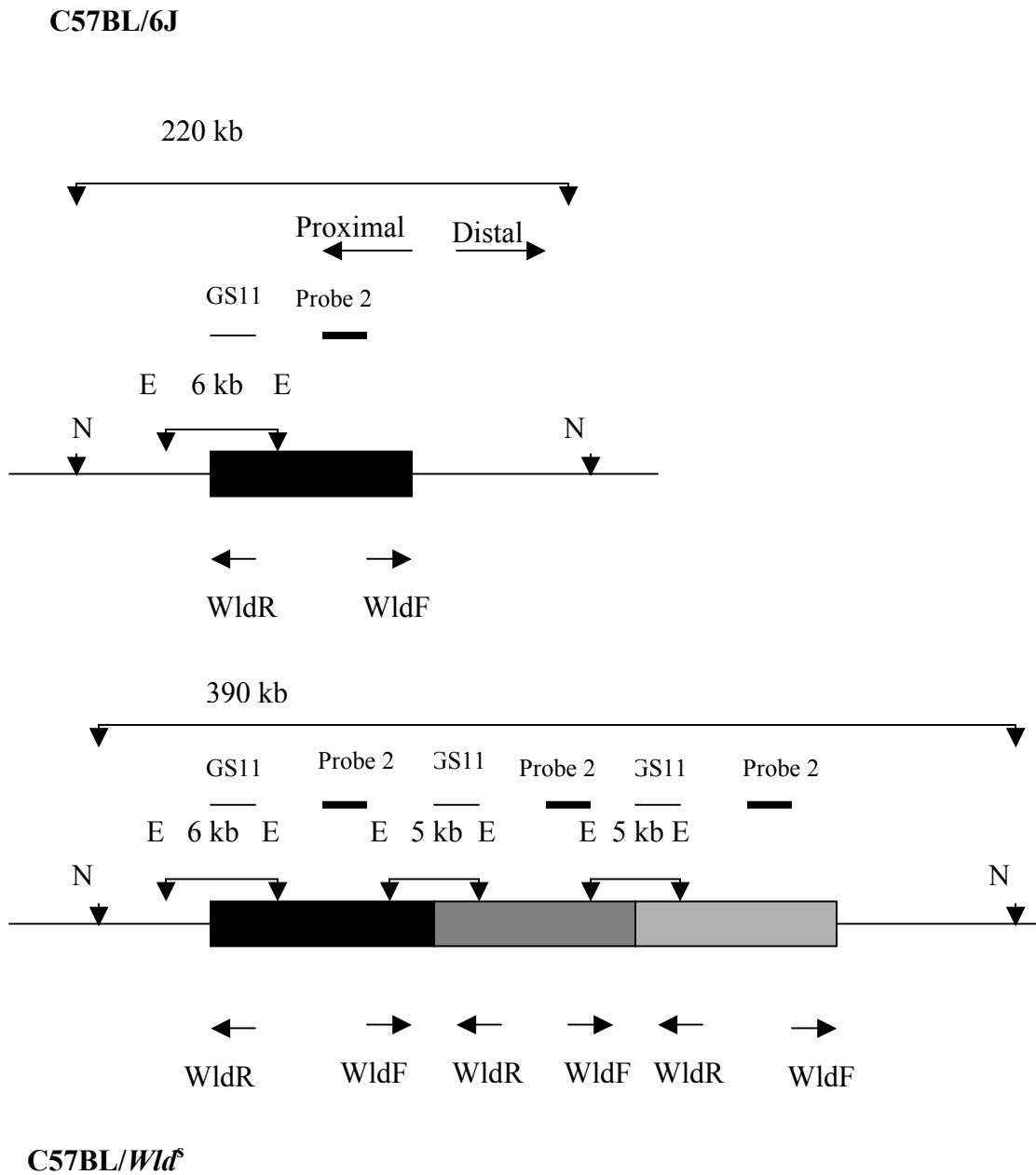
Figure 3.2 PCR showing the detection of a 182 bp *Wld*^{s}-specific band in *Wld*^{S} homo- and heterozygotes, but not in C57BL/6J.

Figure 3.3 Southern blotting showing the detection of 6 kb constant band in wild type (C57 BL/6J) and *Wld*^{s}, plus a 5 kb *Wld*^{s}-specific band. Probe used for Southern blotting is GS11 (see the localization of probe in Figure 3.1). Lane 1-2: C57BL/6J samples; lane 3-4: *Wld*^{S} heterozygous; lane 5-6: *Wld*^{S} homozygous.

Figure 3.4 Pulsed-field gel analysis of C57BL/*Wld*^{s} and C57BL/6J genomic DNA digested with *Not*I. Probe 2 was used in this assay and located centrally within the repeat unit (see the localization of probe in Figure 3.1).

Figure 3.2

6J1 6J2 *Wld*^s/+ *Wld*^s/+ *Wld*^s/s *Wld*^s/s

500 bp

200 bp

WldF + WldR

Figure 3.3

6 Kb
5 Kb

Figure 3.4

6J1   6J2   *Wld*^s/s *Wld*^s/s *Wld*^s/+ *Wld*^s/+

388 Kb

220 Kb
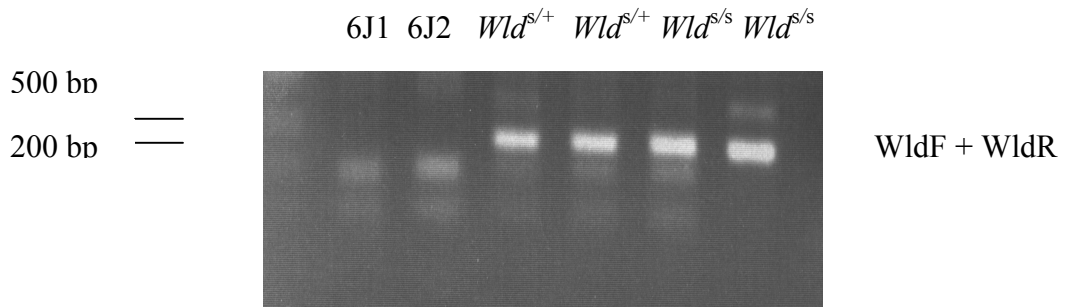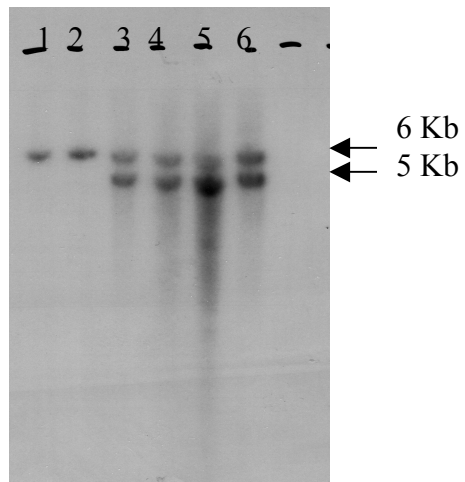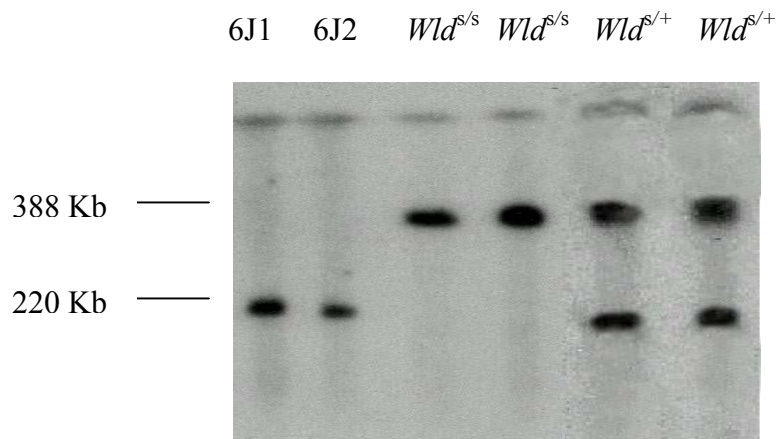
Figure 3.5 Schematic representation of numbers of axons in plantar (A) and median (B) nerves of 3-month-old $P0^{+/+}$ and $P0^{-/-}$ mice with or without the Wld^S mutation. Note that the Wld^S mutation has no influence on axon numbers in $P0^{+/+}$ genotypes. However, in $P0^{-/-}$ mice, loss of axons is significantly reduced in mice carrying the Wld^S mutation. ***$p<0.0001$; **$p<0.002$; *$p<0.05$. n, number of individuals of the respective genotype investigated. hom, Homozygous; het, heterozygous.

Figure 3.5

A Plantar nerve
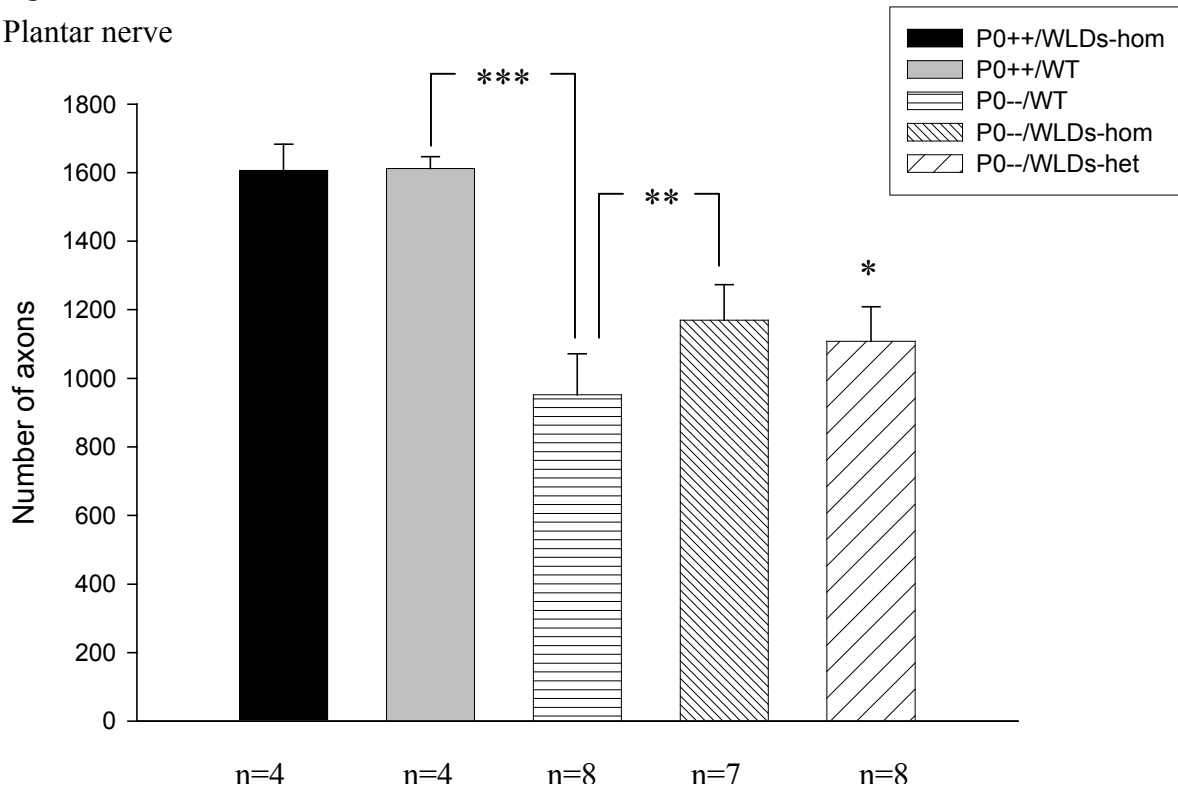
B Median nerves
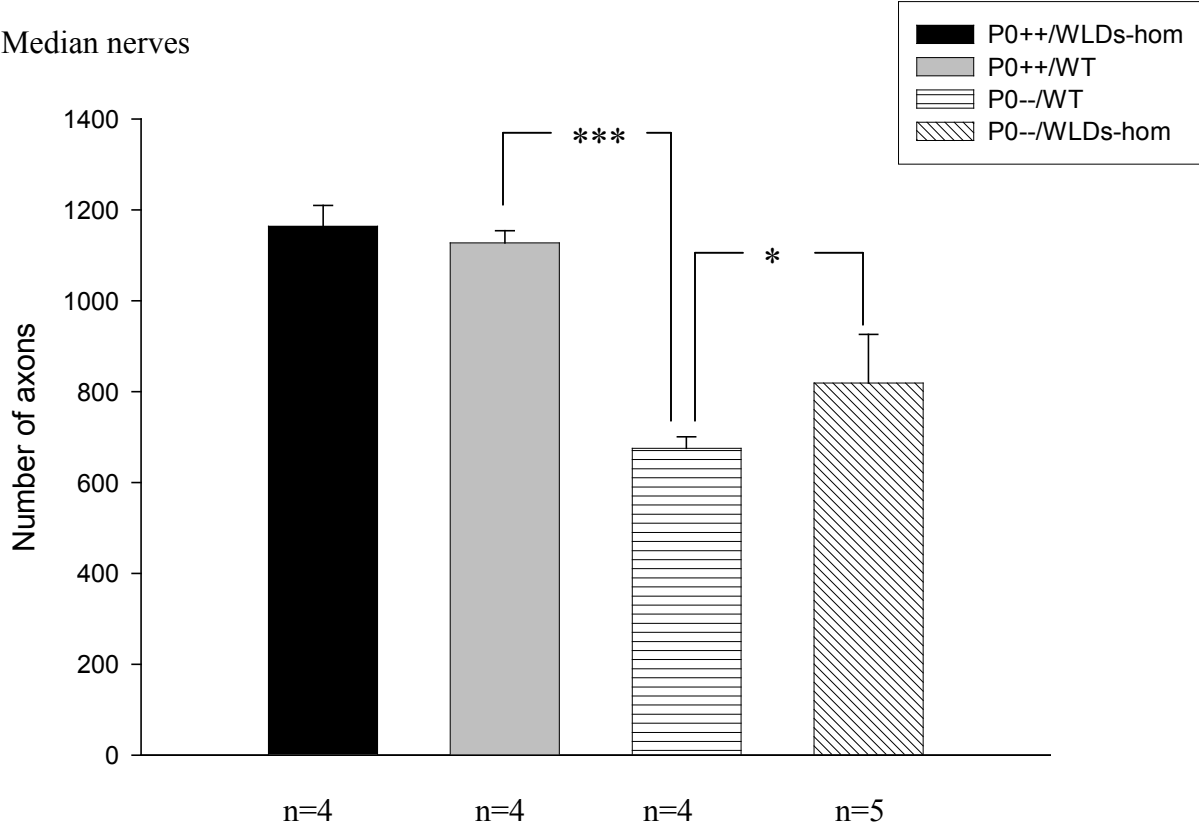
Figure 3.6a Schematic representation of amplitudes of compound action potentials from small foot muscles of 3-month-old $P0^{+/+}$ and $P0^{-/-}$ mice with and without the Wld^S mutation on distal stimulation of sciatic nerves. Note that the Wld^S mutation has no influence on amplitudes in $P0^{+/+}$ genotypes. Amplitudes are markedly reduced in the absence of P0 ($P0^{-/-}$), but reduction is less pronounced in the myelin mutants carrying the homozygous Wld^S mutation. Amplitudes from $P0^{-/-}$ mice heterozygous for the Wld^S mutation show a slight trend toward higher values compared with $P0^{-/-}$ single mutants. ***p<0.0001 and *p<0.05. n, Number of individuals of the respective genotype investigated.

Figure 3.6b Schematic representation of retrogradely labeled spinal motoneurons of 3-month-old mice using Fluorogold. $P0^{-/-}$/WT mice show a significantly lower number of back-labeled spinal (lumbosacral) motoneurons than $P0^{+/+}$/WT mice (*p<0.05). In 3-month-old $P0^{-/-}$/Wld^S double mutants, however, the number of labeled motoneurons is as high as in $P0^{+/+}$ mice, indicating a significant preservation of $P0^{-/-}$ motor axons on Wld^S expression. n, Number of individuals of the respective genotype investigated. WT, wild type; *hom*, homozygous; *het*, heterozygous.

Figure 3.6

a
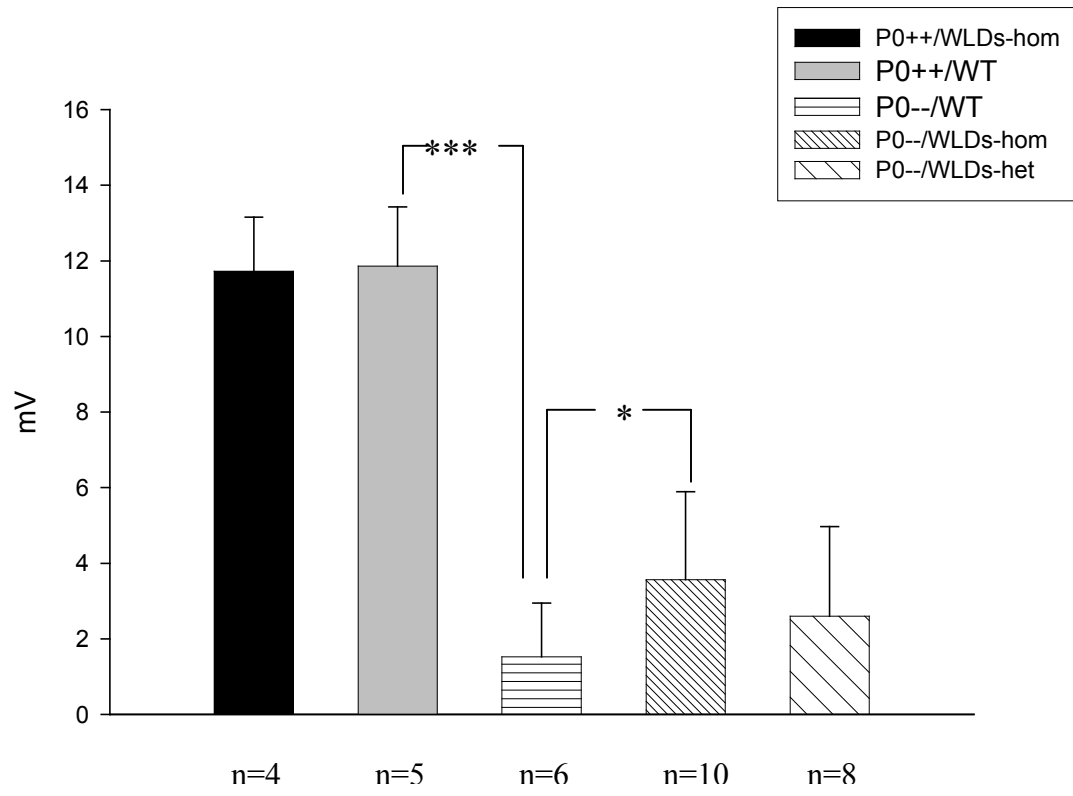
Figure 3.6

b.
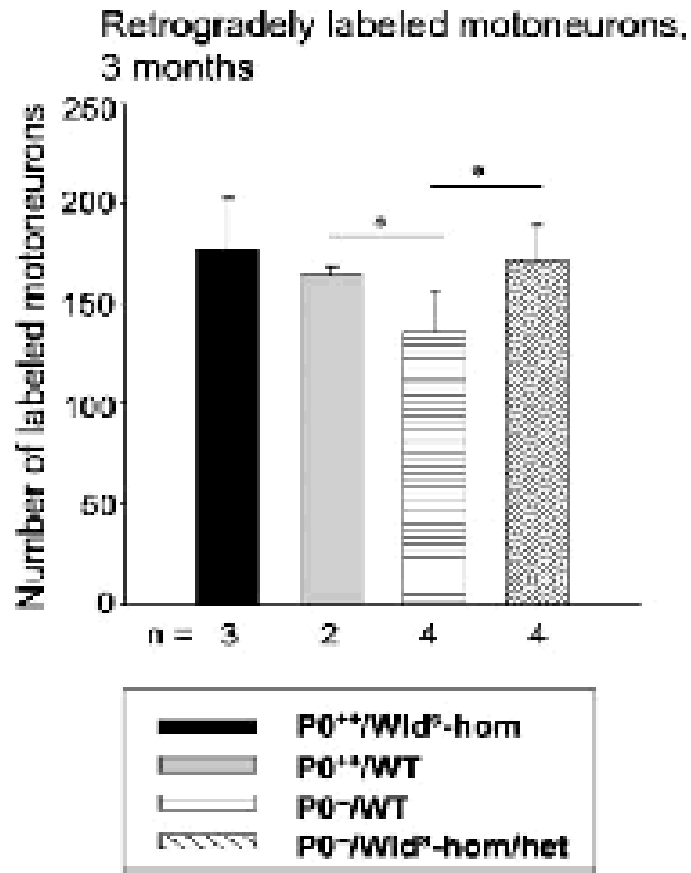
Figure 3.7 Schematic representation of muscle strength (grip test of forelimb) of $P0^{+/+}$ and $P0^{-/-}$ mice (3 months of age) with and without the Wld^S mutation. The Wld^S mutation has no influence on muscle strength in $P0^{+/+}$ genotypes. Muscle strength is strongly reduced in $P0^{-/-}$/WT mice, but reduction is less pronounced in $P0^{-/-}$/Wld^S-homozygous mutants. Muscle strength of $P0^{-/-}$ mice carrying a heterozygous Wld^S mutation show a small, non-significant trend toward higher values compared with $P0^{-/-}$ single mutants. ***$p<0.0005$; *$p<0.05$. n, Number of individuals of the respective genotype investigated. WT, wild type; hom, homozygous; het, heterozygous.

Figure 3.7
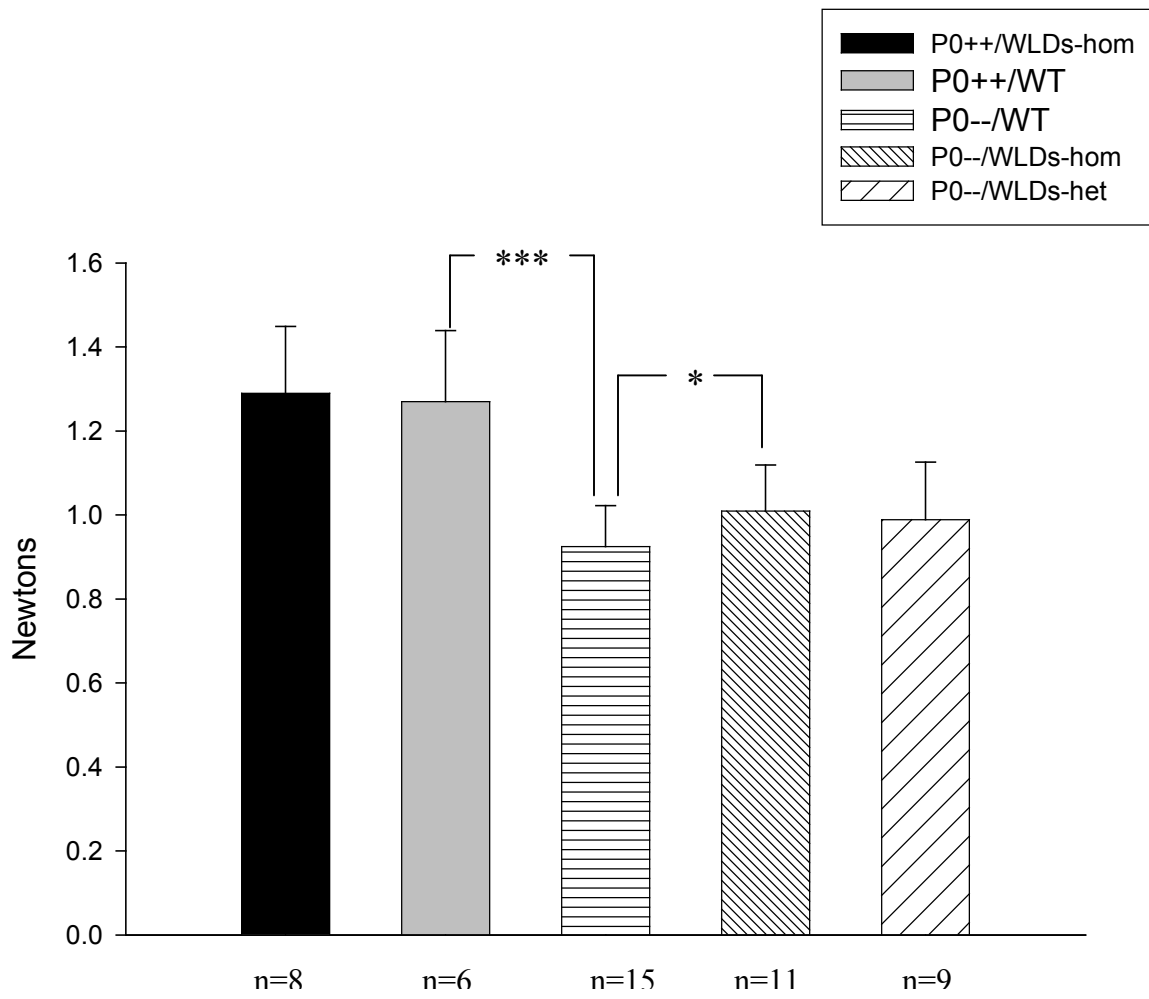
Figure 3.8 Western blot analysis of young versus old P0$^{-/-}$/Wld^S double mutants. Lumbar spinal cord (*SPC*) and lumbar (L4 – L5) dorsal root ganglia (*DRG*) homogenates of 6-week-old versus 6-month-old P0$^{-/-}$/Wld^S double mutants show a similar Wld^S expression (Wld^S). Transgenic (Tg Wld^S) Wld^S and wild-type lanes show that the observed band is specific for Wld^S mice. ß-Tubulin (ß-Tub) expression in spinal cord and dorsal root ganglia homogenates are shown as controls. Hom, Homozygous.

Figure 3.8 Western blot analysis of young versus old P0$^{-/-}$/Wld^S double mutants.
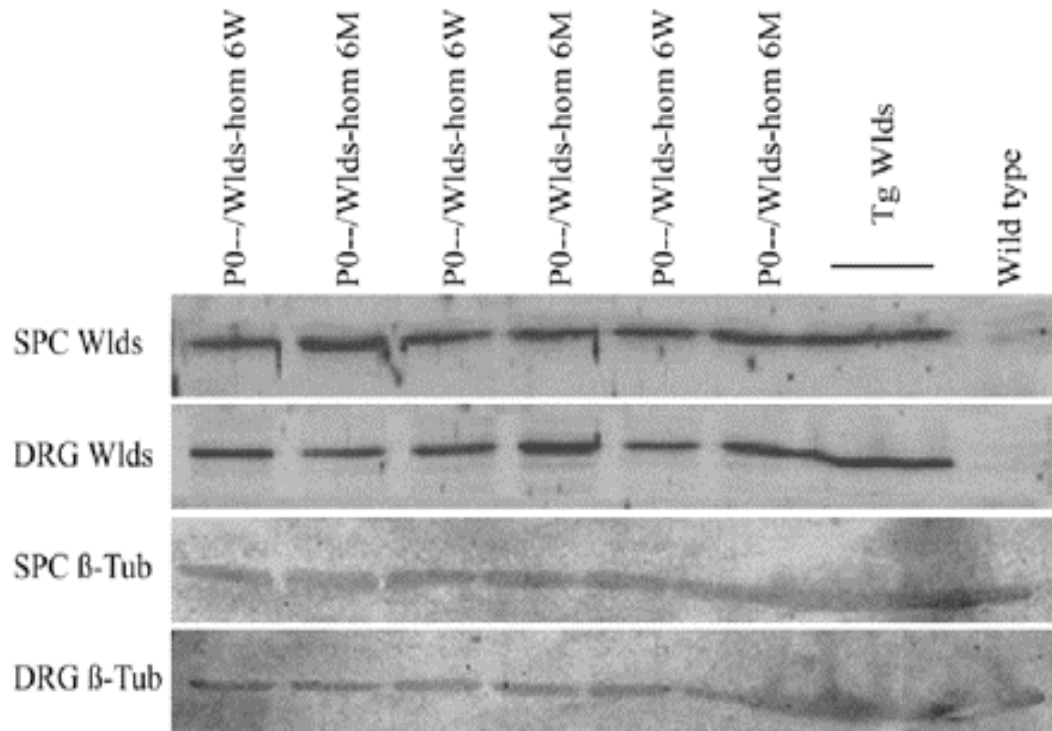
CHAPTER 4

THE 85-kb TRIPLICATION IN C57BL/*Wld*^{S} IS STABLY

INHERITED

4.1 Introduction

Two duplication cases have been identified before in mice bred in the Department of Physiology, University of Oxford in 1996 and 1997 (Coleman *et al*, 1998)(Figure 4.1b) and the tandem triplication in the *Wld*^{S} mouse is very likely to have developed from duplication by homologous, but unequal, crossing-over between tandem head-to-tail repeated DNA sequences (Figure 4.2)(Jeffreys *et al*, 1988; Tartof, 1988) (see details in section 1.3). The duplication-triplication instability could have been a single event, or there could be a dynamic equilibrium between two repeats and three repeats, especially considering the large homologous regions available for recombination, and thus reversion. In addition diverged breeding colonies of *Wld*^{S} have been suggested to have different phenotypic properties (Crawford *et al*, 1995) and one possible explanation proposes that the mutation is not the same. Furthermore, given the dose-dependence of the *Wld*^{S} phenotype (Mack *et al*, 2001), it is important to determine whether all *Wld*^{S} mice carry the same gene dosage or whether they are highly variable. Somatic reversion would also have the possibility to explain the observed reduction in phenotype with age (Perry *et al*, 1992), so it is important to study the mutation in old mice as well. To answer these questions, I carried out a genomic instability study in *Wld*^{S} mouse using pulsed field gel electrophoresis assay (Mi *et al*, 2002). Chromosomes from three diverged breeding colonies were examined, together with chromosomes from aged mice.

4.2 Result

4.2.1 Sources of Wld^S tissues.

C57BL/*Wld*^{S} spleens were obtained from three diverged breeding colonies (Table 4.1):

(1) Harlan-Olac, Bicester, UK, which is the parent colony. Some mice were F1 or F2 from breeding stock derived from Harlan-Olac.

(2) Johns Hopkins Laboratories. This breeding colony was established from the Harlan-Olac colony in 1989 using four breeding pairs and has been maintained separately since then.

(3) Biosonda, Santiago, Chile. This breeding colony was established from the Harlan-Olac colony in 1996 using 4 males and 12 females and maintained separately.

Other breeding colonies, e.g., those originally set up at Edinburg, UK, and Kingston, Canada appeared to have been discontinued. This was also the case for that at the Department of Physiology, Oxford, UK, where the duplication allele was previously observed. Four mice directly from Harlan-Olac were aged to 12 months before genotyping their spleens and three were aged to 15 months. Spleens were stored at -80°C until use.

4.2.2 Stable inheritance of an 85-kb triplication in C57BL/Wld^S.

A total of 132 Wld^S chromosomes from homozygous and heterozygous Wld^S mice no more than two generations beyond those, originally obtained from Harlan-Olac were examined using pulsed field gel electrophoresis (see details in section 3.2.1). The original duplication result was confirmed but there was no clear sign of a duplication allele in the recently obtained Wld^S mice (Figure 4.1). Similarly, no quadruplications were observed, which could be the predicted reciprocal product of partial reversion. Although we cannot rule out a low rate of somatic reversion in the spleen due to the detection limit of pulsed field gel assay, results from these 132 Wld^S chromosomes strongly indicate that occurrence of the duplication allele is a very rare event (Table 4.1).

In order to investigate whether somatic reversion might occur in older mice, we studied an additional 6 chromosomes of 15 month old mice and 8 chromosomes of 12 month old mice. Again, only the triplication allele was observed (Figure 4.1a; Table 4.1), indicating that somatic reversion in spleen is unlikely.

Although these data indicate that the triplication / duplication rearrangement is very rare, it is still important to know the genotype of other Wld^S breeding colonies, in order to facilitate the comparison of results from different breeding colonies. Therefore, in order to test whether the duplication allele might exist in those colonies, we genotyped mice from current breeding colonies that are diverged from Harlan-Olac. 16 Wld^S chromosomes of mice from the Johns Hopkins colony and 18 Wld^S chromosomes of mice from Biosonda, Chile showed only triplication (Figure 4.1; Table 4.1).

In total 180 chromosomes of Wld^S from 3 divergent breeding colonies have been examined and all found to carry the triplication. Thus the triplication mutation is stable during both mitosis and meiosis, and the previously observed duplication is likely to have been surviving alleles of the original mutation rather than a partial reversion. The

triplication has now been shown to be the causative mutation, acting through an *Ube4b/Nmnat* chimeric gene (Mack *et al*, 2001), indicating the possibility of Wld preventing axon degeneration in diverse pathologies and altering the symptoms. The fact that triplication is stable rules out instability as a source of phenotypic variation. Thus this result is essential for accurate interpretation of studies the effect of Wld^S on neurodegenerative phenotypes. It is necessary to track Wld^S inheritance ($Wld^{+/+}$, or $Wld^{+/S}$, or $Wld^{S/S}$) when crossing Wld^S with mice model of neurodegenerative diseases, such as $P0^{-/-}$ and *gad* (see details in section 3.2.2), thus the drawing conclusion of stable inheritance of triplication in Wld^S will facilitate the evaluation of such studies.

Conclusions: all current Wld^S is triplication. Any reversion rate is extremely low; much lower than comparably-sized mammalian duplications such as pink-eyed unstable mutation (Gondo *et al*, 1993).

4.3 Discussion

Results from 180 Wld^S chromosomes of mice from 3 diverged breeding colonies indicate that the rate of occurrence of duplication in Wld^S mice is very low. Thus, we conclude that the Wld^S triplication is stable under normal conditions and that it is the predominant, and possibly exclusive, allele in the current Wld^S breeding colonies.

Wld^S is thus more stable than some other rearrangements of comparable size in mammals, such as the pink-eyed unstable mutation (p^{un}). It would be interesting to know whether mutagenic treatment such as radioactivity or carcinogens would make it less stable, as it is the case with pink-eyed (Schiestl *et al*, 1994; Schiestl *et al*, 1997).

We did not find any duplication in aged mice (1 year or more) also, which suggests that the "different mutation" theory (e.g., triplication reverts to duplication) does not underlie observed differences in age effect (Crawford *et al*, 1995) and further supports stability during mitosis as well as during meiosis. This is further supported by the observation that there are no age-dependent changes in expression level of the Wld^S protein (Gillingwater *et al*, 2002; Samsam *et al*, 2003). While we cannot rule out other genetic explanations, the observed difference in age-effect is more likely to be explained by different experimental approaches.

Results from 3 breeding colonies do not show any duplication, suggesting that the parent colony (Harlan-Olac, UK) must have been predominantly triplication as far back as 1989. The alternative explanation that the triplication arose and became fixed independently in three different breeding colonies seems unlikely. The duplication alleles identified in mice bred in the Department of Physiology, University of Oxford in 1996 and 1997 were probably persisting original duplication mutations that are now extinct. However, we cannot rule out the possibility that a single rare meiotic partial reversion occurred in this subline. Somatic instability occurring independently in the two respective mice, however, now seems extremely unlikely, given the far greater number of mice studied in the present paper without signs of somatic instability.

Finally, the fact that the triplication is stable rules out instability as a source of phenotypic variation. It is important to know this for studies addressing the effect of Wld^S on neurodegenerative phenotype.

Table 4.1 Triplication results of Wld^S chromosomes examined by PFGE

	Mice origin (source of breeding colony)	Wld^S chromosomes No.	Results	
			Triplications No.	Duplications No.
1a	Harlan-Olac, U.K.	132	132	0
1b	Harlan-Olac, U.K. 12 months old	8	8	0
1c	Harlan-Olac, U.K. 15 months old	6	6	0
2	Johns Hopkins. USA (diverged from Harlan-Olac)	16	16	0
3	Biosonda, Chile (diverged from Harlan-Olac)	18	18	0
Total		180	180	0

Figure 4.1a Pulsed field gel analysis of C57BL/*Wld*^S chromosomes from 3 diverged breeding colonies. Probe located within triplication detected a single fragment of approximately 390 kb in C57BL/*Wld*^S, a fragment of 305 kb in duplication allele and a fragment of 220 kb in C57BL/6J wild type mouse. a) three samples (1-3) from Harlan-Olac, Bicester, UK. b) three samples (4-6) from Johns Hopkins Laboratories. c) three samples (7-9) from Biosonda, Santiago, Chile. d) three samples (10-12) from older mice (12 months). e) one sample from C57BL/6J and one from the Department of Physiology, Oxford, UK, where the duplication allele was previously observed.

Figure 4.1b Identification of 170- kb (triplication) and 85-kb (duplication) insertions in C57BL/*Wld*^S from breeding colonies in Department of Physiology, Oxford (Coleman *et al*, 1998). WldA is representative of five of seven DNAs analyzed, whereas WldC and WldD were unique. Probe located centrally within the repeat unit. 1: WldA; 2: C57BL/6J; 3: WldC; 4: C57BL/6J; 5: WldD.

Figure 4.1a

388 kb

305 kb

220 kb
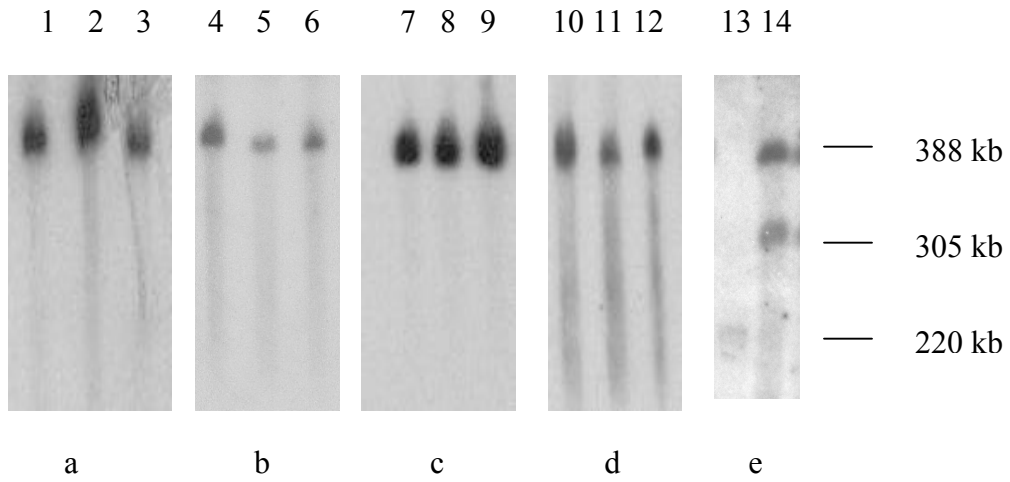
Figure 4.1b

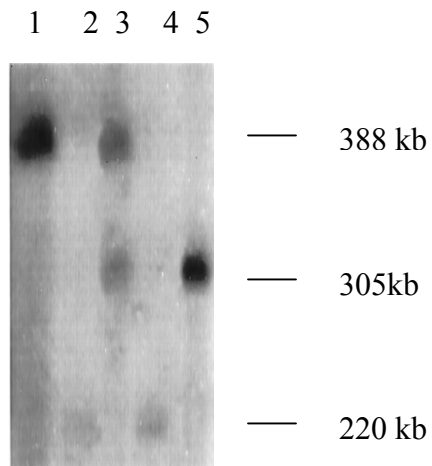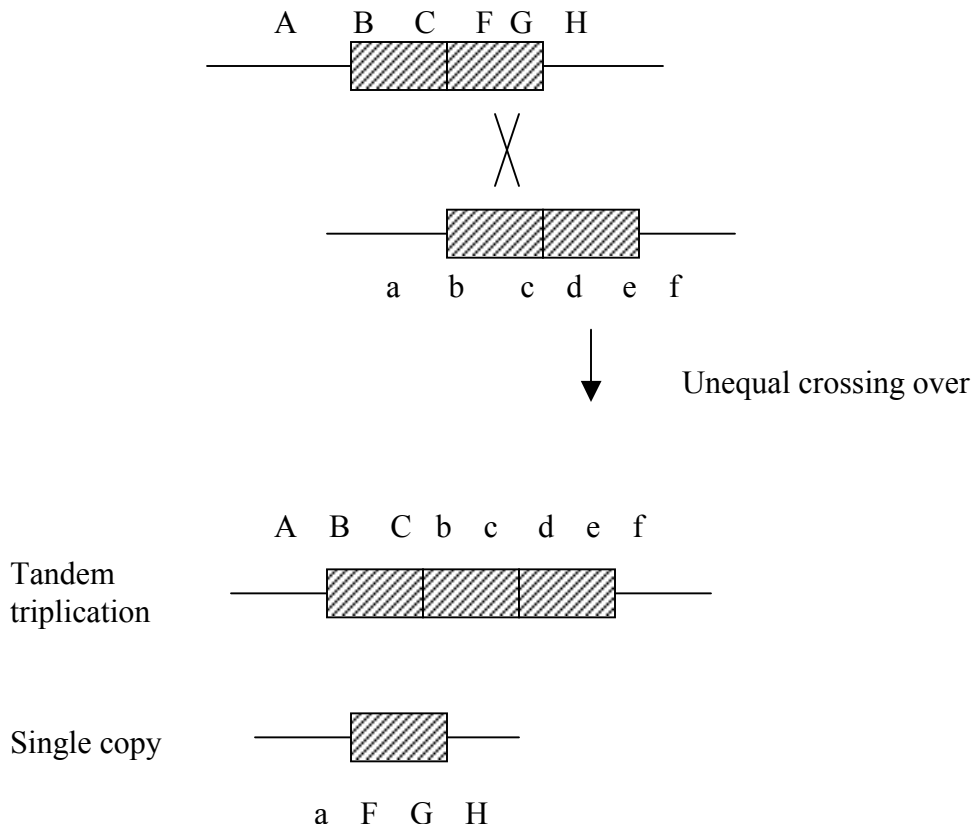Figure 4.2 Unequal crossing-over between tandem head-to-tail repeated DNA sequences

produces one copy and tandem triplication respectively.

Figure 4.2

A   B   C   F G   H

a   b   c   d   e   f

Unequal crossing over

A   B   C   b   c   d   e   f

Tandem
triplication

Single copy

a   F   G   H

CHAPTER 5

THE *Wld*^{S} MUTATION REDUCES AXONAL SPHEROID

PATHOLOGY IN GRACILE AXONAL DYSTROPHY (*gad*) MICE

5.1 Introduction

The gracile axonal dystrophy (*gad*) mouse is an autosomal recessive mutant characterized by 'dying-back' axonal degeneration and formation of spheroid bodies primarily in the gracile tract (Yamazaki *et al*, 1988; Saigoh *et al*, 1999). The gracile tract consists of thoracic, lumbar and sacral DRG axons that travel up the dorsal column of the spinal cord within the gracile fascicle, where they terminate in the medulla oblongata within the gracile nucleus. The *gad* mutation is an in-frame deletion of *Uch-l1*, and disrupts Uchl1's function in generating free monomeric ubiquitin and thus its essential role in continuing the function of the proteasome-ubiquitin system (Saigoh *et al*, 1999).

Axonal spheroids morphologically and immunochemically similar to those of *gad* mice also occur widely in CNS neurodegenerative pathology, including myelin disorders (Griffiths *et al*, 1998), tauopathies (Lewis *et al*, 2000; Probst *et al* 2000), ALS (Tu *et al*, 1996; Oosthuyse *et al*, 2001; Howland *et al*, 2002), traumatic brain injury (Cheng and Povlishock, 1988), Alzheimer's disease (Brendza *et al*, 2003), Parkinson's disease (Galvin *et al*, 1999), Creutzfeldt-Jakob disease (Liberski *et al*, 1999) and Niemann-Pick disease (Bu *et al*, 2002). They also occur during normal ageing and secondarily in some serious illnesses (Sung *et al*, 1981). In contrast, PNS axons undergo 'Wallerian-like' or 'dying-back' degeneration, even in the same disease such as *gad* in mouse and human ALS and Alzheimer's disease (Miura *et al*, 1993; Oosthuyse *et al*, 2001; Lewis *et al*, 2000), although swellings occur in some rare PNS disorders (Miike *et al*, 1986; Bomont *et al*, 2000).

Spheroids are focal 10-50 μm diameter swellings, filled with disorganized neurofilaments, tubules, organelles or multi-lamellar inclusions, mostly in long axons. In 'dying-back' disorders they predominate in distal axons, appearing further proximal with increasing age (Mukoyama *et al*, 1989; Bu *et al*, 2002), whereas proximal spheroids occur in spinal cord motor neurons of ALS patients and mouse model (transgenic mice carrying a human mutant SOD1) (Tu *et al*, 1996), and spinal cord of transgenic mice overexpression of human four-repeat tau with tauopathy (Probst *et al*, 2000) (Figure 5.9). Most spheroids contain neurofilament and amyloid precursor proteins, and sometimes ubiquitin, tau or synuclein.

The role of axonal spheroids in disease is poorly understood. Although a common axonal response to diverse insults, spheroids could arise by disease-specific mechanisms. Although manifestations of axon degeneration, they could also contribute, impairing axonal transport to and from more distal sites. Distal and proximal spheroids might arise by related mechanisms or distal spheroids could originate distinctly as 'dying back' axonal endbulbs. Why spheroids are rarer in PNS pathology, and whether preventing them in CNS preserves axon function is unknown. These questions could be addressed if a method to prevent or delay spheroids were available.

Wld^S can protect axons from vincristine toxicity *in vitro* (Wang *et al*, 2001)*,* and delay axon loss and symptom in diverse PNS disorders, such as myelin-related peripheral neuropathy (in the *P0*$^{-/-}$ mouse)(Samsam *et al*, 2003; section 3.2.2) and progressive motor neuronopathy (in the *pmn* mouse)(Ferri *et al*, 2003; section 3.2.2) *in vivo*. Since the *gad* mouse is the first mammalian model of neurodegeneration with a defect in the ubiquitin system and with dying-back type degeneration with formation of spheroids as primary defect (gracile tract) in CNS, crossing gracile axonal dystrophy (*gad*) with *Wld*^S will provide important information on: 1) whether *Wld*^S could have an effect on axonal spheroids in CNS; 2) whether the mechanism of Wallerian degeneration, dying-back axonal degeneration and axonal spheroid pathology are related, which would be crucial to the pathogenesis of some neurodegenerative disease characterized with dying-back degeneration.

5.2 Result

5.2.1 *Wld*^S can function to protect axons in *gad* mice

gad causes axon degeneration through defective ubiquitin metabolism (Osaka *et al*, in press), while *Wld*^S protects axons probably through a ubiquitin-related mechanism too, such as N-terminal 70 amino acids of Ube4b sequestering of ubiquitination factors by protein-protein interactions and ubiqutination within nucleus altering transcription factor stability or RNA processing, leading to an axon effect mediated by unknown protein (Mack *et al*, 2001; Coleman and Perry, 2002). In order to test for direct antagonism between *gad* and *Wld*^S and to show that *Wld*^S delays Wallerian degeneration in the presence of *gad*, we transected sciatic nerves before onset of hindlimb weakness in two

gad homozygotes that were heterozygous for Wld^S. These mice also carried a YFP-H transgene (Feng *et al*, 2000) to allow a rapid assessment of Wallerian degeneration (Beirowski *et al*, submitted). No degradation of heavy neurofilament protein could be detected in distal sciatic nerves five days after nerve lesion (Figure 5.2a) and all YFP-labeled axons were unfragmented (Figure 5.2b) compared to total fragmentation at 52 hours in non-Wld^S mice (Beirowski *et al*, submitted). The Wld^S phenotype is highly dose-dependent (Mack *et al*, 2001) so the complete preservation of axons for five days in a Wld^S heterozygote convincingly demonstrates that *gad* does not significantly weaken the Wld^S phenotype. Thus it is feasible to test the effect of Wld^S on *gad* pathology and likely that Wld^S and *gad* are not directly antagonistic.

5.2.2 Genotyping of *gad* and Wld^S status.

In the following text, $gad^{+/+}$, $gad^{+/-}$ and $gad^{-/-}$ refer to wild-type, heterozygous and homozygous *gad* mice respectively. Crossing $gad^{+/-}$ with $Wld^{S/S}$ results in exclusively $Wld^{+/S}$, so double heterozygous mice ($gad^{+/-}/Wld^{S/+}$) could be identified by genotyping for *gad* as described below and intercrossed. Before any further behavioral and pathological analysis of *gad* homozygotes amongst the offspring ($gad^{-/-}/Wld^{S/S}$, $gad^{-/-}/Wld^{S/+}$, $gad^{-/-}/Wld^{+/+}$), a method is needed to genotype the *gad* status.

Genomic DNA extracts from tail tips from 3-4 week-old mice were digested by *Pvu*II at 37˚C overnight, and run on 1 % TAE gel overnight. DNA on the gel was Southern-blotted overnight onto Hybond N+ (Amersham) in 0.4 M NaOH. It was then hybridized with a ^{32}P labeled 764 bp probe generated by PCR from *gad* homozygous genomic DNA using primers 5' ATCCAGGCGGCCCATGACTC 3' and 5'AGCTGCTTTGCAGAGAGCCA 3'. The *gad* mutation is caused by an in-frame deletion of exon 7 and exon8 (3.5 kb of genomic DNA) of *Uchl1* (Figure 1.4), so a 764 bp *gad*-specific probe (Saigoh *et al*, 1999) could detect 726 bp *gad*-specific fragment in *gad* homozygote, ~1.6 kb wild type specific fragment in *gad* wild type, and both fragments in *gad* heterozygote (Figure 5.1). $gad^{+/-}/Wld^{S/+}$ were selected for intercrossing, and the resulting $gad^{-/-}$ (with or without Wld^S) were chosen for further behavioral and pathological analysis.

The *Wld* status ($Wld^{+/+}$, $Wld^{S/+}$ or $Wld^{S/S}$) in $gad^{-/-}$ mice was genotyped postmortem by pulsed-field gel electrophoresis (see section 3.2.1).

5.2.3 Axonal spheroid pathology is reduced by Wld^S

In order to determine the effectiveness of Wld^S on *gad* axonal spheroid pathology, I counted axonal spheroids in approximately 90 H&E stained 6 μm paraffin sections from throughout the gracile nucleus and 30 sections from throughout the cervical spinal cord of each 18-week old *gad* mouse and *gad*/Wld^S double homozygote. 50% fewer spheroids were found in gracile nucleus of *gad*/Wld^S mice than in *gad* mice (p=0.0004) and 63% fewer in cervical gracile fascicle (p=0.0011) (Figure 5.3). These highly significant reductions indicate a strong protective effect of Wld^S that lasts well into late-stage disease. Intermediate values were observed in Wld^S heterozygotes, further supporting the result. No spheroids were observed in control animals of this age (data not shown).

A reduction in the number of axonal spheroids could result theoretically from either reduced axon pathology or pathology so extensive that the axons are completely destroyed. However, when *gad* pathology is made worse by crossing with *Uch-l*3 null mice, extensive axon pathology with a significant increase in the number of spheroids becomes detectable at more caudal locations in cervical and thoracic gracile fascicle when compared with *Uch-l1*^{gad} single homozygotes (Kurihara *et al*, 2001). We did not observe this, and Wld^S homozygotes maintain a rostral-caudal gradient of axonal spheroid pathology, suggesting that *gad* remains a 'dying-back' pathology in Wld^S mice but that its progress is delayed.

5.2.4 Secondary myelin loss and astrocyte activation are reduced by Wld^S

To determine the integrity of axon-myelin units in *gad*/Wld^S mice, the density of luxol fast blue myelin staining was measured in two 6 μm poly-L-lysine coated paraffin sections from the gracile nucleus and two sections from the cervical spinal cord of each 18-week old *gad* mouse and *gad*/Wld^S double homozygote. Further evidence of a reduced loss of axon-myelin units in *gad*/Wld^S mice came from a significant reduction (p=0.018) in secondary myelin loss in cervical gracile fascicle in the same animals (Figure 5.4 a, b, c). A similar protective trend in the medulla oblongata did not reach statistical significance (p=0.059), probably due to the naturally weaker myelination in this region, but Wld^S clearly did not cause any deterioration so the reduction in axonal spheroid numbers (Figure 5.3) must reflect reduced pathology and not wholesale axon loss. It is difficult to conduct electrophysiology study in axonal tract of central nerve system,

however, as the rescued axons remain myelinated, they potentially retain normal conductance properties, at least in these locations. It is unlikely that Wld^S has any direct effect on myelin because expression of Wld^S in glia does not alter Wallerian degeneration (Glass *et al*, 1993). Thus reduced myelin loss in *gad*/Wld^S mice is likely to reflect the maintenance of functional axon-myelin units.

Increased immunostaining by GFAP has also been reported in *gad* mice, reflecting astrocyte activation in response to axon damage (Yamazaki *et al*, 1988). We quantified this in *gad*/Wld^S mice and found it to be significantly reduced (p=0.015) in gracile nucleus compared to *gad* mice (Figure 5.4 d, e, f), with a non-significant trend in the same direction in cervical gracile fascicle (p=0.121). Thus, both direct and indirect measures of spheroidal axon pathology in the gracile tract are reduced by the Wld^S gene.

5.2.5 Behavioral changes due to Wld^S are complex

In the absence of any behavioral test to target specifically the gracile tract that contains the primary sensory central projections of dorsal root ganglion, we carried out several other tests to determine the effect of Wld^S on the general *gad* phenotype. No significant change was found in splay test or hindlimb clasping (Figure 5.6 and 5.7), but, paradoxically, the steady deterioration in Rotarod performance of *gad* mice was anticipated by 5.5 weeks in Wld^S homozygotes (Figure 5.5) and by 5 weeks in heterozygotes (data not shown). The statistical significance was greatest beyond 14 weeks (p=0.002 at 18 weeks when data for both homo- and heterozygous Wld^S are combined). This may reflect either failure of Wld^S to preserve motor nerve terminals in older mice or the fact that a constant difference becomes proportionately greater as performance declines. In parallel to the decline in Rotarod performance, mice began to drag their back legs during normal walking (not shown), indicating that progressive hindlimb paralysis, rather than any learning, balance or coordination defect underlies the poor Rotarod performance. All non-*gad* mice remained on the Rotarod for 300 seconds regardless of the presence of Wld^S (data not shown).

5.2.6 *gad*/Wld^S motor nerve terminals degenerate extensively by 15 weeks (done by collaborators Dr. Thomas Gillingwater and Dr. Richard Ribchester, University of Edinburgh)

The neuromuscular junction is an additional major site of pathology in *gad* mice (Miura *et al*, 1993) and having observed that developing hindlimb paralysis is the cause of falling from the Rotarod we examined neuromuscular junctions for evidence of altered endplate denervation in *gad*/*Wld*^{S} mice. Extensive denervation was observed in lumbrical muscles from 15 week old mice, even in the presence of *Wld*^{S} (Figure 5.8), as 53.5 ± 11.8% of endplates were at least partially denervated in *gad*/*Wld*^{S} mice and 32.3 ± 14.8% fully denervated (n=4). Thus, the reason why *gad*/*Wld*^{S} mice do not perform better in Rotarod than their *gad* littermates is likely to be that neuromuscular innervation is the limiting factor. However, we found a similar degree of denervation in *gad* without *Wld*^{S}, so the reason for the worse performance of *gad*/*Wld*^{S} remains unclear. One possibility is that delayed clearance of intramuscular nerve branches in *Wld*^{S} mice might delay a compensatory sprouting reaction. It remained possible that *Wld*^{S} might protect motor nerve terminals at younger ages, particularly as its ability to protect synapses after axotomy decreases dramatically with age: with 50%-90% of endplates partially or fully occupied after 5 days axotomy in 2-month-old *Wld*^{S} mice and with less than 5% of endplates occupied after 3 days axotomy in 7-month-old *Wld*^{S} mice (Gillingwater *et al*, 2002). However, at 9 weeks one *gad* mouse and one *gad*/*Wld*^{S} mouse showed almost no denervation (Figure 5.8 c and d) suggesting that there is little or no time window in which both *gad* and *Wld*^{S} exert their effects on the neuromuscular synapse. Our data differ from Miura *et al*. (1993), who reported extensive denervation at 9 weeks, perhaps because of the different staining methods employed or because of different genetic backgrounds of the mice. However, our data reveal two important points. First, protection of motor nerve terminals by *Wld*^{S} in a disease setting is weaker than its protection of axons, as spheroid numbers in gracile tract remained low in mice even three weeks older (Figure 5.3). This matches similar observations made in axotomy experiments. Second, the Rotarod deficiency in *gad* mice is more likely to be linked to denervation of neuromuscular junctions than to gracile tract pathology.

5.3 Discussion

Wld^S protection from axonal spheroids in *gad* is the first indication that *Wld*^{S} can alleviate axon pathology in chronic CNS disease, and indicates that *Wld*^{S} delays a central

step of axon pathology. Pathological mechanisms, whether initiated by defective ubiquitin metabolism or other degenerative stimuli (Lunn *et al*, 1989; Wang *et al*, 2002; Samsam *et al*, 2003; Ferri *et al*, 2003), converge on a step delayed by *Wld*[S] (Figure 5.11). Divergent pathological manifestations result, namely axonal spheroids in *gad*, Wallerian degeneration in injury models, and dying back axon loss without spheroids in peripheral neuropathy and motor neuronopathy. Alternatively, *Wld*[S] could alter multiple steps of axon pathology, but either way an unexpected mechanistic or regulatory relationship is revealed between axonal spheroids and Wallerian degeneration.

It is now essential to determine whether *Wld*[S] reduces axonal spheroids in other CNS diseases, where their occurrence is widespread. The mechanistic relationship between proximal spheroids in ALS, dystrophic axons in amyloid plaques and distal spheroids in *gad* can now be studied. The clinical implications of preventing spheroids in ALS, Alzheimer's disease, Parkinson's disease, brain trauma and CNS myelin disorders would be considerable, but more immediately, reducing spheroid pathology in animal models helps to understand the consequences of spheroid pathology. Further studies should also ask whether reducing axonal spheroid formation in *gad* or elsewhere translates into maintenance of axon function.

gad/Wld[S] mice suffered extensive synapse loss by 15 weeks (Figure 5.8) whereas axon pathology was still strongly reduced three weeks later (Figure 5.3). We could not study whether *gad/Wld*[S] synapses were protected in younger mice, where *Wld*[S] delays synapse loss after axotomy (Gillingwater *et al*, 2002), because consistent synapse pathology developed only later, even with *gad* alone. However, our data do indicate the importance of synapse loss for *gad* symptoms and suggest that synapse pathology contributes to the eventual decline in other models protected by *Wld*[S] (Samsam *et al*, 2003; Ferri *et al*, 2003). The data also support the hypothesis that different mechanisms underlie synaptic and axonal degeneration, with *Wld*[S] affording only limited protection to synapses (Gillingwater and Ribchester, 2001; Gillingwater *et al*, 2002).

A link between axonal spheroids, 'dying-back', and Wallerian degeneration is supported by previous observations. First, axons degenerate in a single disease with spheroids in the CNS and without spheroids in the PNS, indicating that CNS spheroid pathology and PNS 'dying-back' are related. In *gad* mice, this occurs even within the same cell, as gracile

tract central projections of lumbar primary sensory neurons have spheroids, while peripheral muscle spindles degenerate without swelling (Oda *et al*, 1992). Similarly, ALS in humans (Tu *et al*, 1996; Takahashi *et al*, 1997), mice (Tu *et al*, 1996; Oosthuyse *et al*, 2001) and rats (Howland *et al*, 2002), together with tauopathy in mice (Lewis *et al*, 2000; Probst *et al*, 2000), all show axonal spheroids in spinal cord and other CNS areas but extensive 'Wallerian-like' degeneration without spheroids in ventral roots and peripheral nerves. Second, 'dying-back' axonopathy and Wallerian degeneration are related, as Wld^S delays axon loss in Taxol toxicity (Wang *et al*, 2002), peripheral neuropathy (Samsam *et al*, 2003) and motor neuronopathy (Ferri *et al*, 2003). Our studies now complete the three-way relationship, with spheroids, 'dying-back' and Wallerian degeneration all delayed by a single mutation.

The striking contrast between the morphology of axonal spheroids and Wallerian degeneration makes these findings particularly surprising. However, even injury-induced Wallerian degeneration shows different morphology depending on experimental circumstances. First, when injured gracile tract axons undergo Wallerian degeneration they swell to spheroid-like dimensions quite unlike Wallerian degeneration in the PNS (George and Griffin, 1994)(Figure 5.10). Second, crush injury in the PNS causes a retrograde degeneration that is clearly distinct from degeneration induced by transection (Lunn *et al*, 1990) but these processes are related because both are delayed by Wld^S (Beirowski *et al*, unpublished data). Third, Wld^S nerve terminals degenerate differently according to their age, withdrawing gradually from young endplates but degenerating synchronously at older junctions (Gillingwater *et al*, 2002). Thus, differences in morphology in this field do not necessarily indicate totally distinct mechanisms.

It is intriguing how related mechanisms cause swelling in spheroids but axon fragmentation in Wallerian degeneration. Cytoskeletal changes are common to both, so a loosening of cytoskeletal structure could cause disorganised cytoskeleton to accumulate in spheroids but to undergo rapid granular disintegration in Wallerian degeneration. Wallerian degeneration of injured gracile tract axons displays elements of both processes, possibly having an intermediate mechanism: like spheroids, these axons dilate considerably but, typical of Wallerian degeneration, they also rapidly lose their cytoskeletal proteins (George and Griffin, 1994). In traumatic brain injury, observation of

Wallerian degeneration and spheroids in the same transverse thin section has been interpreted as some axons having a more proximal spheroid that blocks axonal transport (Cheng and Povlishock, 1988)(Figure 5.10). In view of our findings, an additional explanation needs to be considered, that spheroids and Wallerian degeneration are alternative responses of different axons to the same lesion. Methods for real-time or long-range longitudinal analysis of individual spheroid-containing axons are required to resolve this, similar to new methods already applicable in PNS axons (Beirowski *et al*, submitted). What determines whether an axon develops a spheroid or undergoes Wallerian degeneration? Possible explanations include the different glial and haematopoietic cell content of the CNS and the slower rate of axonal transport there (Wujek and Lasek, 1983) but injury type may also be important. Finally, since the discovery of the *Wld*^{S} mouse, Wallerian degeneration is no longer considered a passive wasting of distal axons but a regulated self-destruction programme (Buckmaster *et al*, 1995; Raff *et al*, 2002). The reduction of axonal spheroid pathology by the same gene raises similar questions: rather than being a passive consequence of blocked axonal transport they could be, like Wallerian degeneration, a programmed response to axon damage.

Altered ubiquitin metabolism plays important roles in neurodegenerative diseases of the CNS. Genetic mutations in Parkinson's disease include an E3 ligase (Kitada *et al*, 1998) and possibly *Uchl*1, the human homologue of the gene mutated in *gad* (Leroy *et al*, 1998). Indeed there is a protective effect of *Wld*^{S} in a Parkinson's model as well (Sajadi *et al*, submitted). Ubiquitin positive inclusions and other evidence indicate abnormal ubiquitination in Alzheimer's disease (Mori *et al*, 1987; van Leeuwen *et al*, 1998), polyglutamine disorders (DiFiglia *et al*, 1997; Cummings *et al*, 1999; Bence *et al*, 2001) and ALS (Tu *et al*, 1996; Bruijn *et al*, 1997). Axons and synapses are particularly vulnerable, as proteasome inhibitors cause specific degeneration of distal neurites (Laser *et al*, in press) and ubiquitin-related mutations alter synapse growth (DiAntonio *et al*, 2001) and stability (Wilson *et al*, 2002). As *Wld*^{S} can counter a downstream effect of defective ubiquitin metabolism, it now becomes important to study its effects on the above disorders. Ironically, ubiquitin-proteasome pathway alterations also delay Wallerian degeneration (Mack *et al*, 2001; Zhai *et al*, 2003).

Wld^S is a unique tool to explore the relationship between axon pathology and disease symptoms. For example, the poor Rotarod performance of *ga*d/*Wld*^{S} mice, despite multiple indications of reduced pathology in the gracile tract, suggests that gracile tract axons are not responsible for this particular behavioral deficit. Poor preservation of neuromuscular junctions, especially in older *ga*d/*Wld*^{S} mice, is a more likely explanation. Why the phenotype actually worsens, however, is unclear. An interesting possibility is impairment of functional compensation, such as nodal or terminal sprouting, as *Wld*^{S} is known to impair axon regeneration secondarily (Brown *et al*, 1994). The Rotarod deficit in *gad/Wld*^{S} mice contrasts both with the lack of significant change in other tests we report and with the distinct improvements seen in peripheral neuropathies, motor neuronopathy and a Parkinson's model (Wang *et al*, 2002; Samsam *et al*, 2003; Ferri *et al*, 2003; Sajadi *et al*, submitted). However, the behavior in the Parkinson's study was also not as expected from the histopathology with unexpected effects on drug-induced turning behavior in mice showing distal protection of their dopaminergic fibers. Thus, although *Wld*^{S} protects axons in a widening range of diseases, it is clear that we have much to learn about the behavioral consequences of axon protection, which need to be studied on a disease-specific and test-specific basis. Rapid removal of sick but "undead" cells is sometimes beneficial (Schulz and Nictotera, 2000) so when the regulation of Wallerian degeneration is sufficiently understood, it might be used to amputate sick axons selectively to facilitate their rapid clearance where appropriate. In other circumstances, however, we may wish to prolong axon survival long enough to overcome or treat a temporary insult and then allow the axon to return to normal.

In summary, *Wld*^{S} alleviates chronic CNS axon pathology in *gad* mice and that formation of distal axonal spheroids shares a regulatory step with Wallerian degeneration and 'dying-back' axon loss without spheroids. The effect of *Wld*^{S} on other CNS disorders with ubiquitination deficits or proximal axonal spheroid pathology should now be studied. Behavioral consequences of axon rescue are sometimes complex and must be assessed on a disease- and test-specific basis. Finally, it is clear that future studies need to identify factors protecting synapses as strongly as *Wld*^{S} protects axons.

Figure 5.1 Southern blot genotyping of *gad*. 1) Southern blot genotyping $gad^{+/+}$, $gad^{+/-}$, and $gad^{-/-}$, genomic DNA were digested by *Pvu*II, southern blotted and detected by radiolabelled g*ad* probe (764bp). 2) Scheme of the deleted region of *Uchl1* in *gad* mice. Predicted sizes of genomic level sequences of exon 6 to exon 9 of $gad^{+/+}$ and $gad^{-/-}$ are shown. The restriction cutting sites for *Pvu*II and predicted sizes of detected fragments by *gad* probe are shown.

Figure 5.1 Southern blot genotyping of *gad*^{-/-}, *gad*^{+/-}, *gad*^{+/+}.
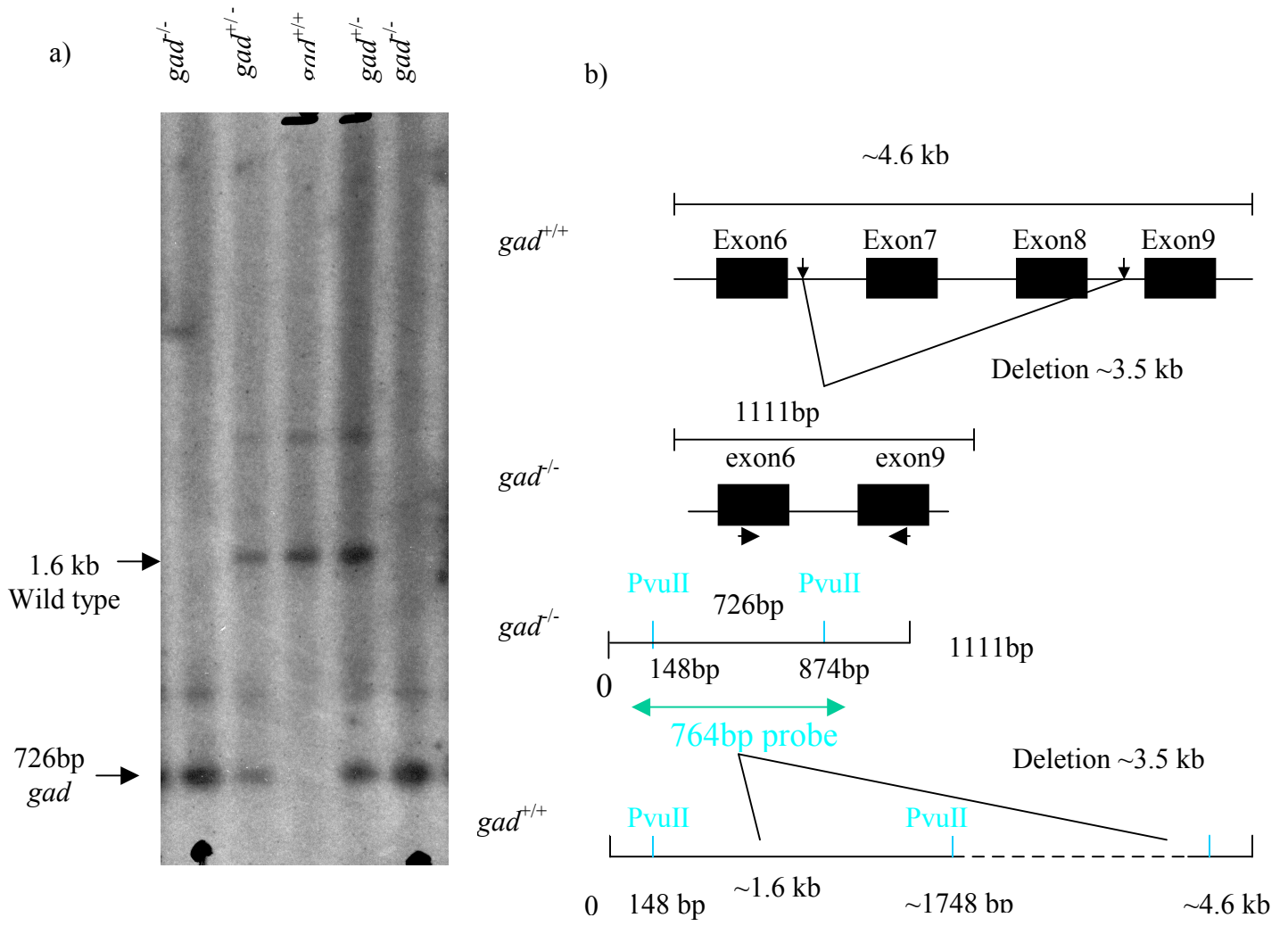
Figure 5.2 Slow Wallerian degeneration in Wld^S heterozygotes carrying homozygous *gad* alleles. (a) Western blot showing complete preservation of heavy neurofilament protein in distal sciatic nerve of *gad* homozygous plus Wld^S heterozygous mice five days after nerve transection. (b) Complete preservation of distal axon integrity in the same mice visualised using the YFP-H transgene. Scale bar: 100 µm.

Figure 5.2

a)

200 kDa ‒

gad + Wld$^{S/+}$

Wild-type

Uncut
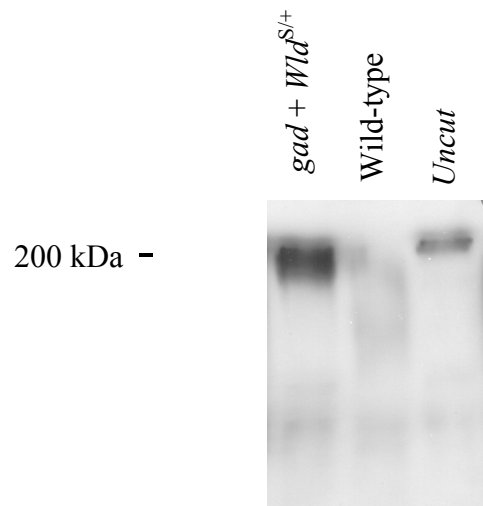
b)
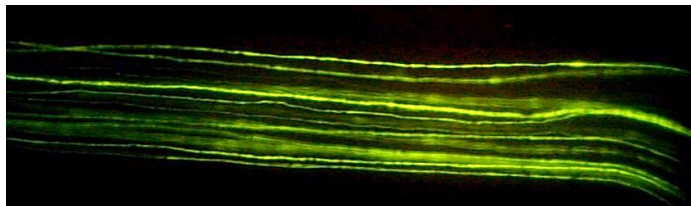
Figure 5.3 Wld^S reduces spheroid body numbers in the gracile tract of *gad* mice. (a and c) Representative sections from gracile nucleus of (a) *gad* and (c) *ga*d/Wld^S mice stained with H & E, showing a large reduction in the number of axonal spheroids (arrows) when Wld^S is present. (b and d) Representative sections from cervical gracile fascicle of (b) *gad* and (d) *ga*d/Wld^S mice. Scale bar (a to d): 25 μm. (e and f) Quantification (mean ± SD) of spheroid counting data in (e) gracile nucleus and (f) cervical gracile fascicle (n=6). ** $p < 0.01$; *** $p < 0.001$.

Figure 5.3
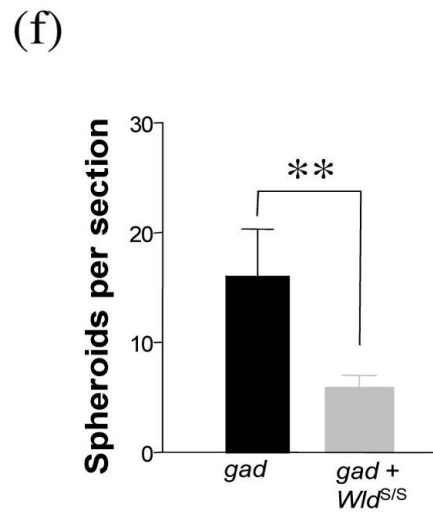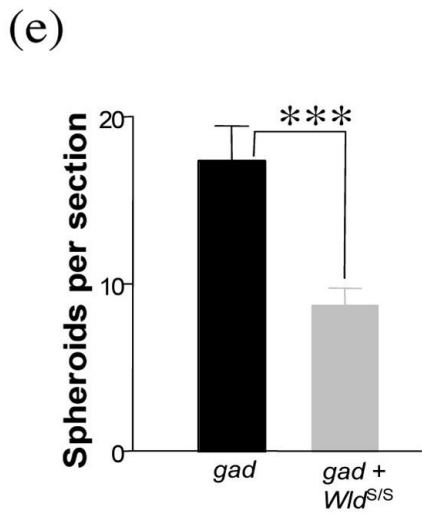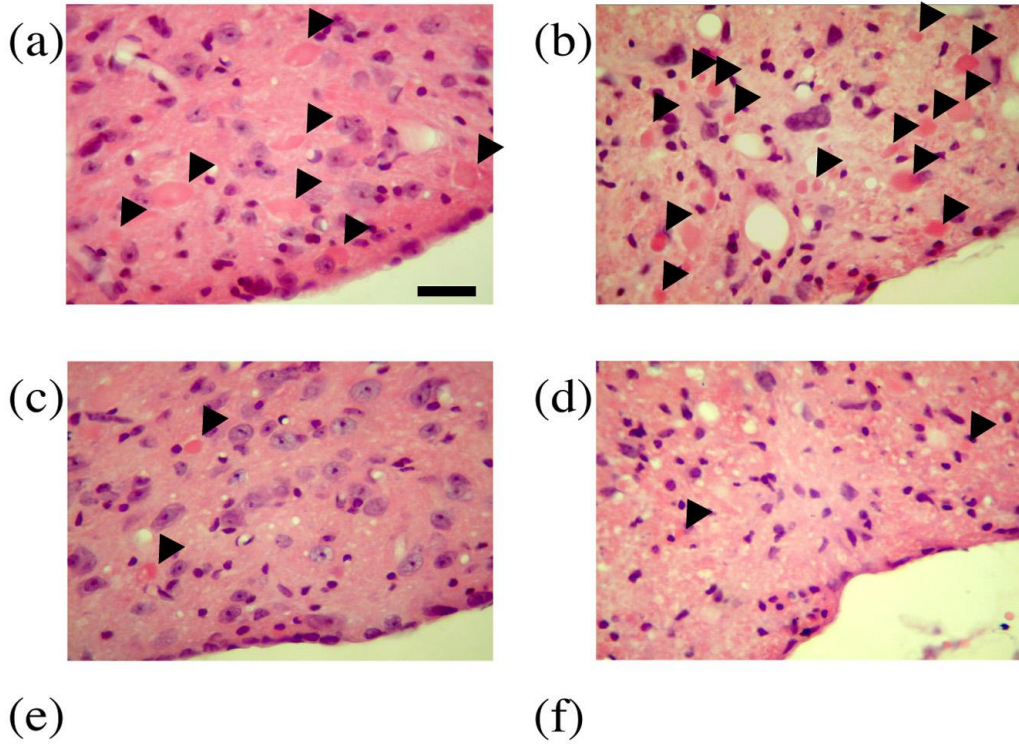
Figure 5.4 Wld^S reduces also other measures of gracile tract pathology. (a) and (b) Representative gracile fascicles from cervical gracile fascile of (a) *gad* and (b) *ga*d/Wld^S mice stained with Luxol Fast Blue and Nuclear Fast Red, showing the reduction in myelin loss when Wld^S is present. Scale bar (a and b): 25 µm. (c) Densitometric quantification (mean ± SD) of Luxol Fast Blue staining (n=5). (d) and (e) Representative gracile nuclei of (d) *gad* and (e) *ga*d/Wld^S mice immunostained for GFAP, showing lower astrocyte activation when Wld^S is present. Scale bar (c and d): 25 µm. (f) Densitometric quantification (mean ± SD) of GFAP immunocytochemistry signal (n=5). * $p < 0.05$.

Figure 5.4
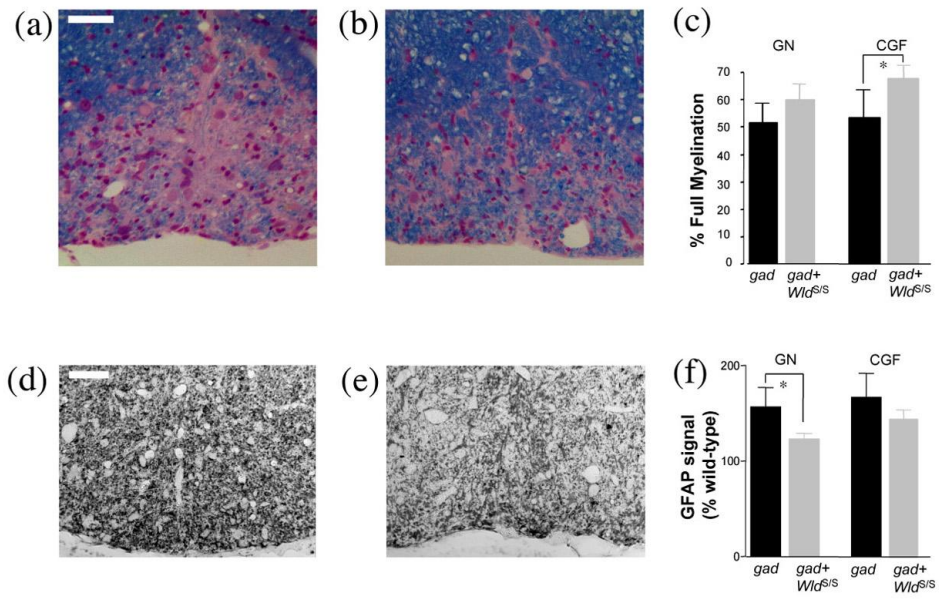
Figure 5.5 *gad* mice perform worse on Rotarod when they carry a Wld^S allele. Time taken for *gad* mice of increasing ages to fall from an accelerating Rotarod in the presence of homozygous mutant (n=9) or wild-type (n=6) alleles for Wld^S. Homozygous Wld^S causes deterioration to be anticipated by approximately 5.5 weeks, with significant (* $p < 0.05$) differences in performance at several individual timepoints, especially beyond 14 weeks. The Rotarod performance of Wld^S heterozygotes was also significantly worse than wild-type and, when combined with Wld^S homozygote data, gave a highly significant difference from wild-type *(p = 0.002)* at 18 weeks (data not shown).

Figure 5.5
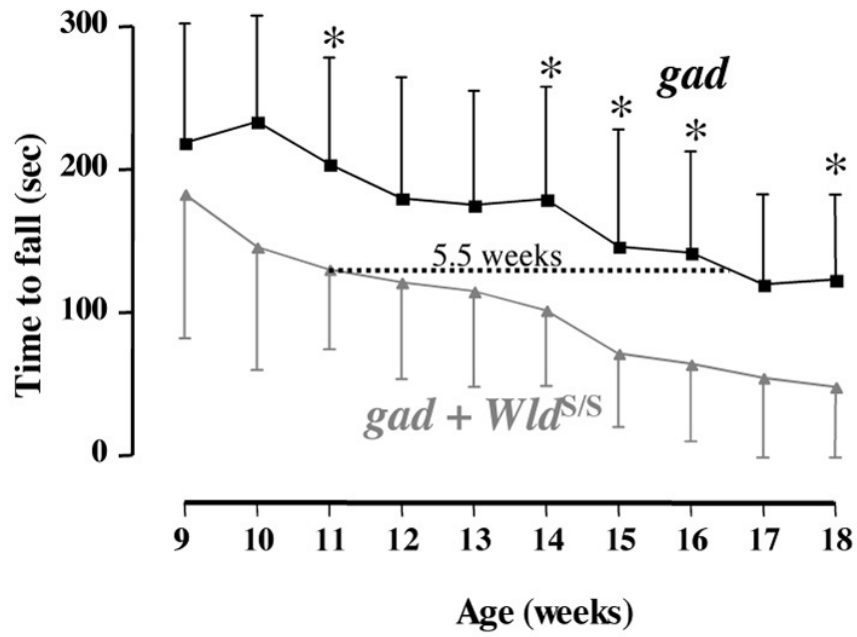
Figure 5.6 There is no significant difference on footsplay test in *gad* mice with *Wld*[S] allele or without *Wld*[S] allele. Distance of hind limbs measured for *gad* mice of 9 weeks and 13 weeks to drop from a height of 15 cm to land on white paper in the presence of homozygous mutant (n=8) or wild-type (n=7) alleles for *Wld*[S]. White blocks stand for *gad* wild type (wt) or heterozygotes (hetero); black blocks stand for *gad*/*Wld* homozygotes (homo); blue blocks stand for *gad*/*Wld* wild type (*Wld* wt).

Figure 5.6

Footsplay test

hindlimb spread (cm)

$P = 0.3$

$P = 0.09$

6,00

5,00

4,00

3,00

2,00

1,00

0,00

9   13

weeks

gad wt and hetero
gad/wld homo
gad/wld wt
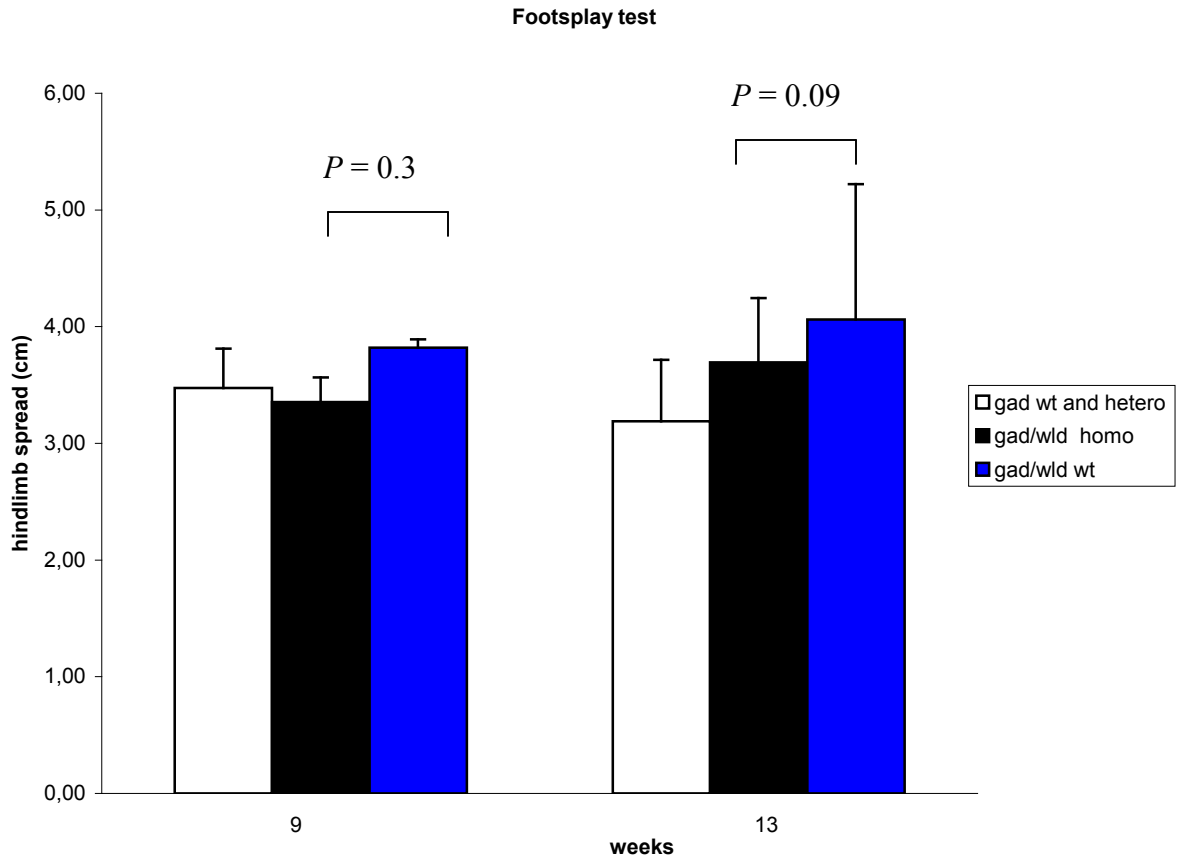
Figure 5.7 There is no significant difference on hind limbs clasping test between *gad* mice with Wld^S allele (Wld^S homozygous or heterozygotes) or without Wld^S. Time taken for *gad* mice of increasing ages (from 6 week to 16 week) to clasp their hind limbs (Figure 2.3) within 1 minute in the presence of homozygous mutant (n=10), heterozygous mutant (n=14) or wild-type (n=7) alleles for Wld^S.

Figure 5.7

Clasping comparation

Legend:
- wld wt
- wld hetero
- wld homo

X-axis: weeks (6 to 16)
Y-axis: seconds (0.00 to 70.00)

Figure 5.8 Denervation at the neuromuscular junction. At 15 weeks both (a) *gad* and (b) *ga*d/*Wld*^S have extensive denervation, with partial occupancy of endplates by motor nerve terminals occurring frequently. At 9 weeks mice denervation had hardly begun in some mice of either genotype (c and d respectively). Scale bar: 25 µm
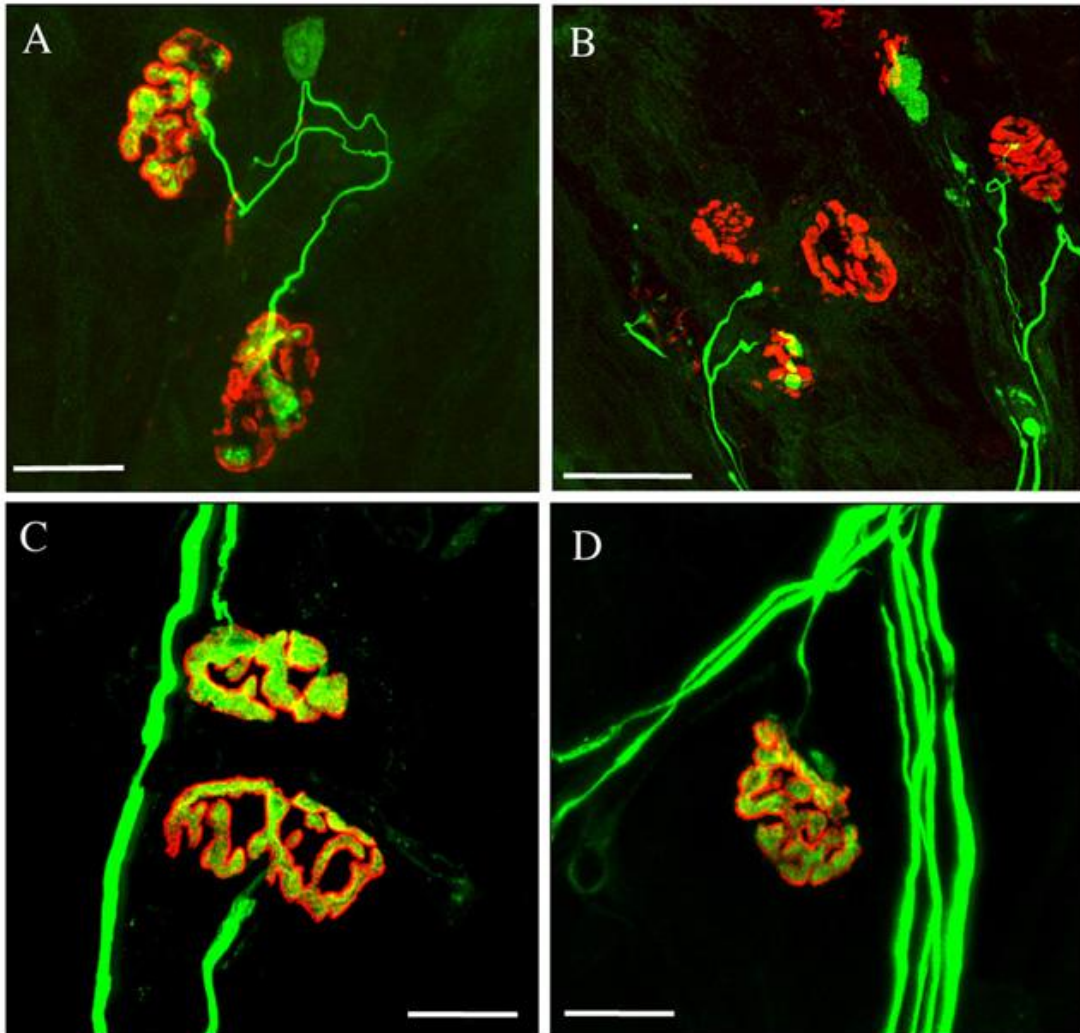
Figure 5.8

Figure 5.9 Axonal spheroids are present widely in degenerative pathology.

a) Axonal spheroids were present in the brainstem of 7-week old *npc*-1$^{-/-}$ mice. *Npc*-1$^{-/-}$ is a mice model of human Niemann-Pick type C (NPC, a neurodegenerative storage disease), primary antibody: SMI 32 (Sternberger Monoclonals, Inc. USA), staining nonphospho-NF-H (Bu *et al*, 2002). 40 x.

b) NF-rich spheroids were found in the anterior horn of SOD1-G93A mice at 130 days old, a mice model of human familial amyotrophic lateral sclerosis. Primary antibody: rabbit anti-NFL polyclonal anti-serum (Tu *et al*, 1996). Scale bar: 20 µm.

c) Axonal spheroid swellings are present in the ventral horns of the spinal cords in *Vegf*$^{\delta/\delta}$ mice with ALS-like motoneuron de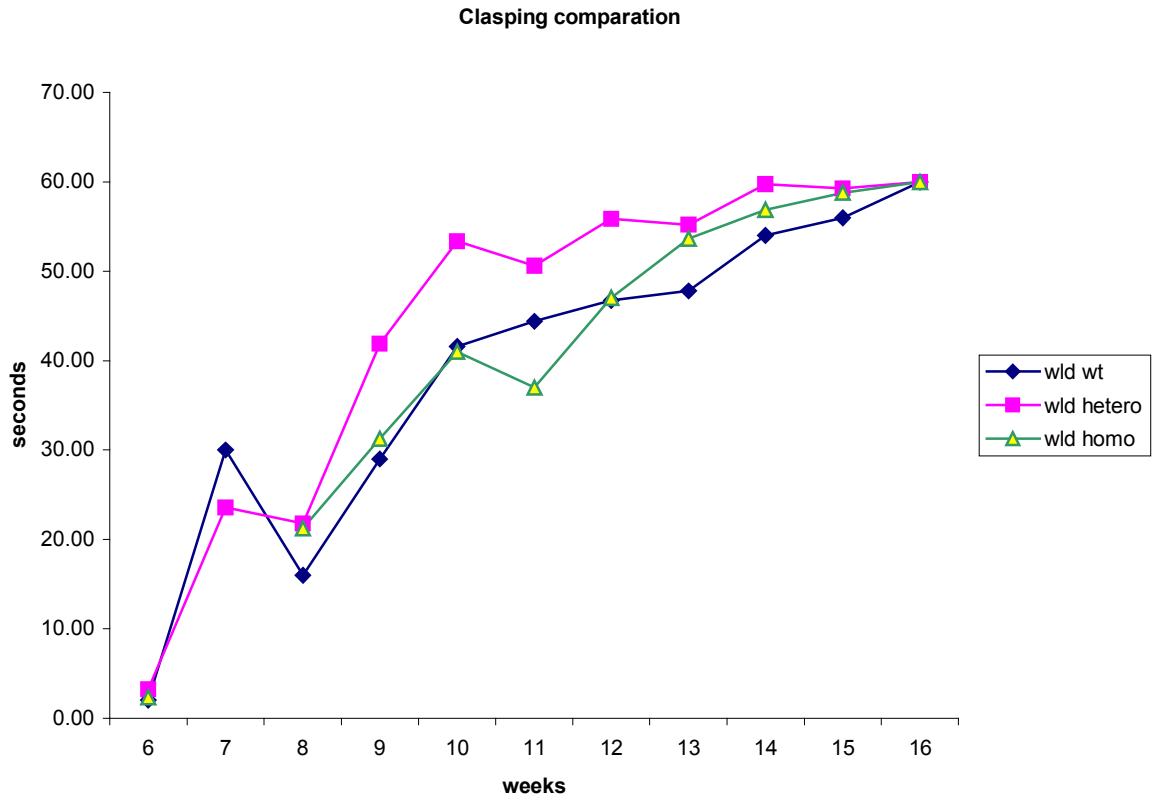generation and d) Toluidine blue staining shows a marked deficit or abnormal appearance of axons, endoneural fibrosis and macrophage infiltration (Wallerian-like degeneration) in the sciatic nerve of a *Vegf*$^{\delta/\delta}$ mice (Oosthuyse *et al*, 2001). Scale bar: 20 µm.

e) and f) Electron microscopy of axonal spheroids from the raphe of the brain stem of 10-month transgenic mice expressing human four-repeat tau protein. Both spheroids in e) and f) are surrounded by a thin myelin sheath. The axon in e) contains mostly intermediate-size filaments. The axon in f) contains mainly concentrically structured dense bodies in an electron-dense background (Probst *et al*, 2000). Scale bar: 2.5 µm.

Figure 5.9

a)

b)
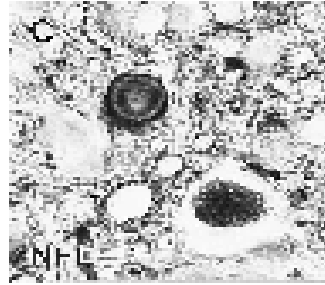
c)
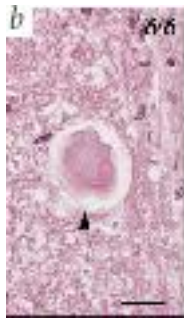
d)
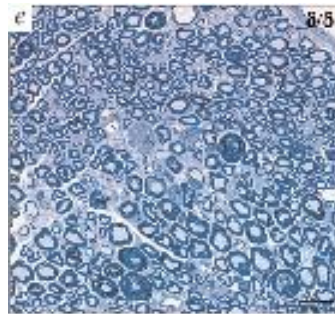
e)
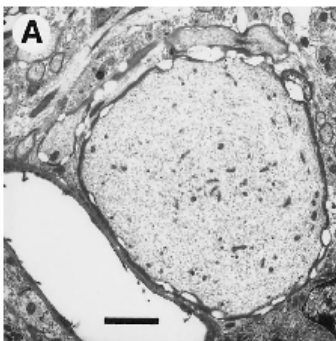
f)
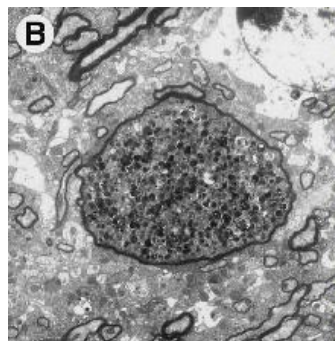
Figure 5.10 Evidences show that Wallerian degeneration and axonal spheroid are related.

    a) Gracile tract axons (Lumbar cord) 46 h post-axotomy in 18-week-old rat undergo Wallerian degeneration with spheroid-like dimensions quite unlike Wallerian degeneration in the PNS. Scale bar, 0.1 μm.

    b) In traumatic brain injury, Wallerian degeneration and spheroids in the same transverse thin section has been observed. At 14 days posttrauma, electron microscopy demonstrates a reactive swelling with a focally disrupted axolemma, degenerating mitochondria and electron-dense bodies. Wallerian change (arrows) of segments of injured axons distal to the reactive swelling is reflected in the appearance of electron-dense and collapsed axonal profiles. 5600 x.

Figure 5.10

a)
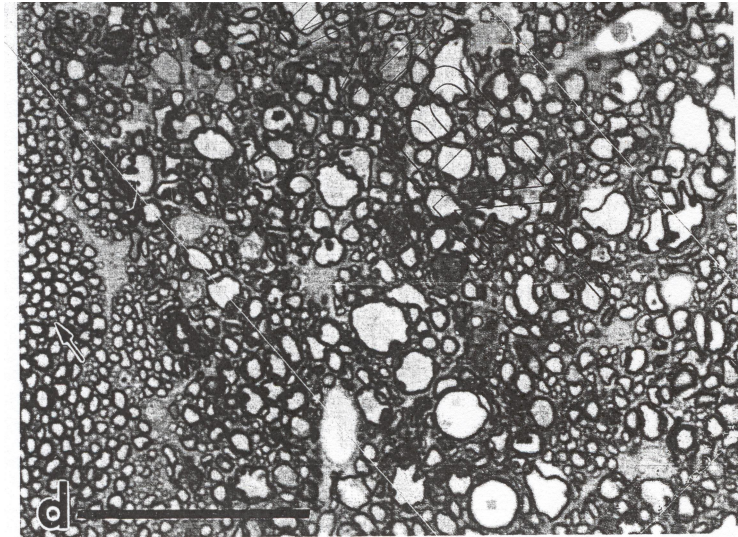
b)
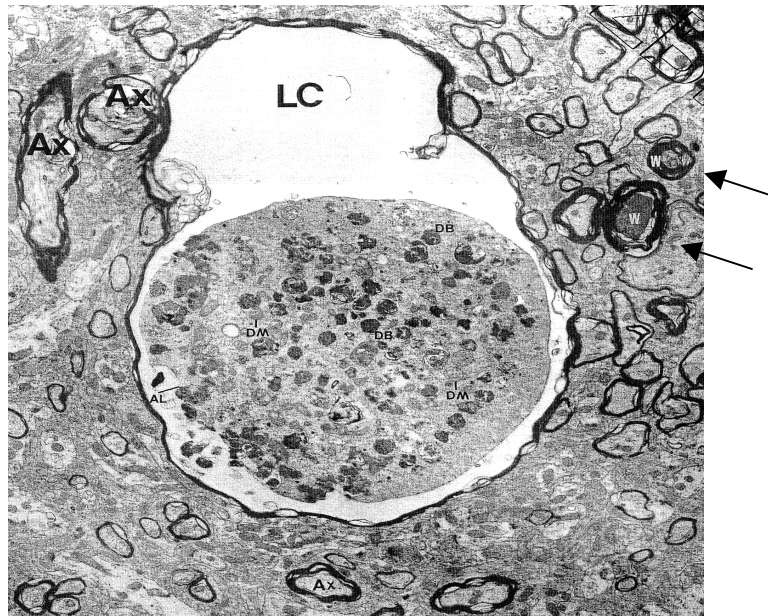
Figure 5.11 *Wld*[S] delays a central step of axonal pathology that lies after the convergence point of multiple degenerative stimuli but upstream of the divergence of several pathological manifestations.

Figure 5.11

Defective ubiquitin metabolism (*gad*)

Myelin defect (P0$^{-/-}$)

Axonal transport block (*pmn*)

Injury

Taxol, vincristine toxicity

Apoptotic death of cell body

Wld^S

?

Axonal spheroids

Wallerian degeneration

'Dying-back' axon loss
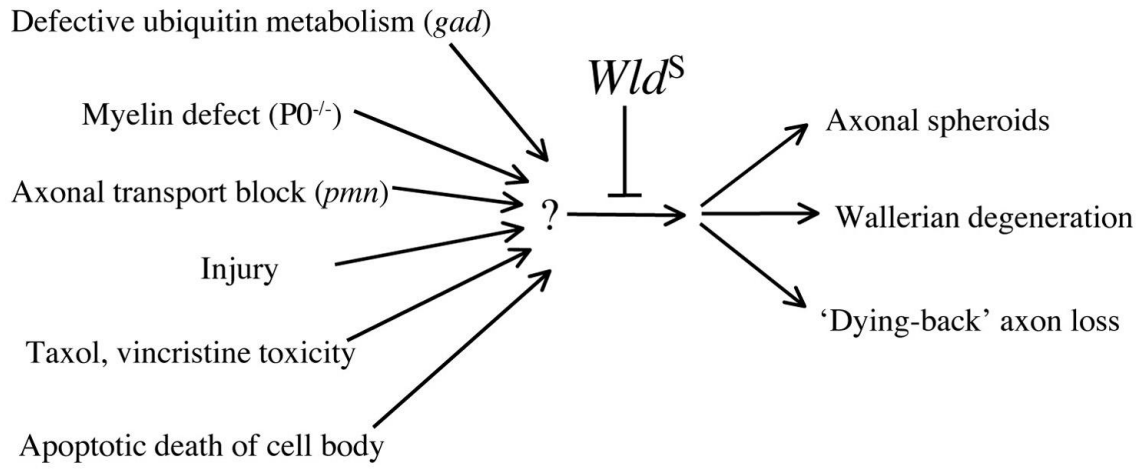
CHAPTER 6

STUDY OF THE *Wld^S* MECHANISM

6.1 Introduction

Axons and their synapses distal to an injury undergo rapid Wallerian degeneration, but axons in the C57BL/Wld^S mouse are protected in such processes for 3 weeks after transection (Lunn *et al*, 1989). The degenerative and protective mechanisms are unknown. However the protective gene was identified in our lab (Mack *et al*, 2001), and encodes an N-terminal fragment of ubiquitination factor E4B (*Ube4b*) fused to nicotinamide mononucleotide adenylytransferase (*Nmnat*). The yeast homolog of Ube4b is required to multi-ubiquitinate some substrate proteins (Koegl *et al*, 1999) and a direct link between ubiquitination and axon degeneration comes from the *Uch-l1* mutation in gracile axonal dystrophy (Saigoh *et al*, 1999). However, the Wld^S protein contains only 70 of 1,173 amino acids from Ube4b, and these are absent from the yeast homolog. They are therefore unlikely to confer multi-ubiquitination activity but may have a related role. However, the protective mechanism could still work through Ube4b sequences, possibly due to sequestering of ubiquitination factors by protein-protein interactions. Nmnat is a nuclear protein and known to catalyze the reaction $NMN + ATP \rightarrow NAD^+ + Ppi$ (Magni *et al*, 1999), a reaction generally assumed not to be at equilibrium because of the constitutive action of pyrophosphatases. Chimeric protein Wld^S contains full-length sequence of Nmnat, however, whether it has Nmnat enzyme activity was unknown.

Several projects to characterize Wld^S protein are ongoing in the lab, such as studying the localization of Wld^S protein, finding the binding partners of N-terminal fragment of Wld^S, knocking out Ube4b, the parent gene of N-terminal 70 amino acids of Wld^S. All of these projects use the N70 antibody that I generated (see below). In addition, I describe how I expressed Wld^S fusion protein for analysis of intrinsic Nmnat enzyme activity by a collaborating group and my generation and analysis of transgenic N70 with nucleus localization signal (NLS) or nucleus export signal (NES) etc.

6.2 Results

6.2.1 Identifying the *Wld*^{S} gene and its initial characterization

Prior to the beginning of this work, a transgenic mouse line had been made (E34) to test the hypothesis that the chimeric gene was the *Wld*^{S} gene. This formal proof was necessary because there is only one mutant allele for *Wld*^{S} and other genes are also

altered by the triplication. Thus, the correlation between inheritance of chimeric gene and the Wld^S phenotype is not alone proof of causality. E34 was made using a construct with *Nmnat* plus 54 nucleotides at the junction and 33 nucleotides of truncated N-terminal 210 nucleotides of *Ube4b* from a β-actin promoter. It was known not to show the Wld^S phenotype (Figure 6.1a), but at the beginning of the work, it was not known whether this line expressed protein. Two antibodies had been made using synthetic peptides (amino acids shown in bold in Figure 1.4, were used to make peptides for generation of polyclonal antisera), but had not been tested on Western blots, and it was important to know whether line E34 did express the protein. If it did not, we could not have made any conclusion about the identity of the gene; if it did, it would have suggested that this construct did not contain a fully-functioning Wld^S gene. In joint work by myself and Dr. Till Mack, line E34 was found to express the unique protein but, surprisingly, it was 6-7 kDa smaller than Wld^S-specific protein showed in brain homogenates in C57BL/Wld^S mouse. To sort out the possible explanation of the difference between transgenic and Wld^S, Dr. Michael Coleman re-examined the sequence, and found out there were 177 nucleotides (59 amino acids) missing at the N-terminus. Thus new transgenic lines were made which included the missing N-terminus (full sequence of Wld^S gene shown in Figure 1.4 and the transgenic construct shown in Figure 6.1a).

While generation of the new transgenics was in progress, I generated a new antiserum. This was necessary because the anti-peptide antibodies recognised the Wld^S protein only weakly, along with many non-specific background bands. Recombinant N70 protein, whose sequence is shared between Wld^S and wild-type Ube4b (ubiquitination factor E4B) was made to raise rabbit polyclonal antibody using the services of Eurogentec (Eurogentec, Belgium). N-terminal 210 nucleotides of chimeric Wld^S (sequence see Figure 1.4) was amplified by PCR, cloned into *NheI* / *XhoI* double-digested pET-28b (+) vector (Figure 2.2) and expressed in BL21 (DE3) *E.coli* strain (data not shown). The Nickel-chelating resin was used to purify recombinant N70 protein with polyhistidine (6 x His) (ProBond^{TM}, Invitrogen) and purified recombinant protein was frozen (-20°C) and shipped to Eurogentec for raising polyclonal antisera in two rabbits.

The polyclonal antibodies against recombinant N70 from both rabbits did recognize Wld^S protein and Ube4b (Figure 6.3). The further affinity purification of antibody was done by

Postdoctoral fellow Dr. Till Mack in the lab (2.1.7). The purified antibody was used for the Wld^S localization study in isocortex and motor neurons (done by Bogdan Beirowski), showing the predominant nuclear localization of Wld^S protein (Figure 6.2). Dr. Till Mack also used it to show that Ube4b expression is unaltered in Wld^S mice and to study Wld^S expression in Wld^S mice at different ages, showing age-independent protection of axons (Gillingwater *et al*, 2002) (Figure 6.3). Dr. Heike Laser used it to study binding interactions between N70 and other proteins. Finally, I describe below how I used it myself in the transgenic N70 project (see section 6.2.2).

Since the Wld^S gene was confirmed by at least 3 lines of transgenic mice (Mack *et al*, 2001), and it encodes an N-terminal fragment of ubiquitination factor E4B (*Ube4b*) fused to nicotinamide mononucleotide adenylytransferase (*Nmnat*), the questions were addressed: which part of the gene does the job to delay Wallerian degeneration in axons, or does the protective effect needs both parts, and what could the mechanism be? Part of my contribution to this was to make recombinant Wld^S protein for *Nmnat* enzyme activity analysis, since nucleotides 282-1140 of Wld^S spans the entire *Nmnat* open reading frame. Full-length chimeric gene (sequence see Figure 1.4) was amplified by PCR, cloned into *NheI* / *XhoI* double-digested pET-28b (+) vector (Figure 2.2) and expressed in BL21 (DE3) *E.coli* strain (data not shown). The Nickel-chelating resin was used to purify recombinant chimeric protein with polyhistidine (6 x His) (ProBond^{TM}, Invitrogen) and purified recombinant protein was frozen (-20°C) and shipped to our collaborator's lab in Italy (Professor Giulio Magni) for Nmnat enzyme activity assay. The purified protein was found to have Nmnat enzyme activity, but a meaningful specific activity could not be calculated since protein had partly degraded during shipping. However, the observed specific activity in a Wld^S bacterial lysate (0.96 U/ mg) was comparable with that of a bacterial lysate containing recombinant human Nmnat (1.74 U / mg) (Figure 6.4) (Emanuelli *et al*, 2001), suggesting that the degree of activity in Wld^S protein is considerable. To determine whether there is a corresponding increase in Nmnat activity in Wld^S mice, our collaborators studied Nmnat activity in brain homogenates and found a fourfold increase in Wld^S brain compared to C57BL/6J ($p<0.05$, Figure 6.4). The total content of NAD$^+$, however, was not significantly altered ($p=0.2$; Figure 6.4).

Therefore, the Wld protein confers an increase in Nmnat activity without altering the steady-state level of NAD^+.

6.2.2 Transgenic N70 plus NLS or NES does not show *Wld*[S] phenotype

The failure of Wld[S] protein to alter resting NAD^+ levels, together with the absence of a *Wld*[S] phenotype in E34 mice, suggested that the N-terminal region (N70) of the Wld[S] protein is necessary for the phenotype. I then made transgenic mice with N70 plus Nucleus Localization Signal (NLS) or Nucleus Export Signal (NES). The aim was to clarify two question 1) whether N70 itself is enough to delay Wallerian degeneration and 2) whether the nucleus localization is essential for the phenotype since Wld[S] protein is predominantly expressed in nucleus (Mack *et al*, 2001) (Figure 6.2).

I cloned N70-NLS or N70-NES with flag tag downstream of β-actin promoter in *BamH*I-digested pHβApr-1 (Figure 2.1, Figure 6.1b and Figure 6.1c) and confirmed their orientation by sequencing. To check whether Nucleus Localization Signal (NLS) and Nucleus Export Signal (NES) do confer the localization of recombinant protein in nucleus (N70-NLS) or cytoplasm (N70-NES), I transfected transgenic construct pHβApr-1-N70-NLS or pHβApr-1-N70-NES into COS-7 cells, and it showed that pHβApr-1-N70-NLS was expressed in nucleus, and pHβApr-1-N70-NES was expressed in cytoplasm as expected by anti-flag-tag monoclonal antibody (see above and Figure 6.5).

To further characterize the role of N70-NLS and N70-NES, transgenic mice expressing the N70-NLS or N70-NES from a β-actin promoter were generated. The N70-NLS and N70-NES fragments with β-actin promoter was excised from the plasmid, purified using Qiaquick extraction kit and then shipped for injection into C57BL/CBA F1 mouse pronuclei using the service of Professor George Kollias (Alexander Fleming Research Center, Vari, Greece). I then performed DNA extraction and genotype analysis to identify founders and control further breeding. One transgenic line (line 311) was confirmed positive by Southern blotting for N70-NLS expression with multi-copy integration. Three lines of transgenic N70-NES (line 213, 215, and 219) were confirmed positive by a strong PCR signal and chosen for further analysis.

To test whether N70-NLS or N70-NES confer the *Wld*[S] phenotype, the structural preservation of axons several days after axotomy were examined either by western blotting for the preservation of heavy neurofilament protein or by visualizing YFP signal

(Feng *et al*, 2000) for axonal integrity. Following unilateral sciatic nerve transection in ~7, 8 or 12 week old mice, a nerve segment 2-4 mm distal to the lesion after 53 h, 56h or 3 days was taken for western blotting, and tibial nerve was taken for YFP signal visualization. None of transgenic N70-NLS or N70-NES homozygotes or heterozygotes show preservation of axons either in 3 days lesion, 56 hours or 53 hours low stringency lesion (Table 6.1). However no N70-NLS or N70-NES protein expression was detectable in western blotting (data not shown), thus to conclude whether N70 itself could alter Wallerian degeneration may require further transgenic lines to be generated.

6.3 Discussion

We showed that polyclonal antibodies against recombinant N70 are suitable for western blotting and immunocytochemistry studies to examine Wld^S protein expression level and localization (Figure 6.2 and 6.3). Such polyclonal anti-N70 antibodies could also be used for other application, such as confirming Wld^S expression in substantia nigra dopaminergic neurons of *Wld*^{S} mice with 6-hydroxydopamine (6-OHDA) lesion, a mouse model of Parkinson disease (Sajadi *et al*, submitted). It could be applied for studying the potential binding partner of N70 by immunoprecipitation as well, and other studies which should lead towards the mechanism of axon protection by *Wld*^{S}.

The predominant Wld^S protein expression in nucleus and its non-homogeneous intranuclear distribution suggest that the protective mechanism could involve sequestering of ubiquitination factors by protein-protein interactions. Ubiquitination could thus be altered within the nucleus, altering transcription factor stability or RNA processing, leading to an axon effect mediated by unknown proteins. Alternatively, ubiquitination in cytoplasm or axon might be altered by sequestration of ubiquitination factors normally located there. Although there was a fourfold increase in *Wld*^{S} brain homogenates compared to C57BL/6J, the total content of NAD$^+$ was not significantly altered. It thus suggests the putative additional NAD$^+$ is metabolized in *Wld*^{S}. The product of a compensatory reaction could itself be involved in axon protection. For example, mild activation of PARP without NAD$^+$ depletion can be neuroprotective (Nagayama *et al*, 2000); synthesis of the signaling molecule cyclic ADP ribose from

NAD$^+$ regulates calcium release from intracellular stores, potentially influencing calcium activated proteases in Wallerian degeneration (Di Lisa *et al*, 2001).

We did not see *Wld*^{S} phenotype in transgenic N70-NLS or N70-NES, several reasons could account for this: firstly, we did not detect any N70-NLS or N70-NES protein expression by western blotting although we detected convincingly transgene integration into the chromosome by Southern blotting. If there is no N70-NLS or N70-NES expression in transgenic mice at all, we could not make any conclusion to exclude N70's possible role in delaying Wallerian degeneration. Such doubt may be resolved in future studies by making additional transgenic mice. Secondly, it could be that protein expression level (N70-NLS or N70-NES) is not high enough to confer any *Wld*^{S} phenotype, since *Wld*^{S} phenotype is highly dose-dependent (Mack *et al*, 2001). Thirdly, it could be N70 itself could not complete the role in delaying Wallerian degeneration and it does need other parts of the Wld^S protein, such as Nmnat sequence or the 18 amino acid joining region. Ongoing experiments by Dr. Heike Laser to look for the binding partners of N70 by yeast two-hybrid and biochemical analysis might also indicate the role of N70. Alternatively, knock out of N70 parent gene Ubiquitination factor E4B (*Ube4b*) could also give us information as to whether Wld^S works with Ube4b on delaying Wallerian degeneration, or whether defective in *Ube4b* partially mimics the *Wld*^{S} phenotype and thus its downstream effect could possibly play a role on the protective mechanism. Such experiments using a gene-trap ES cell clone are in progress (Dr. Michael Coleman and Dr. Neil Smyth), although early indications are that there may be splicing across the interruption in *Ube4b*. Alternatively, the mechanism of Wld^S could be studied by testing the effect of other mutations (e.g., knock-outs or spontaneous mutants with known altered gene) to find one with a similar effect on axon. A connection between *Wld*^{S} and such a mutation with known defective pathway would shed light on the *Wld*^{S} mechanism.

Figure 6.1a the transgenic construct of *Ube4b/Nmnat*. The chimeric cDNA (consisting of the N-terminal 210 coding nucleotides of *Ube4b*, the entire 855 coding nucleotides of *Nmnat*, and 54 nucleotides formed at the junction) was expressed with non-coding exon 1 of β-actin under the control of a human β-actin promoter and terminated with the SV40 polyadenylation signal.

Figure 6.1b the transgenic construct of N70 plus NLS. N-terminal 210 coding nucleotides of chimeric *Wld*^{S} with 3 x NLS of the SV40 large T antigen and Flag tag was expressed with non-coding exon 1 of β-actin under the control of a human β-actin promoter and terminated with the SV40 polyadenylation signal.

Figure 6.1c the transgenic construct of N70 plus NES. N-terminal 210 coding nucleotides of chimeric *Wld*^{S} with NES and Flag tag was expressed with non-coding exon 1 of β-actin under the control of a human β-actin promoter and terminated with the SV40 polyadenylation signal.

Figure 6.1a the transgenic construct of chimeric gene.
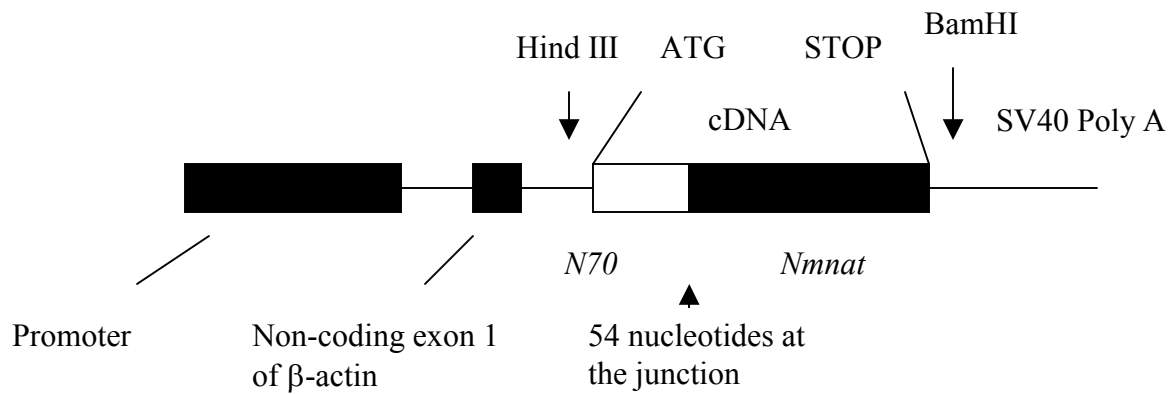
Figure 6.1b the transgenic construct of N70 plus NLS.
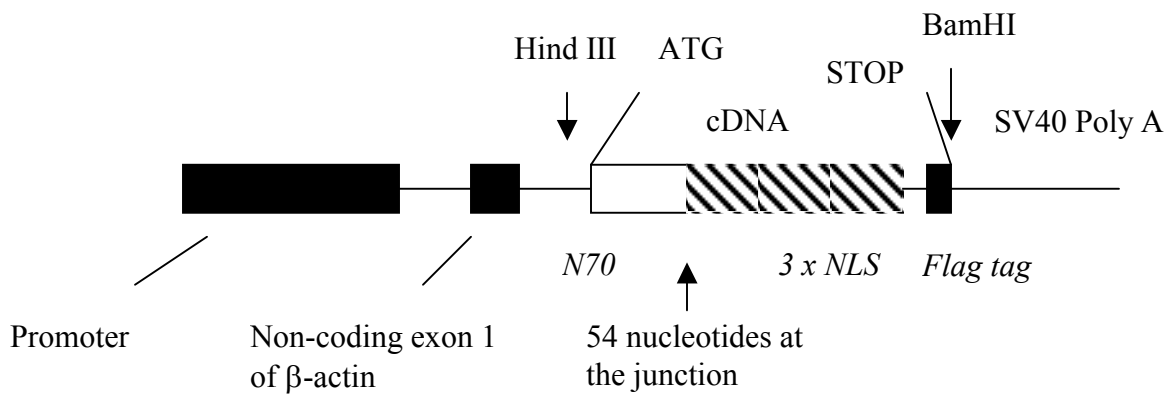
Figure 6.1c the transgenic construct of N70 plus NES.
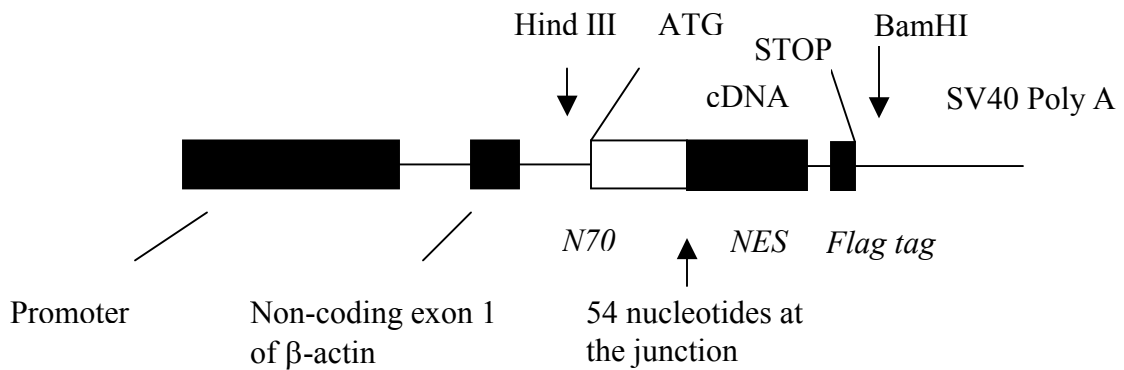
Figure 6.2 The intracellular location of the Wld^S protein. a) presence of the Wld^S protein in neuron nuclei of isocortex and b) its absence from C57BL/6J control tissue. Red, anti-N70 antibody, which detects Wld^S and Ube4b. Green, anti-MAP2 antibody markedly outlining neuronal cell bodies. (c-e) Motor neurons in thoracic spinal cord of both *Wld*^{S} (c) and transgenic line 4836 (d) (see details in section 1.4) expressed the Wld^S protein (red) in their nuclei, whereas those of C57BL/6J (e) did not. Cytoplasmic signals may be Ube4b or low level Wld^S protein. Counter stain, neurofilament (green) (Mack *et al*, 2001).

Figure 6.2

Isocortex
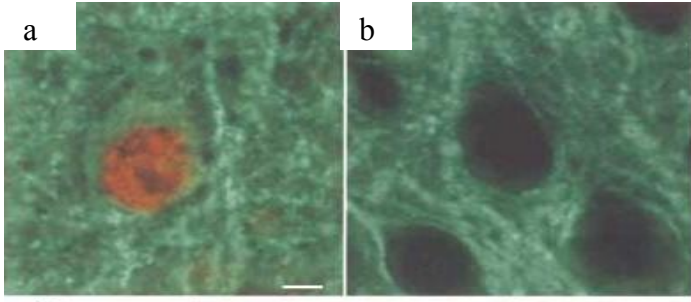
Motor neurons in thoracic spinal cord
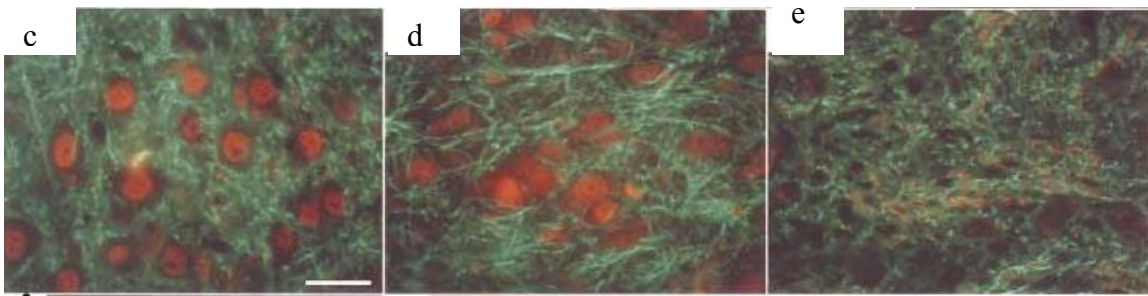
Figure 6.3 Western blotting shows Ube4b, Wld^S and β-tubulin (loading control) expression in *Wld*^{S} mice of different ages (2 months, 4 months, 7 months and 12 months) compared to a 6J mouse control (Gillingwater *et al*, 2002).

Figure 6.3

A

2 m | 4 m | 7 m | 12 m | 6J

N70 (415) antiserum -Ube4b- -Wld-

β-tubulin
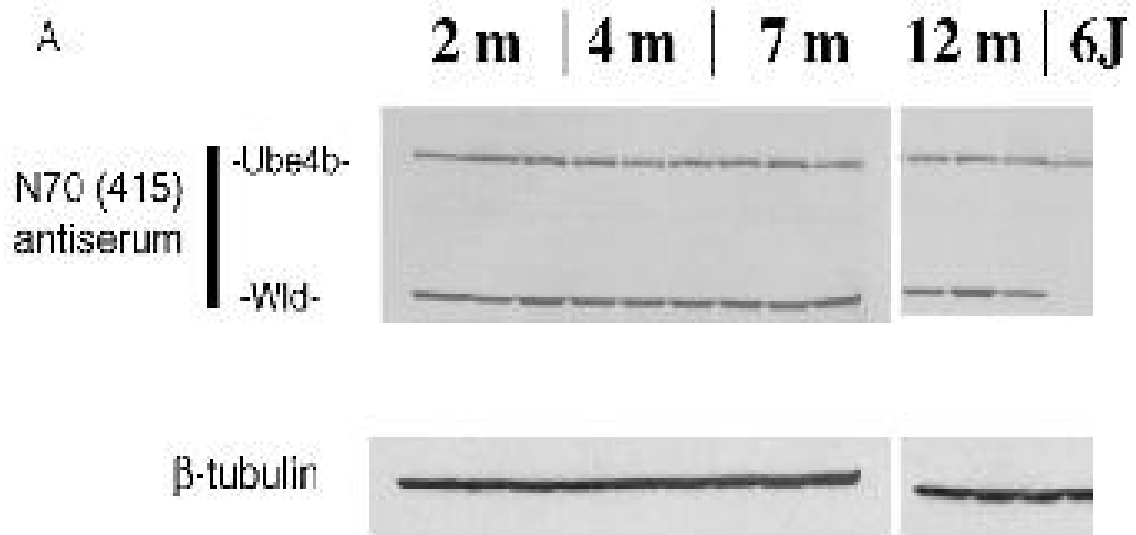
Figure 6.4 a) Commasie-blue protein gel show the chimeric gene lysate (recombinant chimeric protein expressed in *E.coli*) and the control lysate (*Ecoli* without recombinants chimeric protein expression), the observed specific activity for Nmnat of chimeric protein bacterial lysate is 0.96 U/mg, which is comparable with that of a bacterial lysate containing recombinant human NMNAT (1.74 U/mg) (Emanuelli *et al*, 2001).

b) Increased Nmnat activity and unaltered NAD^+ content in Wld^S brain. Bar charts show Nmnat specific activity and NAD^+ content in homogenates of fresh brain from homozygous Wld^S and C57BL/6J mice. Means and standard error are shown (n=3) (Mack *et al*, 2001).

Figure 6.4

a

Chimeric gene lysate   Control lysate

43 kDa

Activity (U/ml)	9.28
Protein concentration	9.60
Specific activity (U/mg)	0.96

b
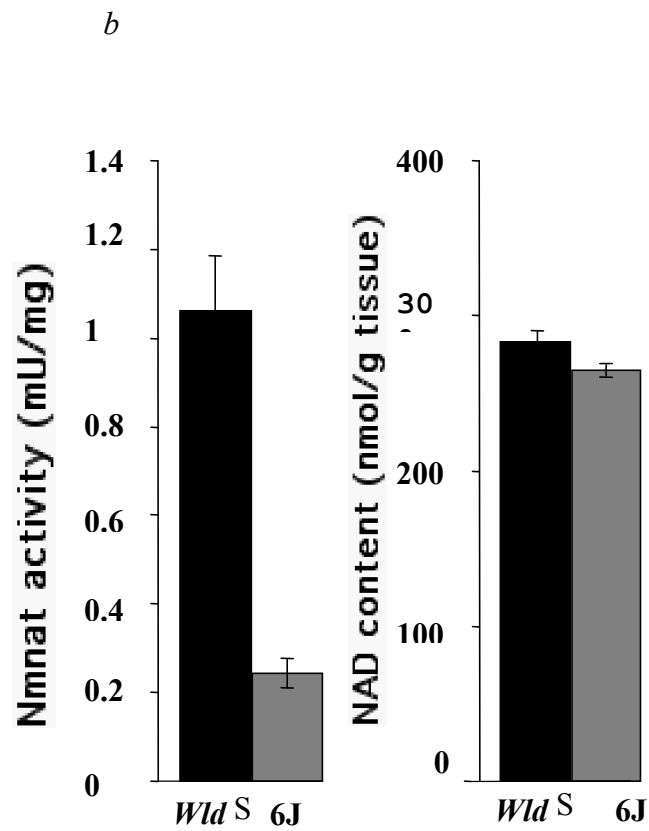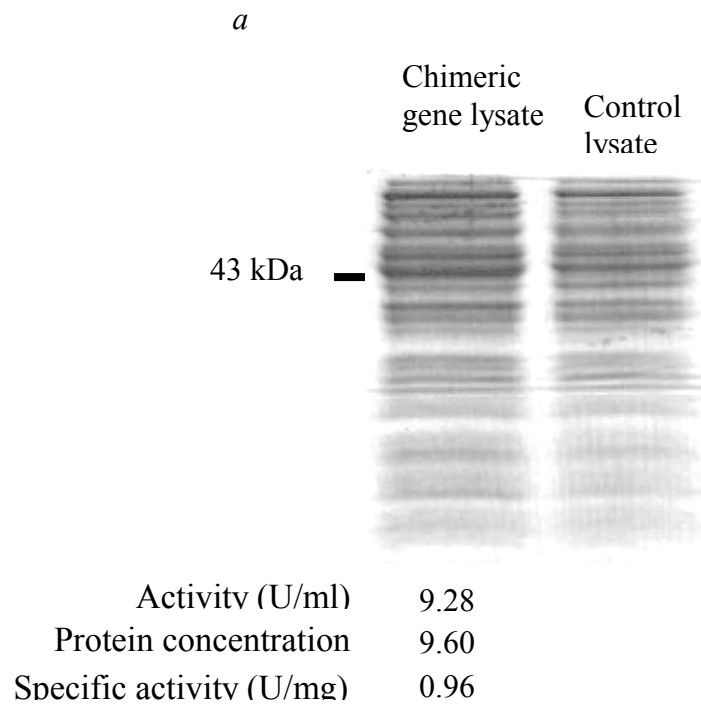
Figure 6.5 Transfection of COS-7 cell with pHβApr-1-N70-NLS or pHβApr-1-N70-NES, shows the predominant nucleus expression with N70-NLS (a), and cytoplasm expression with N70-NES (b). Red, anti-flag-tag M2 monoclonal antibody (Sigma, Germany); Blue, DAPI nucleus staining.

Figure 6.5

a)
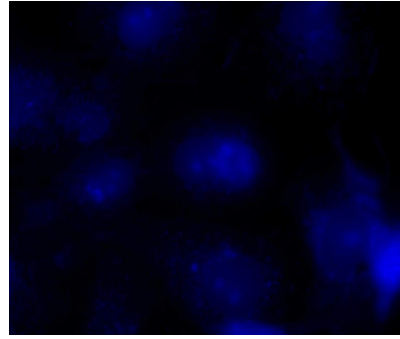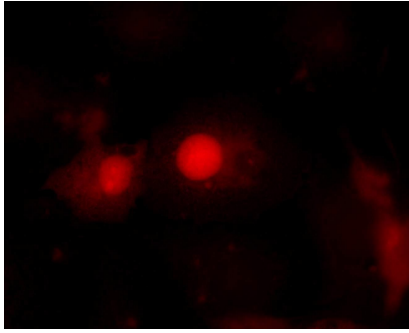
b)
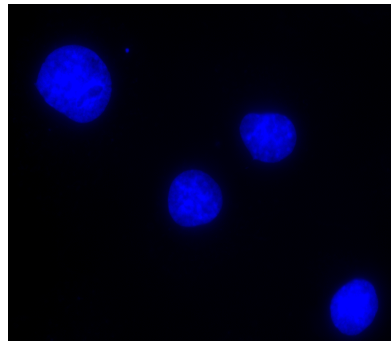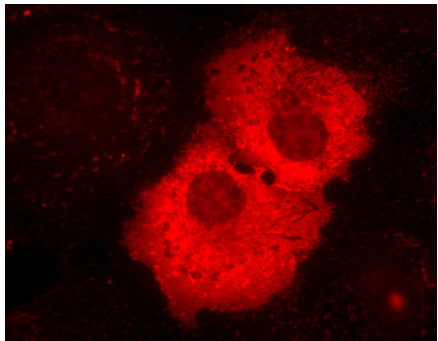
Figure 6.6 Transgenic N70-NLS and N70-NES do not show Wld^S phenotype.

a) Western blot showing the extent of 200-kD neurofilament protein degradation in distal sciatic nerve of N70-NLS or N70-NES heterozygotes/homozygote 56 hours after nerve transection. Complete preservation of NF-200 in uncut contralateral nerve was shown as well.

b) Fragmentation of distal axon integrity in N70-NLS or N70-NES homozygotes 53 hours after nerve transection using the YFP-H transgene. Scale bar: 100 μm.

Figure 6.6

a)

NLS hetero NLS hetero NLS homo Uncut (wt) NES hetero NES hetero NES homo

NF200 →
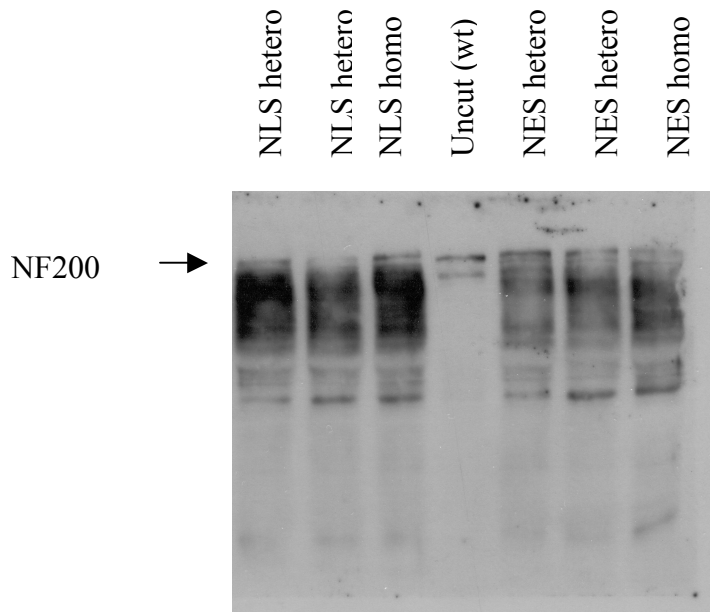
b)

NES 53 h lesion

NLS 53 h lesion

Table 6.1 Results of preservation of axons in transgenic N70-NLS or N70-NES mice by western blot (for preservation of neurofilaments) or visualizing YFP signal (for axonal integrity). Hetero = heterozygote; Homo = homozygote; WB = western blot.

a) Transgenic N70-NLS

Mice No.	Genotype	Lesion time	Result	Age
38m2	NLS hetero + YFP	3 days	No preservation in WB and YFP	~7 week old
38m4	NLS hetero + YFP	3 days	No preservation in WB and YFP	~7 week old
39m3	NLS hetero	3 days	No preservation in WB	~7 week old
37f2	NLS hetero + YFP	56 h	No preservation in WB and YFP	~8 week old
37f5	NLS hetero + YFP	56 h	No preservation in WB and YFP	~8 week old
37f6	NLS hetero + YFP	56 h	No preservation in WB and YFP	~8 week old
37m2	NLS hetero +YFP	56 h	No preservation in WB and YFP	~8 week old
36f3	NLS homo + YFP	56 h	No preservation in WB and YFP	~8 week old
36m4	NLS homo + YFP	56 h	No preservation in WB and YFP	~8 week old
34m3	NLS homo + YFP	53 h	No preservation in WB and YFP	~12 week old

b) Transgenic N70-NES

Mice No.	Genotype	Lesion time	Result	Age
34 f3	NES hetero	3 days	No preservation in WB	~8 week?
34f4	NES hetero + YFP	3 days	No preservation in WB and YFP	~8 week?
42m1	NES hetero	3 days	No preservation in WB	~7 week old
42m2	NES hetero	3 days	No preservation in WB	~7 week old
41f4	NES hetero	3 days	No preservation in WB	~7 week old
42f5	NES hetero	3 days	No preservation in WB	~7 week old
47f2	NES hetero	56 h	No preservation in WB	~8 week old
47m3	NES hetero	56 h	No preservation in WB	~8 week old
47m4	NES homo	56 h	No preservation in WB	~8 week old
39f3	NES homo + YFP	53 h	No preservation in WB and YFP	~12 week old

Summary

The slow Wallerian degeneration mouse, C57BL/Wld^S, carries a dominant mutation which delays Wallerian degeneration in the distal stump of an injured axons for several weeks in both central and peripheral nervous system (CNS and PNS). A highly unusual 85 kb tandem triplication was previously identified in the Wld^S mouse and during the period of my PhD work was shown to be the causative mutation, acting through a *Ube4b/Nmnat* chimeric gene contained within it.

The aims of project described in this thesis were 1) to develop a suitable method to track the inheritance of the 85 kb tandem triplication Wld^S allele; 2) to investigate the instability of 85 kb triplication at the chromosomal level; 3) to explore whether Wld^S could alleviate or rescue axon loss in PNS and CNS neurodegenerative disease by crossing Wld^S with mouse models of neurological disorders; 4) to characterize Wld^S protein and 5) to investigate the possible mechanism involving in delaying Wallerian degeneration.

Three genotyping methods for Wld^S were developed, namely PCR, Southern blotting and pulsed field gel electrophoresis (PFGE) (Chapter 3). The relative merits of these three methods for genotyping of Wld^S are discussed: PFGE is the only qualitative method to distinguish homozygotes from heterozygotes, but usually needs to be done post-mortem; PCR is a quick assay, however it is difficult to distinguish homozygotes from heterozygotes, or wild-type from false negative; Southern blotting could resolve the false negative problem in PCR with a constant wild-type band as an internal control, but could only distinguish homozygotes from heterozygotes partially by the relative strength of Wld^S-specific band and the constant band.

The PFGE method was used to look for any possible instability of the 85 kb tandem triplication in Wld^S at the chromosome level (Chapter 4). In total 180 chromosomes of WldS from three divergent breeding colonies at different ages have been examined and all found to carry the triplication. Thus, the triplication mutation is stable during both mitosis and meiosis. Such a study almost rules out instability as a source of phenotypic variation. It is essential to know this for accurate interpretation of studies the effect of Wld^S on neurodegenerative phenotypes (see Chapter 5).

At the outset of this work, the effect of Wld^S on axon degeneration in disease, as opposed to injury, was completely unknown. I collaborated with the group of Rudolf Martini (University of Würzburg) in a study showing that Wld^S protects axons in a myelin-related peripheral neuropathy (the $P0^{-/-}$ mouse)(Chapter 3). Simultaneously, work in another collaborating group revealed a similar protective effect in progressive motor neuronopathy (*pmn*). To investigate whether Wld^S has effect on axonal loss in CNS neurological disorders, I crossed Wld^S with *gad* (gracile axonal dystrophy) mice (Chapter 5), a simple genetic mouse model (with a defect in Uchl1, ubiquitin carboxy-terminal hydrolase l1) of CNS neurodegenerative disease with a defect in ubiquitin system and axonal spheroid pathology in CNS. Wld^S significantly reduced axonal spheroid numbers and secondary pathology (myelin loss and astrocyte activation). However, neuromuscular synapse pathology still developed with age, leading probably to the complex behavioral changes observed. The observations that Wld^S can alleviate axonal spheroid pathology in *gad* mice in our study and also delay axon loss in PNS disorders with dying-back axon degeneration in our collaborators' studies, suggest that formation of distal axonal spheroids shares a regulatory step with Wallerian degeneration and 'dying-back' axon loss without spheroids, and that Wld^S delays a central step of such axon pathology.

Ube4b/*Nmnat* (Wld^S) is known to delay Wallerian degeneration, however the protective mechanism is unknown. I also contributed to studies to characterize Wld^S and its role in delaying Wallerian degeneration. Firstly, I generated recombinant protein and polyclonal antiserum that were used to show that Wld^S protein is predominantly nuclear. Secondly, I generated transgenic mice carrying the N-terminal 70 amino acid (N70) of Wld^S fused with nuclear localization signal (NLS) or nuclear export signal (NES) to test whether the N70 was sufficient for the Wld^S phenotype and in which intracellular compartment it has to be located. The phenotype was analyzed by examining the preservation of neurofilament protein in lesioned nerves by western blotting or axonal integrity using a YFP marker protein. Transgenic N70-NLS or N70-NES heterozygotes / homozygotes did not show Wld^S phenotype, however there was not detectable N70-NLS or N70-NES protein expression level by western blotting.

In conclusion, pulsed field gel electrophoresis (PFGE) is the only qualitative method to distinguish Wld^S homozygotes from heterozygotes comparing to the alternatives of PCR

and Southern blotting. The Wld^S triplication is stable under normal conditions and is the predominant, and possibly exclusive, allele in the current Wld^S breeding colonies. Wld^S alleviates chromic PNS and CNS axon pathology in *gad* mice. Formation of distal axonal spheroids shares a regulatory step with Wallerian degeneration and 'dying-back' axon loss without spheroids. The N70-NLS or N70-NES experiments were inconclusive with the existing transgenic lines but Wld^S was shown to be a predominantly nuclear protein using the antiserum that I generated.

Zusammenfassung

Die C57BL/*Wld*^S (langsame Waller'sche Degeneration) Maus, besitzt eine dominante Mutation, welche die Waller'sche Degeneration am distalen Ende eines verletzten Axons sowohl im zentralen (ZNS), als auch im peripheren Nervensystem (PNS) über mehrere Wochen hinauszögert. Eine äußerst ungewöhnliche 85 kb Tandem Triplikation wurde vorher in der *Wld*^S Maus identifiziert. Während meiner Dissertationsarbeit konnte gezeigt werden, daß diese Mutation über ein darin enthaltenes *Ube4b*/*Nmnat* chimeres Gen agiert.

Die Ziele des Projektes dieser Dissertation sind: 1) Die Entwicklung einer geeigneten Methode zur Verfolgung der Herkunft des 85 kb Tandem Triplikation *Wld*^S Allels, 2) die Untersuchung der Stabilität der 85 kb Triplikation auf chromosomaler Ebene; 3) die Erkundung ob *Wld*^S den Axonenverlust bei neurodegenerativen Krankheiten im PNS und ZNS durch Kreuzung mit deren Mausmodellen abmildern oder verhindern kann; 4) die Charakterisierung des Wld^S Proteins und 5) die Untersuchung von möglichen Mechanismen, welche die Waller'sche Degeneration verzögern.

Drei Methoden zur Genotypenbestimmung von *Wld*^S wurden entwickelt: PCR, Southern Blotting und Pulsed-Field Gel Electrophorese (PFGE) (Kapitel 3). Die relativen Vorteile dieser drei Methoden zur Genotypisierung von *Wld*^S werden im folgenden diskutiert: PFGE ist die einzige qualitative Methode um Homozygoten von Heterozygoten zu unterscheiden, muß aber post-mortem durchgeführt werden; PCR ist eine rapide Methode, bei der es aber schwierig ist, Homozygoten von Heterozygoten, oder Wildtypen von Falsch-Negativen zu unterscheiden; Southern Blotting würde das Problem der Falsch-Negativen im PCR mithilfe einer konstanten Wildtyp-Bande als Standard lösen, erlaubt aber die Unterscheidung von Homozygoten von Heterozygoten nur über einen Vergleich der relativen Bandintensitäten der Wld^S mit der Standardbande.

Die PFGE Methode wurde verwendet, um eventuelle Instabilitaeten der 85 kb Triplikation in *Wld*^S auf chromosomaler Ebene zu untersuchen (Kapitel 4). Es wurden insgesamt 180 Chromosomen von *Wld*^S aus drei divergenten Kolonien und bei verschiedenen Altersabschnitten untersucht, und alle enthielten die Triplikation. Dies zeigt die Stabilität der Triplikation während der Mitose als auch der Meiose. Diese Untersuchung diente vor allem dazu, Chromosomeninstabilität als Quelle von phänotypischer Variation auszuschließen. Für die genaue Auswertung der Untersuchungen der Wirkung von *Wld*^S auf neurodegenerative Phänotypen (siehe Kapitel 5) war diese Feststellung essentiell.

Im Gegensatz zu den Effekten von *Wld*^S auf Läsionen waren zu Beginn dieser Arbeit die Effekte von *Wld*^S auf axonal degenerative Krankheiten noch völlig unbekannt. In Kollaboration mit der Gruppe von Rudolf Martini (Universität Würzburg) arbeitete ich an einer Studie, die zeigte, daß *Wld*^S Axone in einer Maus mit einer Myelin Neuropathie im PNS (*P0*^-/- Maus) schützt (Kapitel 3). Gleichzeitig konnte in Zusammenarbeit mit einer anderen Gruppe ein ähnlicher Schutzeffekt bei der Progressiven Motorneuropathie (*pmn*) gezeigt werden. Um zu untersuchen, ob *Wld*^S eine Wirkung auf den Axonenverlust in neurologischen Krankheiten des ZNS hat, kreuzte ich *Wld*^S mit *gad* (gracile axonal dystrophy) Mäusen (Kapitel 5). *gad* ist ein einfaches genetisches Mausmodell (Defekt in Uchl1, der Ubiquitin carboxyterminalen Hydrolase l1) einer zentral neurodegenerativen Krankheit mit einem Defekt im Ubiquitin System und axonaler Spheroid Pathologie. *Wld*^S konnte im signifikanten Maße die Anzahl der Spheroide und sekundäre pathologische Symptome wie Myelinverlust und Astrozytenaktivation reduzieren. Pathologische Symptome der Muskelsynapsen entwickelte sich dennoch mit wachsendem Alter, wodurch vermutlich die Entwicklung komplexer Verhaltensänderungen herbeigeführt wurde. Sowohl die Beobachtungen in unseren Studien, daß *Wld*^S die Pathologie der axonalen Spheroide in *gad* Mäusen abmildert, als auch die Beobachtungen der kollaborierenden Gruppe, daß *Wld*^S die Axonverluste in PNS Krankheiten mit Rückdegeneration verzögert, läßt vermuten, daß die Formation eines Spheroids im distalen Axon bei einem regulatorischen Schritt stattfindet, und zwar sowohl bei der Wallerdegeneration und als auch bei rückdegenerierenden Axonverlusten ohne Spheroidformation. *Wld*^S verzögert daher einen zentralen Schritt in der Pathologie von Axonen.

Es ist bekannt, daß *Ube4b*/*Nmnat* (*Wld*^S) die Wallerdegeneration verzögert, jedoch ist der protektive Mechanismus unbekannt. Ich habe daher Untersuchungen durchgeführt, die zur Charakterisierung von *Wld*^S führten, und dessen Rolle in der Verzögerung der Waller Degeneration darstellten. Zunächst generierte ich ein rekombinantes Protein und ein polyklonales Antiserum, mit deren Hilfe es ist gezeigt worden, daß das Wld^S Protein sich überwiegend im Nukleus befindet. Zweitens produzierte ich eine transgene Maus, welche die N-terminalen 70 Aminosäuren (N70) von *Wld*^S in Fusion mit einem Nuklearen Lokalisations Signal (NLS) bzw. Nuclear Export Signal (NES) enthielt. Diese dienten dazu zu testen, ob N70 allein genügte, um den *Wld*^S Phänotyp hervorzurufen, und in welchem Zellkompartiment das Protein lokalisiert war. Der Phänotyp wurde anhand der Erhaltung von Neurofilament Proteinen in den verletzten Nerven untersucht. Die Experimente liefen über Western Blot bzw. über Untersuchungen der Axonenintergrität unter Verwendung eines YFP Marker Proteins. Transgene N70-NLS oder N70-NES Heterozygoen bzw. Homozygoten zeigten keinen *Wld*^S Phänotyp, wobei aber auch keine N70-NLS oder N70-NES Proteine im Western Blot detektiert wurden.

Im Vergleich zu den Methoden PCR und Southern Blotting war PFGE letztendlich die einzige qualitative Methode um *Wld*^S Homozygoten von Heterozygoten zu unterscheiden. Die *Wld*^S Triplikation ist unter Normalbedingungen stabil und ist das prädominierende und möglicherweise einzige Allel in den gegenwärtigen *Wld*^S Züchtungen. *Wld*^S mildert chronische pathologische Sympome in PNS und ZNS Axonen von *gad* Mäusen. Die Formation eines distalen axonalen Spheroids repräsentiert einen Regulationsschritt bei der Wallerdegeneration und bei rückwärtigen Axonenverlusten ohne Spheroide. Die N70-NLS und N70-NES Experimente waren bei den vorhandenen transgenen Kolonien nicht eindeutig, aber unter dem von mir hergestellten Antiserum konnte gezeigt werden, daß Wld^S ein vorüberwiegend nuklear lokalisiertes Protein ist.

CHAPTER 7

References

Alves-Rodrigues A., Gregori L. & Figueiredo-Pereira M. E. Ubiquitin, cellular inclusions and their role in neurodegeneration. *Trends Neurosci*. 21 (1998): 516-520.

Ando M., Yamauchi M., Fujita K., Kakita M., Nagata Y. Induction of tissue transglutaminase in rat superior cervical sympathetic ganglia following in vitro stimulation of retinoic acid. *Neurosci Res*. 24 (1996): 357-62.

Arnold J., Dawson S., Fergusson J., Lowe J., Landon M., Mayer R.J. Ubiquitin and its role in neurodegeneration. *Prog Brain Res*. 117 (1998): 23-24.

Balducci E., Emanuelli M., Raffaelli N., Ruggieri S., Amici A., Magni G., Orsomando G., Polzonetti V., Natalini P. Assay methods for nicotinamide mononucleotide adenylyltransferase of wide applicability. *Anal Biochem*. 228(1995): 64-8.

Beites C.L., Xie H., Bowser R., Trimble W.S. The septin CDCrel-1 binds syntaxin and inhibits exocytosis. *Nat Neurosci*. 2 (1999): 434-439.

Bence N.F., Sampat R.M., Kopito R.R. Impairment of the ubiquitin-proteasome system by protein aggregation. *Science*. 292 (2001): 1552-1555.

Bizz A., Schaetzle B., Patton A., Gambetti P. & Autilio-Gambetti L. Axonal transport of two major components of the ubiquitin system: free ubiquitin and ubiquitin carboxyl-terminal hydrolyse PGP9.5. *Brain Res*. 548 (1991): 292-299.

Bomont P., Cavalier L., Blondeau F., Ben Hamida C., Belal S., Tazir M., Demir E., Topaloglu H., Korinthenberg R., Tuysuz B., Landrieu P., Hentati F., Koenig M. The gene encoding gigaxonin, a new member of the cytoskeletal BTB/kelch repeat family, is mutated in giant axonal neuropathy. *Nat Genet*. 26 (2000): 370-374.

Bordet T., Lesbordes J.C., Rouhani S., Castelnau-Ptakhine L., Schmalbruch H., Haase G., Kahn A. Protective effects of cardiotrophin-1 adenoviral gene transfer on neuromuscular degeneration in transgenic ALS mice. *Hum Mol Genet*. 10 (2001): 1925-33.

Bregman B.S., Kunkel-Bagden E., Schnell L., Dai H.N., Gao D., and Schwab M.E. Recovery from spinal cord injury mediated by antibodies to neurite growth inhibitors. *Nature*. 378(1995): 498-501.

Brendza R.P., O'Brien C., Simmons K., McKeel D.W., Bales K.R., Paul S.M., Olney J.W., Sanes J.R., Holtzman D.M. PDAPP: YFP double transgenic mice: a tool to study amyloid-β associated changes in axonal, dendritic and synaptic structures. *J Comp Neurol*. 456 (2003): 375-383.

Bridges C.B. *Science*. 83 (1936): 210-211.

Brown M.C., Perry V.H., Hunt S.P., Lapper S.R. Further studies on motor and sensory nerve regeneration in mice with delayed Wallerian degeneration. *Eur J Neurosci*. 6 (1994): 420-428.

Bruijn L.I., Becher M.W., Lee M.K., Anderson K.L., Jenkins N.A., Copeland N.G., Sisodia S.S., Rothstein J.D., Borchelt D.R., Price D.L., Cleveland D.W. ALS-linked SOD1 mutant G85R mediates damage to astrocytes and promotes rapidly progressive disease with SOD1-containing inclusions. *Neuron*. 18 (1997): 327-338.

Bu B., Li J., Davies P., Vincent I. Deregulation of cdk5, hyperphosphorylation, and cytoskeletal pathology in the Niemann-Pick Type C murine model. *J Neurosci*. 22 (2002): 6515-6525.

Buckmaster E.A., Perry V.H. & Brown M.C. The rate of Wallerian degeneration in cultured neurons from wild type and C57BL/*Wld*[S] mice depends on time in culture and may be extended in the presence of elevated K^+ levels. *Eur J Neurosci*. 7 (1995): 1596-602.

Chalfie M., and Kain S. (eds). Green fluorescent protein: properties, applications, and protocols (New York: Wiley-Liss). 1998.

Chalfie M., Tu Y., Euskirchen G., Ward W.W., and Prasher D.C. Green fluorescent protein as a marker for gene expression. *Science*. 263 (1994): 802-805.

Cheng C.L.Y., Povlishock J.T. The effect of traumatic brain injury on the visual system: a morphologic characterization of reactive axonal change. *J. Neurotrauma*. 5 (1988): 47-60.

Chung K.K., Zhang Y., Lim K.L., Tanaka Y., Huang H., Gao J., Ross C.A., Dawson V.L., Dawson T.M. Parkin ubiquitinates the α-synuclein-interacting protein synphilin-1: implications for the Lewy body formation in Parkinson's disease. *Nat Med*. 7 (2001): 1144-50.

Conn P.M. (ed.). In methods in enzymology. Green fluorescent protein (New York: Academic Press). Volumn 302: 1999.

Cifuentes-Diaz C., Nicole S., Velasco M.E., Borra-Cebrian C., Panozzo C., Frugier T., Millet G., Roblot N., Joshi V., Melki J. Neurofilament accumulation at the motor

endplate and lack of axonal sprouting in a spinal muscular atrophy mouse model. *Hum Mol Genet*. 11(2002): 1439-47.

Cliffer K.D., Siuciak J.A., Carson S.R., Radley H.E., Park J.S., Lewis D.R., Zlotchenko E., Nguyen T., Garcia K., Tonra J.R., Stambler N., Cedarbaum J.M., Bodine S.C., Lindsay R.M., DiStefano P.S. Physiological characterization of Taxol-induced large-fiber sensory neuropathy in the rat. *Ann Neurol*. 43 (1998): 46-55.

Coleman M. P., Conforti L., Buckmaster E. A., Tarlton A., Ewing R. M., Brown M.C., Lyon M. F. & Perry V. H. An 85-kb tandem triplication in the slow Wallerian degeneration (*Wld^S*) mouse. *Proc Natl Acad Sci*. USA 95 (1998): 9985-9990.

Coleman M.P., and Perry V.H. Axon pathology in neurological disease: a neglected therapeutic target. *Trends Neurosci*. 25(2002): 532-7.

Conforti L., Tarlton A., Mack T. GA., Mi W., Buckmaster E. A., Wagner D., Perry V. H., and Coleman M. P. A *Ufd2/D4Cole1e* chimeric protein and overexpression of Rbp7 in the slow Wallerian degeneration (*Wld^S*) mouse. *Proc Natl Acad Sci*. USA 97(2000): 11377-11382.

Crawford T.O., Hsieh S.T., Schryer B.L., Glass J.D. Prolonged axonal survival in transected nerves of C57BL/Ola mice is independent of age. *J Neurocytol*. 24 (1995): 333-40.

Cummings C.J., Reinstein E., Sun Y., Antalffy B., Jiang Y., Ciechanover A., Orr H.T., Beaudet A.L., Zoghbi H.Y. Mutation of the E6-AP ubiquitin ligase reduces nuclear inclusion frequency while accelerating polyglutamine-induced pathology in SCA1 mice. *Neuron*. 24 (1999): 879-892.

Dal Canto M.C. & Gurney M.E. Neuropathological changes in two lines of mice carrying a transgene for mutant human Cu, Zn SOD, and in mice overexpression wild type human SOD: a model of familial amyotrophic lateral sclerosis (FALS). *Brain Res*. 676 (1995): 25-40.

Dang L.C., Melandri F.D. & Stein R.S. Kinetic and mechanistic studies on the hydrolysis of ubiquitin C-terminal 7-amino-4-methylcoumarin by deubiquitinating enzymes. *Biochemistry*. 37 (1998): 1868-1879.

Day I. N. M. & Thompson R. J. Molecular cloning of cDNA coding for human PGP9.5 protein. A novel cytoplasmic marker for neurons and neuroendocrine cells. *FEBS Lett*. 210 (1987): 157-160.

Day I. N. M., Hinks L. J. & Thompson R. J. The structure of the human gene encoding protein gene product 9.5 (PGP9.5), a neuron-specific ubiquitin C-terminal hydrolase, *Biochem J*. 268 (1990): 521-524.

Deckwerth T. L. & Johnson E. M. Jr. Neurites can remain viable after destruction of the neuronal soma by programmed cell death (apoptosis). *Dev Biol*. 165 (1994): 63-72.

Deng H.X., Hentati A., Tainer J.A., Iqbal Z., Cayabyab A., Hung W.Y., Getzoff E.D., Hu P., Herzfeldt B., Roos R.P., et al. Amyotrophic lateral sclerosis and structural defects in Cu, Zn superoxide dismutase. *Science*. 261(1993): 1047-51.

Dewar D., Yam P., McCulloch J. Drug development for stroke: importance of protecting cerebral white matter. *Eur J Pharmacol*. 375 (1999): 41-50.

Di Lisa F., Ziegler M. Pathophysiological relevance of mitochondria in NAD(+) metabolism. *FEBS Lett*. 492 (2001): 4-8.

DiAntonio A., Haghighi A.P., Portman S.L., Lee J.D., Amaranto A.M., Goodman C.S. Ubiquitination-dependent mechanisms regulate synaptic growth and function. *Nature*. 412 (2001): 449-452.

DiFiglia M., Sapp E., Chase K.O., Davies S.W., Bates G.P., Vonsattel J.P., Aronin N. Aggregation of huntingtin in neuronal intranuclear inclusions and dystrophic neurites in brain. *Science*. 277 (1997): 1990-1993.

Emanuelli M., Amici A., Carnevali F., Pierella F., Raffaelli N., Magni G. Identification and characterization of a second NMN adenylyltransferase gene in Saccharomyces cerevisiae. *Protein Expr Purif*. 27 (2003): 357-64.

Emanuelli M., Carnevali F., Saccucci F., Pierella F., Amici A., Raffaelli N., Magni G. Human NMN adenylyltransferase: molecular cloning, chromosomal localization, tissue mRNA levels, bacterial expression, and enzymatic properties. *J Biol Chem.* 276 (2001): 406-412.

Feng G., Mellor R.H., Bernstein M., Keller-Peck C., Nguyen Q.T., Wallace M., Nerbonne J.M., Lichtman J.W., Sanes J.R. Imaging neuronal subsets in transgenic mice expressing multiple spectral variants of GFP. *Neuron*. 28(2000): 41-51.

Ferri A., Sanes J.R., Coleman M.P., Cunningham J.M., Kato A.C. Inhibiting axon degeneration and synapse loss attenuates apoptosis and disease progression in a mouse model of motoneuron disease. *Curr Biol.* 13 (2003): 1-20.

Finn, J. T., Weil M., Archer F., Siman R., Srinivasan A., Raff M.C. Evidence that Wallerian degeneration and localized axon degeneration induced by local neurotrophin deprivation do not involve caspases. *J Neurosci.* 20 (2000): 1333-1341.

Frei R., Motzing S., Kinkelin I., Schachner M., Koltzenburg M., Martini R. Loss of distal axons and sensory Merkel cells and features indicative of muscle denervation in hindlimbs of P0-deficient mice. *J Neurosci.* 19(1999): 6058-67.

Fujimura H., Lacroix C. & Said G. Vulnerability of nerve fibres to ischaemia. A quantitative light and electron microscope study. *Brain.* 114 (1991): 1929-1942.

Fukuda M., Asano S., Nakamura T., Adachi M., Yoshida M., Yanagida M., Nishida E. CRM1 is responsible for intracellular transport mediated by the nuclear export signal. *Nature.* 390 (1997): 308-311.

Galvin J.E., Uryu K., Lee V.M., Trojanowski J.Q. Axon pathology in Parkinson's disease and Lewy body dementia contains α-, β-, and γ-synuclein. *Proc Natl Acad Sci.* 96 (1999): 13450-13455.

Garbern J.Y., Yool D.A., Moore G.J., Wilds I.B., Faulk M.W., Klugmann M., Nave K.A., Sistermans E.A., van der Knaap M.S., Bird T.D., Shy M.E., Kamholz J.A.,

George R., Griffin J.W. The proximo-distal spread of axonal degeneration in the dorsal columns of the rat. *J Neurocytol.* 23 (1994): 657-667.

Gillingwater T. H., Ribchester R. R. Compartmental neurodegeneration and synaptic plasticity in the *Wld*[S] mutant mouse. *J Physiol.* 534 (2001): 627-639.

Gillingwater T. H., Thomson D., Mack T. G., Soffin E. M., Mattison R. J., Coleman M. P., Ribchester R. R. Age-dependent synapse withdrawal at axotomised neuromuscular junctions in *Wld*[S] mutant and *Ube4*b/*Nmnat* transgenic mice. *J Physiol.* 543 (2002): 739-755.

Glass J.D., Brushart T.M., George E.B. & Griffin J.W. Prolonged survival of transected nerve fibres in C57BL/Ola mice is an intrinsic characteristic of the axon. *J Neurocytol.* 22 (1993): 311-21.

Glass J.D. & Griffin J.W. Retrograde transport of radiolabeled cytoskeletal proteins in transected nerves. *J Neurosci*. 14 (1994): 3915-21.

Gondo Y., Gardner J.M., Nakatsu Y., Durham-Pierre D., Deveau S.A., Kuper C. & Brilliant M.H. High-frequency genetic reversion mediated by a DNA duplication: the mouse pink-eyed unstable mutation. *Proc Natl Acad Sci. USA* 90 (1993): 297-301.

Graham D.I., McIntosh T.K., Maxwell W.L., Nicoll J.A. Recent advances in neurotrauma. *J Neuropathol Exp Neurol*. 59 (2000): 641-51.

Griffiths I., Klugmann M., Anderson T., Yool D., Thomson C., Schwab M.H., Schneider A., Zimmermann F., McCulloch M., Nadon N., Nave K.A. Axonal swellings and degeneration in mice lacking the major proteolipid of myelin. *Science*. 280 (1998): 1610-1613.

Griffiths I.R. Patients lacking the major CNS myelin protein, proteolipid protein 1, develop length-dependent axonal degeneration in the absence of demyelination and inflammation. *Brain*. 125(2002): 551-61.

Gurney A.L., Carver-Moore K., de Sauvage F.J., Moore M.W. Thrombocytopenia in c-mpl-deficient mice. *Science*. 265 (1994): 1445-7.

Ha H.C. & Snyder S.H. Poly (ADP-ribose) polymerase is a mediator of necrotic death by ATP depletion. *Proc Natl Acad Sci. USA*. 96 (1999): 13978-13982.

Hardy J. and Gwinn-Hardy K. Genetic classification of primary neurodegenerative disease. *Science*. 282 (1998): 1075-1079.

Hatakeyama S., and Nakayama K.I. U-box proteins as a new family of ubiquitin ligases. *Biochem Biophys Res Commun*. 302 (2003): 635-645.

Hershko A., and Ciechanover A. The ubiquitin system. *Annu Rev Biochem*. 67 (1998): 425-479.

Hicke L. Protein regulation by monoubiquitination. *Nat Rev Mol Cell Biol*. 2 (2001): 195-201.

Howland D.S., Liu J., She Y., Goad B., Maragakis N.J., Kim B., Erickson J., Kulik J., DeVito L., Psaltis G., DeGennaro L.J., Cleveland D.W., Rothstein J.D. Focal loss of the glutamate transporter EAAT2 in a transgenic rat model of SOD1 mutant-mediated amyotrophic lateral sclerosis (ALS). *Proc Natl Acad Sci. U S A* 99 (2002): 1604-1609.

Ichihara N., Wu J., Chui D.H., Yamazaki K., Wakabayashi T., Kikuchi T. Axonal degeneration promotes abnormal accumulation of amyloid β-protein in ascending gracile tract of gracile axonal dystrophy (GAD) mouse. *Brain Res*. 695 (1995): 173-178.

Imai Y., Soda M., Takahashi R. Parkin suppresses unfolded protein stress-induced cell death through its E3 ubiquitin-protein ligasse activity. *J Biol Chem*. 275 (2000): 35661-35664.

Jafari S.S., Maxwell W.L., Neilson M., Graham D.I. Axonal cytoskeletal changes after non-disruptive axonal injury. *J Neurocytol*. 26 (1997): 207-21.

Jeffreys A.J., Royle N.J., Wilson V., Wong Z. Spontaneous mutation rates to new length alleles at tandem-repetitive hypervariable loci in human DNA. *Nature*. 332 (1988): 278.

Joazeiro C.A., and Weissman A.M. RING finger proteins: mediators of ubiquitin ligase activity. *Cell*. 102 (2000): 549-552.

Kajimoto Y., Hashimoto T., Shirai Y., Nishino N., Kuno T., Tanaka C. cDNA cloning and tissue distribution of a rat ubiquitin carboxyl-terminal hydrolase PGP9.5. *J Biochem*. 117 (1992): 28-32.

Katzmann D.J., Babst M. & Emr S.D. Ubiquitin-dependent sorting into the multivesicular body pathway requires the function of a conserved endosomal protein sorting complex, ESCRT-1. *Cell*. 106 (2001): 145-155.

Kenward N., Hope J., Landon M., Mayer R.J. Expression of polyubiquitin and heat-shock protein 70 genes increases in the later stages of disease progression in scrapie-infected mouse brain. *J Neurochem*. 62 (1994): 1870-1877.

Kitada T., Asakawa S., Hattori N., Matsumine H., Yamamura Y., Minoshima S., Yokochi M., Mizuno Y., Shimizu N. Mutations in the parkin gene cause autosomal recessive juvenile parkinsonism. *Nature*. 392 (1998): 605-608.

Kikuchi T., Mukoyama M., Yamazaki K. & Moriya H. Axonal degeneration of ascending sensory neurons in gracile axonal dystrophy mutant mouse. *Acta Neuropathol*. (Berl.) 80 (1990): 145-151.

Koegl M., Hoppe T., Schlenker S., Ulrich H. D., Mayer T. U., Jentsch S. A novel ubiquitination factor, E4, is involved in multiubiquitination chain assembly. *Cell*. 96(1999): 635-644.

Kornek B., Storch M. K., Weissert R., Wallstroem E., Stefferl A., Olsson T., Linington C., Schmidbauer M., Lassmann H. Multiple sclerosis and chronic autoimmune encephalomyelitis: a comparative quantitative study of axonal injury in active, inactive, and remyelinated lesions. *Am J Pathol*. 157(2000): 267-76.

Kurihara L.J., Kikuchi T., Wada K., Tilghman S.M. Loss of Uch-L1 and Uch-L3 leads to neurodegeneration, posterior paralysis and dysphagia. *Hum Mol Genet*. 10(2001): 1963-70.

Larsen C. N., Price J. S. & Wilkinson K. D. Substrate binding and catalysis by ubiquitin C-terminal hydrolases: Identification of two active site residues. *Biochemistry*. 35 (1996): 6735-6744.

Larsen C.N., Krantz B.A., Wilkinson K.D. Substrate specificity of deubiquitinating enzymes: ubiquitin C-terminal hydrolases. *Biochemistry*. 37 (1998): 3358-3368.

Laser H., Mack T.G.A., Wagner D., Coleman M.P. Proteasome inhibition arrests neurite outgrowth and causes 'dying-back' degeneration in primary culture. *In press*.

Leroy E., Boyer R., Auburger G., Leube B., Ulm G., Mezey E., Harta G., Brownstein M.J., Jonnalagada S., Chernova T., Dehejia A., Lavedan C., Gasser T., Steinbach P.J., Wilkinson K.D., Polymeropoulos M.H. The ubiquitin pathway in Parkinson's disease. *Nature*. 395 (1998): 451-452.

Lewis J., McGowan E., Rockwood J., Melrose H., Nacharaju P., Van Slegtenhorst M., Gwinn-Hardy K., Paul Murphy M., Baker M., Yu X., Duff K., Hardy J., Corral A., Lin W. L., Yen S. H., Dickson D. W., Davies P., Hutton M. Neurofibrillary tangles, amyotrophy and progressive motor disturbance in mice expressing mutant (P301L) tau protein. *Nat Genet*. 25 (2000): 402-405.

Liberski P.P., Budka H. Neuroaxonal pathology in Creutzfeldt-Jakob disease. *Acta Neuropathol* (Berl). 97 (1999): 329-334.

Lubinska L. Early course of Wallerian degeneration in myelinated fibres of the rat phrenic nerve. *Brain Res*. 130 (1977): 47-63.

Ludwin S.K., Bisby M.A. Delayed wallerian degeneration in the central nervous system of Ola mice: an ultrastructural study. *J Neurol Sci*. 109 (1992): 140-7.

Lunn E.R., Perry V.H., Brown M.C., Rosen H. & Gordon S. Absence of Wallerian degeneration does not hinder regeneration in peripheral nerve. *Eur J Neurosci.* 1 (1989): 27-33.

Lunn E.R., Brown M.C., Perry V.H. The pattern of axonal degeneration in the peripheral nervous system varies with different types of lesion. *Neuroscience.* 35 (1990): 157-165.

Lyon M. F., Ogunkolade B. W., Brown M.C., Atherton D. J. & Perry V. H. *Proc Natl Acad Sci.* USA 90 (1993): 9717-20.

Mack T. G. A., Reiner M., Beirowski B., Mi W., Coleman M. P. *et al.* Wallerian degeneration of injured axons and synapses is delayed by a Ube4b/Nmnat chimeric gene. *Nat Neurosci.* 4 (2001): 1199-206.

Magni G., Amici A., Emanuelli M., Raffaelli N. & Ruggieri S. Enzymology of NAD^+ synthesis. *Adv Enzymol Relat Areas Mol Biol.* 73 (1999): 135-182.

Martini R. The effect of myelinating Schwann cells on axons. *Muscle Nerve.* 24(2001): 456-66.

Mi W., Glass J. D., Coleman M. P. Stable inheritance of an 85-kb triplication in C57BL/*Wld*[S] mice. *Mutat Res.* 526(2003): 33-7.

Mi W., Conforti L., Coleman M. P. A genotyping method to detect a unique europrotective factor for axon (*Wld*[S]). *J Neurosci Meth.* 113(2002): 215-8.

Miike T., Ohtani Y., Nishiyama S., Matsuda I. Pathology of skeletal muscle and intramuscular nerves in infantile neuroaxonal dystrophy. *Acta Neuropathol* (Berl). 69 (1986): 117-23.

Miura H., Oda K., Endo C., Yamazaki K., Shibasaki H., Kikuchi T. Progressive degeneration of motor nerve terminals in *gad* mutant mouse with hereditary sensory axonopathy. *Neuropathol Appl Neurobiol.* 19 (1993): 41-51.

Mori H., Kondo J., Ihara Y. Ubiquitin is a component of paired helical filaments in Alzheimer's disease. *Science.* 235 (1987): 1641-1644.

Myung J., Kim K.B., Crews C.M. The ubiquitin-proteasome pathway and proteasome inhibitors. *Med Res Rev.* 21(2000): 245-73.

Mukoyama M., Yamazaki K., Kikuchi T. & Tomita T. Neuropathology of gracile axonal dystrophy (GAD) mouse (an animal model of central axonopathy in primary sensory neurons). *Acta Neuropathol.* 79 (1989): 294-299.

Muller H.J., Prokofieva-Belgovskaya A.A. & Kossikov K.V. *Acad Sci. USSR*. 1 (1936): 87-88.

Narayanan S., Fu L., Pioro E., De Stefano N., Collins D.L., Francis G.S., Antel J.P., Matthews P.M., Arnold D.L. Imaging of axonal damage in multiple sclerosis: spatial distribution of magnetic resonance imaging lesions. *Ann Neurol*. 41(1997): 385-91.

Nagayama T., Simon R.P., Chen D., Henshall D.C., Pei W., Stetler R.A., Chen J. Activation of poly (ADP-ribose) polymerase in the rat hippocampus may contribute to cellular recovery following sublethal transient global ischemia. *J Neurochem*. 74 (2000): 1636-45.

Oda K., Yamazaki K., Miura H., Shibasaki H. & Kikuchi T. Dying back type axonal degeneration of sensory nerve terminals in muscle spindles of the gracile axonal dystrophy (GAD) mutant mouse. *Neuropathol Appl Neurobiol*. 18 (1992): 265-281.

Oosthuyse B *et al*. Deletion of the hypoxia-response element in the vascular endothelial growth factor promoter causes motor neuron degeneration. *Nat Genet*. 28 (2001): 131-8.

Osaka H., Wang Y-L., Takada K., Takizawa S., Setsuie R., Li H., Sato Y., Nishikawa K., Sun Y.J., Sakurai M., Harada T., Hara Y., Kimura I., Chiba S., Namikawa K., Kiyama H., Noda M., Aoki S., Wada K. Ubiquitin carboxy-terminal hydrolase L1 binds to and stabilizes monoubiquitin in neurons. *Hum Mol Genet.* In press.

Pardo C.A., Xu Z., Borchelt D.R., Price D.L., Sisodia S.S., Cleveland D.W. Superoxide dismutase is an abundant component in cell bodies, dendrites, and axons of motor neurons and in a subset of other neurons. *Proc Natl Acad Sci. U S A* 92 (1995): 954-8.

Parson S.H., Mackintosh C.L., Ribchester R.R. Elimination of motor nerve terminals in neonatal mice expressing a gene for slow wallerian degeneration (C57BL/*Wld^S*). *Eur J Neurosci*. 9(1997): 1586-92.

Perry V.H., Lunn E.R., Brown M.C., Cahusac S. & Gordon S. Evidence that the rate of Wallerian degeneration is controlled by a single autosomal dominant gene. *Eur J Neurosci*. 2 (1990): 408-413.

Perry V.H., Brown M.C., Lunn E.R. Very Slow Retrograde and Wallerian Degeneration in the CNS of C57BL/Ola Mice. *Eur J Neurosci*. 3 (1991): 102-105.

Perry V.H., Brown M.C., and Tsao J.W. The effectiveness of the gene which slows the rate of Wallerian degeneration in C57BL/Ola mice declines with age. *Eur J Neurosci*. 4 (1992): 1000-1002.

Personett D., Fass U., Panickar K., McKinney M. Retinoic acid-mediated enhancement of the cholinergic/neuronal nitric oxide synthase phenotype of the medial septal SN56 clone: establishment of a nitric oxide-sensitive proapoptotic state. *J Neurochem*. 74 (2000): 2412-24.

Probst A., Gotz J., Wiederhold K.H., Tolnay M., Mistl C., Jaton A.L., Hong M., Ishihara T., Lee V.M., Trojanowski J.Q., Jakes R., Crowther R.A., Spillantini M.G., Burki K., Goedert M. Axonopathy and amyotrophy in mice transgenic for human four-repeat tau protein. *Acta Neuropathol*. (Berl) 99 (2000): 469-81.

Raff M.C., Whitmore A.V., and Finn J.T. Axonal self-destruction and neurodegeneration. *Science*. 296 (2002): 868-871.

Raffaelli N., Sorci L., Amici A., Emanuelli M., Mazzola F., Magni G. Identification of a novel human nicotinamide mononucleotide adenylyltransferase. *Biochem Biophys Res Commun*. 297(2002): 835-40.

Reddy K. S. and Logan J. J. Intrachromosomal triplications: molecular cytogenetic and clinical studies. *Clin Genet*. 58 (2000): 134-141.

Sagot Y., Dubois-Dauphin M., Tan S.A., Bilbao F.de., Aebischer P., Martinou J.C., Kato A.C. Bcl-2 overexpression prevents motoneuron cell body loss but not axonal degeneration in a mouse model of a neurodegenerative disease. *J Neurosci*. 15(1995): 7727-7733.

Sagot Y., Tan S.A., Hammang J.P., Aebischer P., and Kato A.C. GDNF slows loss of motoneurons but not axonal degeneration or premature death of *pmn/pmn* mice. *J Neurosci*. 16 (1996): 2335-2341.

Sagot Y., Toni N., Perrelet D., Lurot S., King B., Rixner H., Mattenberger L., Waldmeier P.C., Kato A.C. An orally active anti-apoptotic molecule (CGP 3466B) preserves mitochondria and enhances survival in an animal model of motoneuron disease. *Br J Pharmacol*. 131(2000): 721-8.

Saigoh K., Wang Y.L., Suh J.G., Yamanishi T., Sakai Y., Kiyosawa H., Harada T., Ichihara N., Wakana S., Kikuchi T., Wada K. Intragenic deletion in the gene encoding ubiquitin carboxy-terminal hydrolase in gad mice. *Nat Genet*. 23 (1999): 47-51.

Samsam M., Mi W., Wessig C., Zielasek J., Toyka K.V., Coleman M.P. and Martini R. The *Wld*^S mutation delays robust axonal loss in a genetic model for myelin-related axonopathy. *J Neurosci*. 23 (2003): 2833-2839.

Schmid C.D., Stienekemeier M., Oehen S., Bootz F., Zielasek J., Gold R., Toyka K.V., Schachner M., Martini R. Immune deficinecy in mouse models for inherited peripheral neuropathies leads to improve myelin maintenance. *J Neurosci*. 20 (2000): 729-735.

Schiestl R.H., Khogali F., Carls N. Reversion of the mouse pink-eyed unstable mutation induced by low dose of x-rays. *Science*. 266 (1994): 1573-6.

Schiestl R.H., Aubrecht J., Khogali F., Carls N. Carcinogens induce reversion of the mouse pink-eyed unstable mutation. *Proc Natl Acad Sci U S A*. 94 (1997): 4576-81.

Schlaepfer W.W., and Hasler M.B. Characterization of the calcium-induced disruption of neurofilaments in rat peripheral nerve. *Brain Res*. 168 (1979): 299-309.

Schmalbruch H., Jensen H.S., Bjaerg M., Kamieniecka Z., Kurland L. A new mouse mutant with progressive motor neuropathy. *J Neuropath Exp Neurol*. 50 (1991): 192-204.

Schulz J.B., Nicotera P. Targeted modulation of neuronal apoptosis: a double-edged sword? *Brain Pathol*. 10 (2000): 273-275.

Sherriff F.E., Bridges L.R., Sivaloganathan S. Early detection of axonal injury after human head trauma using immunocytochemistry for beta-amyloid precursor protein. *Acta Neuropathol (Berl)*. 87(1994): 55-62.

Shih S.C., Sloper-Mould K.E., Hicke L. Monoubiquitin carries a novel internalization signal that is appended to activated receptors. *EMBO J*. 19(2000): 187-198.

Shimura H., Hattori N., Kubo S., Mizuno Y., Asakawa S., Minoshima S., Shimizu N., Iwai K., Chiba T., Tanaka K., Suzuki T. Familial Parkinson disease gene product, parkin, is a ubiquitin-protein ligase. *Nat Genet*. 25 (2000): 302-305.

Shimura H., Schlossmacher M.G., Hattori N., Frosch M.P., Trockenbacher A., Schneider R., Mizuno Y., Kosik K.S., Selkoe D.J. Ubiquitination of a new form of α-synuclein by parkin from human brain: implications for Parkinson's disease. *Science*. 293 (2001): 263-269.

Sidell N., Altman A., Haussler M.R. & Seeger R.C. Effects of retinoic acid (RA) on the growth and phenotypic expression of several human neuroblastoma cell lines. *Exp Cell Res*. 148 (1983): 21-30.

Sidman R.L., Angevine J.B., Pierce E.T. Atlas of mouse brain and spinal cord. Harvard University Press, Cambridge.

Smith K.J., Kapoor R., Hall S.M., Davies M. Electrically active axons degenerate when exposed to nitric oxide. *Ann Neurol*. 49 (2001): 470-6.

Smith R. S. & Bisby M. A. Persistence of axonal transport in isolated axons of the mouse. *Eur. J Neurosci*. 5 (1993): 1127-35.

Smith S. The world according to PARP. *Trends Biochem Sci*. 26 (2001): 174-179.

Southern E. M. Detection of specific sequences among DNA fragments separated by gel electrophoresis. *J Mol Biol*. 98 (1975): 503.

Sturtevant A. H. *Genetics*. 10 (1925): 117-147.

Stys P.K. Anoxic and ischemic injury of myelinated axons in CNS white matter: from mechanistic concepts to therapeutics. *J Cereb Blood Flow Metab*. 18(1998): 2-25.

Sung J.H., Angeline R.M., Park S.H. Axonal dystrophy in the gracile nucleus in children and young adults. *J Neuropath Exp Neurol*. 40 (1981): 73-45.

Takahashi T., Yagishita S., Amano N., Yamaoka K., Kamei T. Amyotrophic lateral sclerosis with numerous axonal spheroids in the corticospinal tract and massive degeneration of the cortex. *Acta Neuropathol (Berl)*. 94 (1997): 294-9.

Tartof K. D. Unequal crossing over then and now. *Genetics*. 120 (1988): 1.

Towbin H., Staehelin T and Gordon J. Electrophoretic transfer of proteins from polyacrylamide gels to nitrocellulose sheets: procedure and some applications. *Proc Natl Acad Sci*. 76 (1979): 4350.

Trapp B.D., Peterson J., Ransohoff R.M., Rudick R., Mork S., Bo L. Axonal transection in the leisons of multiple sclerosis. *N Engl J Med*. 338 (1998): 278-285.

Tsien R.Y. The green fluorescent protein. *Annu Rev Biochem*. 67(1998): 509-544.

Tu P.H., Raju P., Robinson K.A., Gurney M.E., Trojanowski J.Q., Lee V.M. Transgenic mice carrying a human mutant superoxide dismutase transgene develop neuronal cytoskeletal pathology resembling human amyotrophic lateral sclerosis lesions. *Proc Natl Acad Sci U S A*. 93 (1996): 3155-3160.

van Leeuwen F.W., de Kleijn D.P., van den Hurk H.H., Neubauer A., Sonnemans M.A., Sluijs J.A., Koycu S., Ramdjielal R.D.J., Salehi A., Martens G.J.M., Grosveld F.G., Peter J., Burbach H., Hol E.M. Frameshift mutants of beta amyloid precursor protein and ubiquitin-B in Alzheimer's and Down patients. *Science*. 279 (1998): 242-247.

Villegas A., Sanchez J., Carreno D. L., Ropero P., Gonzales F. A., Espinos D., Penalver M. A. & Lozano M. Molecular Characterization of a new family with alpha-thalassemia-1 (-- MA mutation). *Am J Hematol*. 49 (1995): 294-298.

Waller A. Philos. Trans. R. Soc. London. Experiments on the section of glossopharyngeal and hypoglossal nerves of the frog, and observations on the alterations produced thereby in the structure of their primitive fibres. *Philos. Trans. R. Soc. Lond. B Biol. Sci*. 140 (1850): 423-429.

Wang M.S., Wu Y., Culver D.G. & Glass J.D. The gene for slow Wallerian degeneration (*Wld*^{S}) is also protective against vincristine neuropathy. *Neurobiol Dis*. 8 (2001): 155-161.

Wang M.S., Davis A.A., Culver D.G., Glass J.D. *Wld*^{S} mice are resistant to paclitaxel (taxol) neuropathy. *Ann Neurol*. 52 (2002): 442-7.

Watson D.F., Glass J.D., Griffin J.W. Redistribution of cytoskeletal proteins in mammalian axons disconnected from their cell bodies. *J Neurosci*. 13 (1993): 4354 – 60.

Wen W., Meinkoth J. L., Tsien R. Y., Taylor S. S. Identification of a signal for rapid export of proteins from the nucleus. *Cell*. 82 (1995): 463-473.

Wen W., Harootunian A.T., Adams S.R., Feramisco J., Tsien R.Y., Meinkoth J.L., Taylor S.S. Heat-stable inhibitors of cAMP-dependent protein kinase carry a nuclear export signal. *J Biol Chem*. 269(1994): 32214-20

Wilson S.M., Bhattacharyya B., Rachel R.A., Coppola V., Tessarollo L., Householder D.B., Fletcher C.F., Miller R.J., Copeland N.G., Jenkins N.A. Synaptic defects in ataxia mice result from a mutation in Usp14, encoding a ubiquitin-specific protease. *Nat Genet*. 32 (2002): 420-425.

Wilkinson K.D., Lee K.M., Deshpande S., Duerksen-Hughes P., Boss J.M., Pohl J. The neuron specific protein PGP9.5 is a ubiquitin carboxyl-terminal hydrolase. *Science*. 246 (1989): 670-673.

Wilson S.M., Bhattacharyya B., Rachel R.A., Coppola V., Tessarollo L., Householder D.B., Fletcher C.F., Miller R.J., Copeland N.G., Jenkins N.A. Synaptic defects in ataxia

mice result from a mutation in *Usp14*, encoding a ubiquitin-specific protease. *Nat Genet*. 32(2002): 420-5.

Wu J. et al. Abnormal ubiquitination of dystrophic axons in central nervous system of gracile axonal dystrophy (GAD) mutant mouse. *Alzheimer's Res*. 2 (1996): 163-168.

Wujek J.R., Lasek R.J. Correlation of axonal regeneration and slow compound b in two branches of a single axon. *J Neurosci*. 3 (1983): 243-251.

Yamazaki K., Wakasugi N., Tomita T., Kikuchi T., Mukoyama M., Ando K. Gracile axonal dystrophy (GAD), a new neurological mutant in the mouse. *Proc Soc Exp Biol Med*. 187 (1988): 209-215.

Zhai Q., Wang J., Kim A., Liu Q., Watts R., Hoopfer E., Mitchison T., Luo L., He Z. Involvement of the ubiquitin-proteasome system in the early stages of wallerian degeneration. *Neuron*. 39 (2003): 217-25.

Zhang Y., Gao J., Chung K.K., Huang H., Dawson V.L., Dawson T.M. Parkin functions as an E2-dependent ubiquitin-protein ligase and promotes the degradation of the synaptic vesicle-associated protein, CDCrel-1. *Proc Natl Acad Sci. USA*. 97 (2000): 13354-13359.

Zhao C., Takita J., Tanaka Y., Setou M., Nakagawa T., Takeda S., Yang H.W., Terada S., Nakata T., Takei Y., Saito M., Tsuji S., Hayashi Y., Hirokawa N. Charcot-Marie-Tooth disease type 2A caused by mutation in a microtubule motor KIF1Bbeta. *Cell*. 105 (2001): 587-597.

Curriculum Vitae

<u>Persönliche Angaben</u>

Name: Mi

Vorname: Weiqian

Geburtsdatum: 20.01.1973

Geburtsort: Fuzhou, V. R. China

Staatsangehörigkeit: V. R. China

Familienstand: Ledig

<u>Ausbildung</u>

Sept. 1980-Juni. 1986 Schülerin in der Gu-lou No.1 Grundschule in Fuzhou, V. R.China

Sept. 1986-Juni. 1992 Schülerin im Gymnasium No. 3 in Fuzhou, V. R. China

Sept. 1992-Juni. 1996 Studium an der Nankai Universität für Biologie, V. R. China

August. 1997-Nov. 1999 Master studium an der National Universität zu Singapore

Apr. 2000-Nov. 2003 Promotionsstudiengang Biologie (Fachrichtung Genetik) am Institut für Genetik, Universität zu Köln, in der Abteilung von Prof. Dr. Sigrun Korshing und Prof. Dr. Michael Coleman.

<u>Teilpublikationen</u>

Mi W, Glass JD, Coleman MP. Stable inheritance of an 85-kb triplication in C57BL/Wld^S mice. Mutat. Res. May 15; 526(1-2): 33-7 (2003).

Samsam M, **Mi W**, Wessig C, Zielasek J, Toyka KV, Coleman MP and Martini R. The Wld^S mutation delays robust axonal loss of motor and sensory axons in a genetic model for myelin-related axonopathy. J. Neurosci. Apr 1; 23(7): 2833-9 (2003).

Mi W, Conforti L, Coleman MP. A genotyping method to detect a unique europrotective factor for axon (Wld^S). J. Neurosci. Meth. Jan 30; 113(2): 215-8 (2002).

Mack TGA, Reiner M, Beirowski B, **Mi W**, Coleman MP *et al*. Wallerian degeneration of injured axons and synapses is delayed by a *Ube4b/Nmnat* chimeric gene. Nat. Neurosci. Dec;4(12): 1199-1206 (2001).

Conforti L, Tarlton A, Mack TGA, **Mi W**, Coleman MP *et al*. A chimeric protein and overexpression of Rbp7 in the slow wallerian degeneration (Wld^S) mouse. Proc. Natl. Acad. Sci. Oct 10; 97(21): 11377-11382 (2000).